Chlamydiae host cell interaction and immune evasion strategies

Dissertation

zur Erlangung des Grades
Doktor der Naturwissenschaften

am Fachbereich Biologie
der Johannes Gutenberg-Universität Mainz

Susi Krämer

geb. am 15.08.1986 in Kehl am Rhein

Mainz, 2015

Dekan

1. **Berichterstatter**
2. **Berichterstatter**

Tag der mündlichen Prüfung: 24. Juli 2015

During this thesis the obtained research data and collaborative studies led to the following publications:

Krämer S, Crauwels P, Bohn R, Radzimski C, Szaszák M, Klinger M, Rupp J, van Zandbergen G. 2015. AP-1 transcription factor serves as a molecular switch between *Chlamydia pneumoniae* replication and persistence. Infect Immun 83:2651–2660. PMID: 25895972

Peter Crauwels, Rebecca Bohn, Meike Thomas, Stefan Gottwalt, Florian Jäckel, **Susi Krämer**, Elena Bank, Stefan Tenzer, Paul Walther, Max Bastian & Ger van Zandbergen (2015) Apoptotic-like Leishmania exploit the host´s autophagy machinery to reduce T-cell-mediated parasite elimination, Autophagy, 11:2, 285-297 PMID: 25801301

Summary

Chlamydiae are obligate intracellular bacteria with a strong global prevalence. They cause infections of the eye, lung and the genital tract and can either replicate in inclusion compartments or persist inside their host cell. In this thesis we focused on two aspects of chlamydiae infection. We hypothesize that transcription factor AP-1 is crucial for a replicative chlamydiae infection in epithelial cells. In addition we suggest that chlamydiae hide inside apoptotic blebs for a silent uptake by macrophages as immune evasion strategy.

Focusing on AP-1, we could demonstrate that during *Chlamydia pneumoniae* infection, protein expression and phosphorylation of the AP-1 family member c-Jun significantly increased in a time and dose dependent manner. A siRNA knockdown of c-Jun in HEp-2 cells reduced chlamydial load, resulting in smaller inclusions and a significant lower chlamydial recovery. Furthermore, inhibition of the c-Jun containing AP-1 complexes, using Tanshinone IIA, changed the replicative infection into a persistent phenotype, characterized by (i) smaller, aberrant inclusions, (ii) a strong decrease in chlamydial load, as well as by (iii) its reversibility after removal of Tanshinone IIA. As chlamydiae are energy parasites, we investigated whether Tanshinone IIA interferes with energy/metabolism related processes. A role for autophagy or gene expression of *glut-1* and *c-jun* in persistence could not be determined. However we could demonstrate Tanshinone IIA treatment to be accompanied by a significant decrease of ATP levels, probably causing a chlamydiae persistent phenotype.

Regarding the chlamydial interaction with human primary cells we characterized infection of different chlamydiae species in either pro-inflammatory (type I) or anti-inflammatory (type II) human monocyte derived macrophages (hMDM). We found both phenotypes to be susceptible to chlamydiae infection. Furthermore, we observed that upon *Chlamydia trachomatis* and GFP-expressing *Chlamydia trachomatis* infection more hMDM type II were infected. However the chlamydial load was higher in hMDM type I and correspondingly, more replicative-like inclusions were found in this phenotype. Next, we focused on the chlamydial transfer using a combination of high speed live cell imaging and GFP-expressing *Chlamydia trachomatis* for optimal visualization. Thereby, we could successfully visualize the formation of apoptotic, chlamydiae-containing blebs and the interaction of hMDM with these blebs. Moreover, we observed the development of a replicative infection in hMDM.

In conclusion, we demonstrated a crucial role of AP-1 for *C. pneumoniae* development and preliminary time lapse data suggest that chlamydiae can be transferred to hMDMs via apoptotic blebs. In all, these data may contribute to a better understanding of chlamydial infection processes in humans.

Zusammenfassung

Chlamydien sind obligat intrazelluläre Bakterien, welche Infektionen der Schleimhäute im Augen-, Atemwegs- und Genitalbereich hervorrufen können. Die Vermehrung der Chlamydien erfolgt in einem membranumhüllten Kompartiment, der sogenannten Inklusion. Alternativ können Chlamydien auch in ihren Wirtszellen persistieren. Der vorliegenden Arbeit lagen zwei zentrale Hypothesen zugrunde und befasst sich daher mit zwei Aspekten der Chlamydien-Infektion. Im ersten Teil dieser Arbeit untersuchen wir die Rolle des Transkriptionsfaktors AP-1 für die Chlamydien-Infektion in Epithelzellen, da wir annehmen das AP-1 von zentraler Bedeutung für die Vermehrung der Chlamydien in Epithelzellen ist. Im zweiten Teil dieser Arbeit liegt der Fokus auf der Infektion und dem Transfer von Chlamydien in humane Makrophagen, da wir davon ausgehen, dass sich Chlamydien in apoptotischen *Blebs* verstecken, um unbemerkt von Makrophagen aufgenommen zu werden.

Bezüglich der Rolle des Transkriptionsfaktors AP-1 für die Entwicklung der Chlamydien-Infektion in Epithelzellen konnten wir zeigen, dass die Expression und Phosphorylierung der AP-1 Komponente c-Jun während der Infektion mit *Chlamydia pneumoniae* zeit- und dosis-abhängig erhöht wird. Ein c-Jun spezifischer siRNA-Knockdown in HEp-2 Zellen reduzierte die Chlamydienlast, führte zu kleineren Inklusionen sowie einer signifikant verringerten Wiederanzucht. Durch Tanshinone IIA, einem spezifischen AP-1 (c-Jun/c-Fos) Inhibitor, wurde eine persistente Chlamydien-Infektion induziert. Die persistente Infektion war durch kleine, atypische Inklusionen und eine drastische Abnahme der Chlamydienlast gekennzeichnet, was durch Entfernen des Stimulus wieder umkehrbar war. Da Chlamydien als Energieparasiten gelten, wurden mögliche Auswirkungen der Tanshinone IIA-Behandlung auf den Energiestoffwechsel der Wirtszelle untersucht. Eine Beteiligung von Autophagie oder eine Beeinflussung von den AP-1 Zielgenen *glut-1* und *c-Jun* konnte nicht festgestellt werden. Allerdings führte die Tanshinone IIA-Behandlung zu einer signifikanten Abnahme des ATP-Gehalts, was vermutlich die persistente Chlamydien-Infektion bedingt.

In Bezug auf die Interaktion von Chlamydien mit humanen Makrophagen wurde die Infektion verschiedener Chlamydien-Spezies in pro- und anti-inflammatorischen humanen Makrophagen charakterisiert. Dabei zeigte sich, dass beide Makrophagen-Phänotypen mit Chlamydien infiziert werden konnten. Interessanterweise war eine größere Anzahl anti-inflammatorischer Makrophagen mit *Chlamydia trachomatis* (Wildtyp oder eGFP) infiziert, obwohl eine höhere Chlamydienlast sowie mehr replikative Inklusionen in pro-inflammatorischen Makrophagen gefunden wurden. Der Chlamydien-Transfer wurde mittels *Live Cell Imaging* untersucht, wobei GFP-exprimierende Chlamydien zur optimalen Visualisierung genutzt wurden. Dabei konnten wir die Entstehung von apoptotischen, Chlamydien beinhaltenden *Blebs* beobachten, mit welchen die Makrophagen interagierten.

Zudem war es uns möglich, die Entwicklung einer replikativen Infektion in Makrophagen in Echtzeit zu verfolgen.

Zusammenfassend können wir eine wichtige Rolle des Transkriptionsfaktors AP-1 für die Entwicklung der Chlamydien-Infektion von *Chlamydia pneumoniae* in Epithelzellen nachweisen. Vorläufige mikroskopische Echtzeitaufnahmen deuten an, dass Chlamydien in apoptotischen *Blebs* von Makrophagen aufgenommen werden können, was somit einen möglichen Transfermechanismus der Chlamydien darstellt. Die hier vorliegenden Ergebnisse können zu einem besseren Verständnis in Bezug auf die Infektion von Chlamydien im Menschen beitragen.

Table of contents

1 Introduction

1.1 Chlamydiae

Chlamydiae are gram-negative, obligate intracellular bacteria with a unique biphasic development cycle and a strong global prevalence (AbdelRahman and Belland, 2005). First hints for chlamydiae infections have already been given in the Ebers papyrus, one of the oldest existing medical texts dating to 1550 BC (Ebers, 1875). For a long time chlamydiae were considered to be viruses as a result of their obligate intracellular lifecycle and their small size (Wang, 1999). In the 1960s however, they were finally identified as bacteria. Chlamydiae occur both as animal pathogens as well as human pathogens and cause a number of different diseases like infections of the eye, lung and the genital tract (Peeling and Brunham, 1996). Currently the most important human pathogenic species are C*hlamydia pneumoniae* and *Chlamydia trachomatis*.

1.2 Taxonomy

Based on their characteristic biphasic lifecycle chlamydiae are grouped in their own order, *Chlamydiales,* which consists of the families *Parachlamydiaecae*, *Waddliaecae*, *Simkaniaceae* and *Chlamydiaceae* (Everett et al., 1999). The representatives of the *Parachlamydiaceae*, *Waddliaceae* and *Simkaniaceae* live as symbionts in amoebae (Amann et al., 1997; Fritsche et al., 2000; Horn et al., 2000). In contrast, the family *Chlamydiaceae* is the only family which includes human pathogens in addition to animal pathogens (Amann et al., 1997; Bush and Everett, 2001; Everett et al., 1999; Ossewaarde and Meijer, 1999). In 2001 the family *Chlamydiaceae* was divided in two genera, *Chlamydia* and *Chlamydophila*, based on the analysis of the 16S rRNA and 23S rRNA (**Figure 1 A**, Bush and Everett, 2001; Everett et al., 1999). To the genus *Chlamydia* belong the species *Chlamydia trachomatis*, *Chlamydia suis* and *Chlamydia muridarum*. The genus *Chlamydophila* consists of the species *Chlamydophila psittaci*, *Chlamydophila abortus, Chlamydophila felis, Chlamydophila caviae*, *Chlamydophila pecorum* and *Chlamydophila pneumoniae.* However, this division of the family *Chlamydiaceae* into two subgenera was not accepted by large parts of the research community because the proposed classification was based on relatively small differences of the 16S rRNA and did not consider the biological relevance of the organisms (Schachter et al., 2006). Therefore in 2009 it was supposed to reunite the genera again and just use the single genus *Chlamydia* (**Figure 1 B**; Stephens et al., 2009). Until now, no consensus was found on the question of how to classify the chlamydiae. Thus, in

publications both ways of notation can be found. This thesis adheres to the taxonomy according to Stephens et al. so consequently the terms *Chlamydia pneumoniae* and *Chlamydia trachomatis* were used (Stephens et al., 2009).

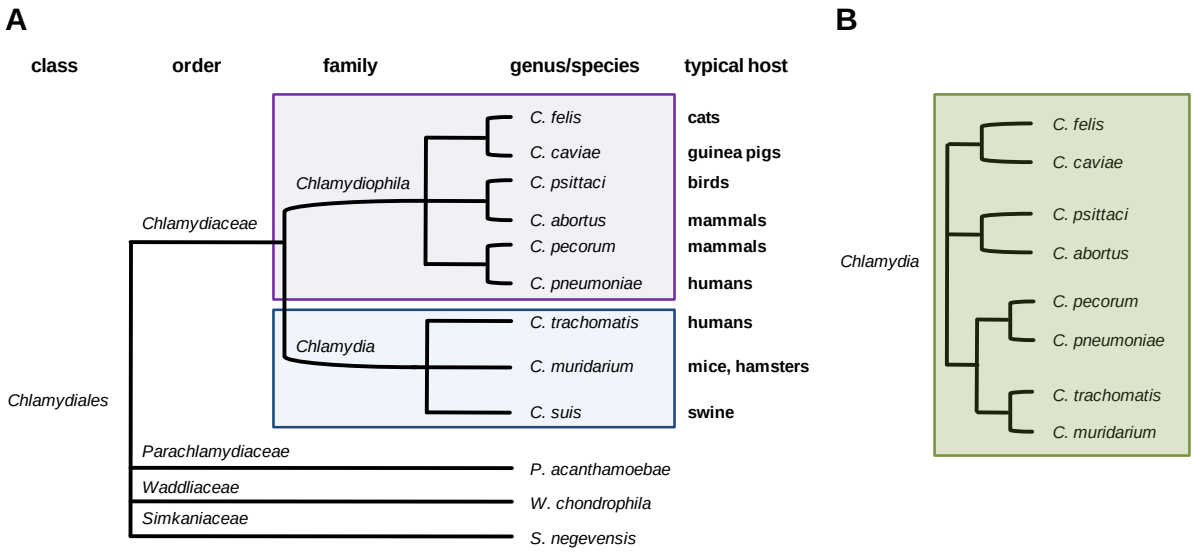

Figure 1: Taxonomy of chlamydiae. Schematic representation of the phylogenetic tree and taxonomy of **A)** the order *Chlamydiaceae* divided in the two genera *Chlamydia* and *Chlamydophila* based on Everett et al. (Everett et al., 1999) and **B)** the phylogenetic tree of *Chlamydiaceae* according to Stephens et al. (Stephens et al., 2009) in whose system all species are united in the genus *Chlamydia*. The length of the lines is arbitrary and does not represent phylogenetic distances.

1.3 Pathogenesis and disease

In humans, three different species are known to cause disease, namely *Chlamydia pneumoniae* and *Chlamydia trachomatis,* which represent the most common ones and *Chlamydia psittaci*, which preferentially infect birds (Beeckman and Vanrompay, 2009).

1.3.1 *Chlamydia pneumoniae*

Chlamydia pneumoniae (*C. pneumoniae*) is an airborne pathogen that infects the respiratory epithelia causing acute and chronic infections of the respiratory tract. Seropositivity in most adult populations ranges from 60% to 90% indicating the high worldwide prevalence of *C. pneumoniae* (Koh et al., 2002). The majority of primary infections proceeds asymptomatic and mostly takes place in adolescence. Up to the age of 20 years, almost 70% of all adults are seropositive for *C. pneumoniae* (Krüll et al., 2005). Lethal infections are rare and occur predominantly in elder and immune-suppressed patients. Since both the upper and the lower respiratory tract can be affected, the infection manifests itself in various diseases such as pharyngitis, sinusitis, bronchitis and pneumonia (Campbell and Kuo, 2009; Grayston et al.,

1993; Peeling and Brunham, 1996). *C. pneumoniae* infection is a major cause of community-acquired pneumonias (CAP) (Grayston, 1992; Kuo et al., 1995; Wreghitt, 1993). An unresolved, persistent *C. pneumoniae* infection is discussed to contribute to the pathological process of chronic inflammatory lung diseases (Blasi et al., 1993; Hahn et al., 1991). Furthermore, *C. pneumoniae* infection has also been associated with bronchial asthma and chronic obstructive pulmonary disease (COPD), the two most common chronic respiratory diseases in man (Droemann et al., 2007; Hahn, 2004; Von Hertzen et al., 1997; Ouellette et al.; 2004, Watson and Alp, 2008). As viable chlamydiae have been cultivated from atherosclerotic plaques and cerebrospinal fluid, *C.pneumoniae* also was associated with several non-respiratory diseases, such as coronary heart disease, multiple sclerosis, and Alzheimer's disease (Fainardi et al., 2008; Hahn; 2004, Ouellette et al. 2004; Palikhe et al., 2008; Sessa et al., 2007; Tang et al., 2009; Watson and Alp, 2008). However the role of *C. pneumoniae* in these diseases is still controversially discussed.

1.3.2 *Chlamydia trachomatis*

Chlamydia trachomatis (*C. trachomatis*) causes infections of the epithelial of the eyes and the genital tract and is, with approximately 90 million new infections per year, among the most common sexually transmitted bacterial pathogens worldwide (Brunham and Rey-Ladino, 2005; WHO, 2011). *C. trachomatis* is divided into three groups of serovars, which display different tissue tropism and establish different clinical outcomes.

Serovars A - C: The serovars A - C cause inflammation of the conjunctiva and the cornea of the eye - called trachoma (Bujger and Ekert; Burton and Mabey, 2009). This trachoma is worldwide the leading cause of preventable infectious blindness and is mostly found endemically in developing countries (Gambhir et al., 2007). The bacteria can be spread through both, direct contact with an infected person or through indirect contact with fomites, e.g. contaminated clothes or towels (WHO, 2015). Worldwide over 50 million people are suffering from active infection, while nearly 2 million people are visually impaired as a result of the disease and of whom 0.5 million are already irreversibly blind (WHO, 2015). The recurring inflammation of the epithelial cells of the conjunctiva is accompanied by swelling of the upper eyelid and scarred tissue. The eyelid then turns inwards, where the eyelashes scratch the ocular surface. This condition is called trichiasis and leads to blindness when left untreated (Burton, 2007; Burton and Mabey, 2009; WHO, 2015).

Serovars D- K: Infections of the genital tract with the serovars D - K represent the most common cause of sexually transmitted bacterial diseases (Thomson et al., 2008; WHO, 2011). Many of these infections remain asymptomatic and therefore unnoticed and subsequently untreated. This promotes chronic infections with serious consequences such as pelvic inflammatory disease, ectopic pregnancy and tubal occlusion (Carlin and Weller,

1995; Faro, 1985; Peeling and Brunham, 1996; Swasdio et al., 1996; Tuffrey et al., 1986). Consequently, these chronic infections are the most common cause of unintentional childlessness due to infection induced infertility of women (Faro, 1985; Haggerty et al., 2010; Swasdio et al., 1996).

Serovars L1 - L3: The serovars L1 - L3 are sexually transmitted as well and infect the lymphatic tissues of the urogenital region causing the more systemic infection lymphogranuloma venereum (LGV) (van Hal et al., 2007; Mabey and Peeling, 2002). The LGV disease is a chronic infection which occurs in three stages. The first stage is often unnoticed as it goes without symptoms causing painless genital ulcer. During the second stage the infection spreads to the lymph nodes and results in painful swelling. The third stage is characterized by fibrosis and edema and mostly remains permanent (Mabey and Peeling, 2002). The dissemination of the chlamydiae is linked to infection of monocytes and macrophages (Mabey and Peeling, 2002; Schachter and Osoba, 1983). In this thesis *C. trachomatis* serovar L2 was used.

1.4 Development cycle of chlamydiae

1.4.1 Replication

All chlamydiae species share a unique biphasic development cycle, in which the bacteria exist in two distinct developmental and functional forms (schematically outlined in **Figure 2 A**). Their development cycle is marked by different transcriptional programs and therefore separated in three diverse intracellular stages, the early, mid and late stage (Shaw et al., 2000). The initial infection starts with the attachment and internalization of the elementary body (EB) by cells of the host's epithelium via phagocytosis or clathrin or calveolin receptor-mediated endocytosis (Dautry-Varsat et al., 2005; Hodinka et al., 1988; Hybiske and Stephens, 2007a; Reynolds and Pearce, 1990). The EB represents the infectious but metabolically inactive form, with a size of about 0.3 µm which can shortly survive outside the cell (Wolf et al., 2000). EBs exhibita rigid outer membrane with three cysteine-rich proteins that are highly cross linked by disulfide bonds (AbdelRahman and Belland, 2005; Hatch et al., 1986). The major outer membrane protein (MOMP) represents one of the most important of these proteins and is not only a major structural component of the chlamydial cell wall, but also an antigen that induces a protective antibody response. After uptake, the EBs still possess their characteristic size and condensed DNA, but just a few hours after infection, the DNA starts to decondense and an increase in size takes place due to the cleavage of the outer membrane disulfide bonds (Grieshaber et al., 2004; Hatch et al., 1986; Wolf et al., 2000; Wyrick, 2000). Thereby the membrane of the bacteria surrounding the vesicular compartment, named the inclusion, is intensely modified. These modifications are required to

prevent the fusion with lysosomes and to provide the necessary supply of various metabolites or nutrients components such as sphingolipids through interaction with the Golgi apparatus (Al-Younes et al., 2001; Hackstadt et al., 1996, 1997; Heuer et al., 2009; Ojcius et al., 1997; Rockey et al., 1995; Scidmore et al., 2003). Within the inclusion the EBs differentiate into the reticulate bodies (RB) with a size of 0.8 - 1.5 µm and this EB to RB conversion is called the early stage of infection (AbdelRahman and Belland, 2005). The RBs are now metabolically active but not infectious anymore. During the mid-stage of the infection, the replication of the RBs, by binary fission, occurs by which the inclusion grows exceptionally large, taking up most of the cytoplasmic space (Hackstadt, 1999; Moulder, 1991)(**Figure 2 B-C**). After replication, the late phase of infection is initiated, in which the chlamydiae start to re-differentiate to infectious EBs. For *C. trachomatis* the late stage begins about 20 hours after infection and for *C. pneumoniae* around 48 hours after infection (Moulder, 1991).

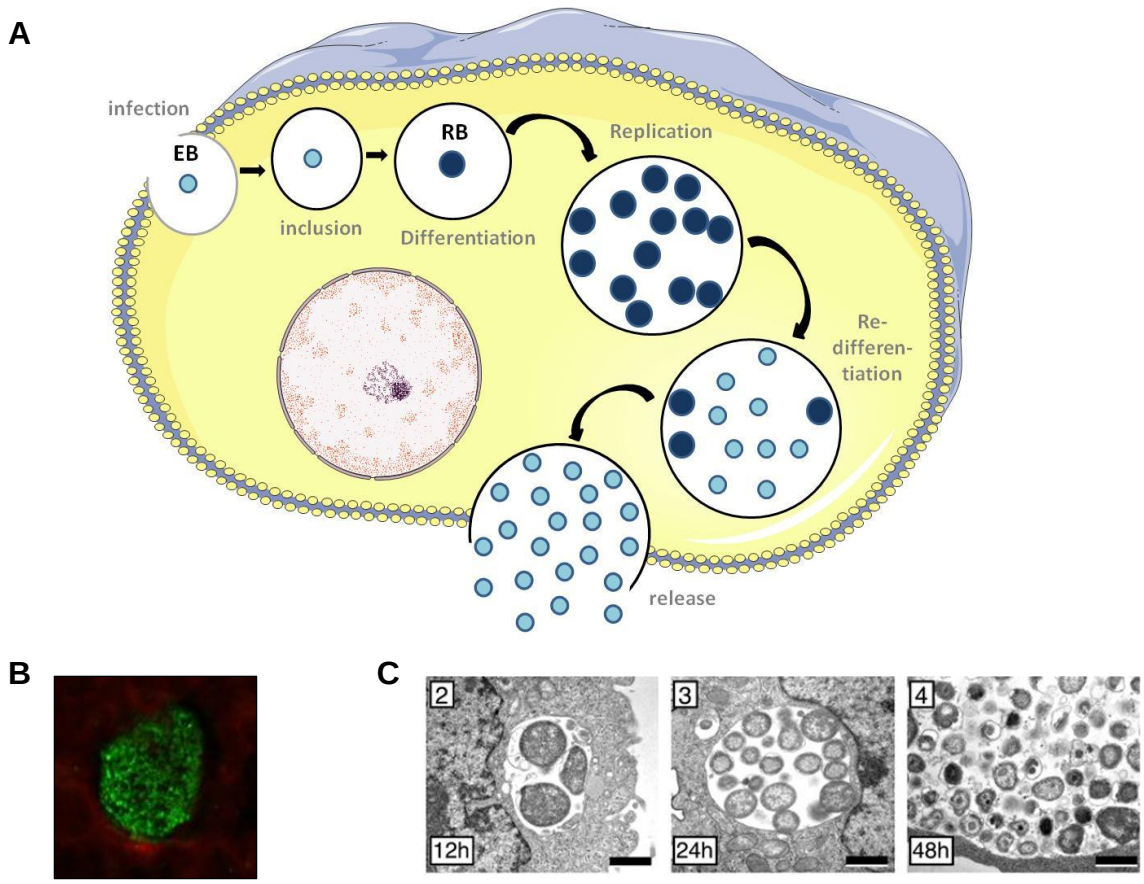

Figure 2: Replicative development cycle of chlamydiae. The replicative development of chlamydiae is schematically outlined in **A**) and begins with attachment and invasion of an elementary body (EB). Inside the cell the inclusion is formed in which the EB differentiates into a reticulate body (RB) which then starts to replicate within the inclusion. After replication the RBs re-differentiate into infectious EBs which are released in order to infect new cells. **B)** Typical replicative inclusion in an epithelial cell stained in green with a specific antibody against chlamydial LPS. **C)** Electron micrograph of a replicative inclusion in an epithelia cell with typical RB developmental forms present at 12 hpi (C2) and 24 hpi (C3) and a mixture of characteristic RBs and EBs 48 hpi (C4) (**adopted and modified from Belland et al. (Belland et al., 2003).**

During the chlamydial development, a high amount of energy is required. Although chlamydiae possess genes required for energy metabolism they are often encoded incompletely and chlamydiae recruit lipids, iron, nucleotides and ATP of their host cell (Hatch et al., 1982; Iliffe-Lee and McClarty, 1999; Kalman et al., 1999; McClarty and Fan, 1993; McClarty and Qin, 1993; Tipples and McClarty, 1993). Thus chlamydiae are discussed to be energy parasites which are highly relying on the supply of nutrients by their host cell (McClarty, 1999; Moulder, 1991). To optimize the energy supply, chlamydiae are also linked to the autophagy machinery, a process used by the host cell to regain energy in times of starvation or stress. Depending on the species, the completion of the developmental cycle takes 48 hours (C. *trachomatis*) to 72 hours (*C. pneumoniae*) after which the chlamydiae finally leave the cell in order to infect new cells (Dautry-Varsat et al., 2005; Hackstadt, 1999; Hybiske and Stephens, 2007b; Moulder, 1991; Wolf et al., 2000). Nevertheless the exact mechanism of chlamydial cell to cell transfer is still largely unknown.

1.4.2 Persistence

Alternatively to the described replication cycle, the infection can also enter a persistence state in response to stress conditions (schematically outlined in **Figure 3 A**). In a persistence state the chlamydiae exist in a strongly altered metabolically and morphologically life form. Persistence is characterized by an incomplete developmental cycle in line with formation of smaller and aberrant inclusions, which harbor only a few but enlarged and aberrant RBs (Beatty et al., 1993, 1994a; Borel et al., 2014; Hogan et al., 2004; Wyrick, 2010)(**Figure 3 B-C**). The inclusions remain small as the chlamydiae do not replicate in this persistent state (Beatty et al., 1994a). Furthermore, persistence is accompanied by reduced infectivity and metabolic activity (Beatty et al., 1994a; Harper et al., 2000; Nelson et al., 2005). In this persistent state, re-differentiation into infectious EBs does not occur, so that a direct cultivation of persistent chlamydiae is not possible, although the chlamydiae remain viable (Beatty et al., 1994b, 1995; Borel et al., 2014). Some chlamydial proteins have been suggested as indicators of chlamydial persistence, such as MOMP and immuno-destructive chlamydial heat shock protein 60 (cHsp60) (Hogan et al., 2004; Villegas et al., 2008). In IFN-γ induced persistence MOMP expression is reduced, while expression of Hsp60 is maintained (Beatty et al., 1994b, 1994c). Furthermore, it was reported that inhibition of autophagy, hereby reducing the nutrient supply, impaired the inclusion size, chlamydial morphology and development of infectious progeny (Al-Younes et al., 2004). In contrast other studies suggest that autophagy can serve as an innate defense mechanism against chlamydiae (Al-Younes et al., 2004, 2011; Yasir et al., 2011). Several host cell pathways have been highlighted to play a role during chlamydiae infection, however the trigger leading

to a persistence phenotype in disease is still controversially debated. *In vitro* persistence can be induced by several conditions for example, by treatment with IFN-γ or certain antibiotics, but also by iron deprivation or nutrient starvation (Beatty et al., 1994c; Coles et al., 1993; Dreses-Werringloer et al., 2000; Harper et al., 2000; Igietseme et al., 1998; Matsumoto and Manire, 1970; Pantoja et al., 2001; Peters et al., 2005; Raulston, 1997; Summersgill et al., 1995). Persistence is a reversible phenotype and after removal of the persistence stimuli the chlamydiae can be reactivated and return to the replicative development cycle (Hogan et al., 2004). In a state of persistence the chlamydiae are resistant to antibiotic treatment. Interestingly, the host cell function is hardly disturbed during persistent infection. Chlamydiae can remain indefinitely in the persistent form which is discussed to be associated with many chronic diseases, such as atherosclerosis, pelvic inflammatory disease, asthma, scarring trachoma and reactive arthritis, as it is difficult for the host cells to eliminate the chlamydiae (Hogan et al., 2004). In general, the molecular switch determining persistent or replicative infection is poorly understood.

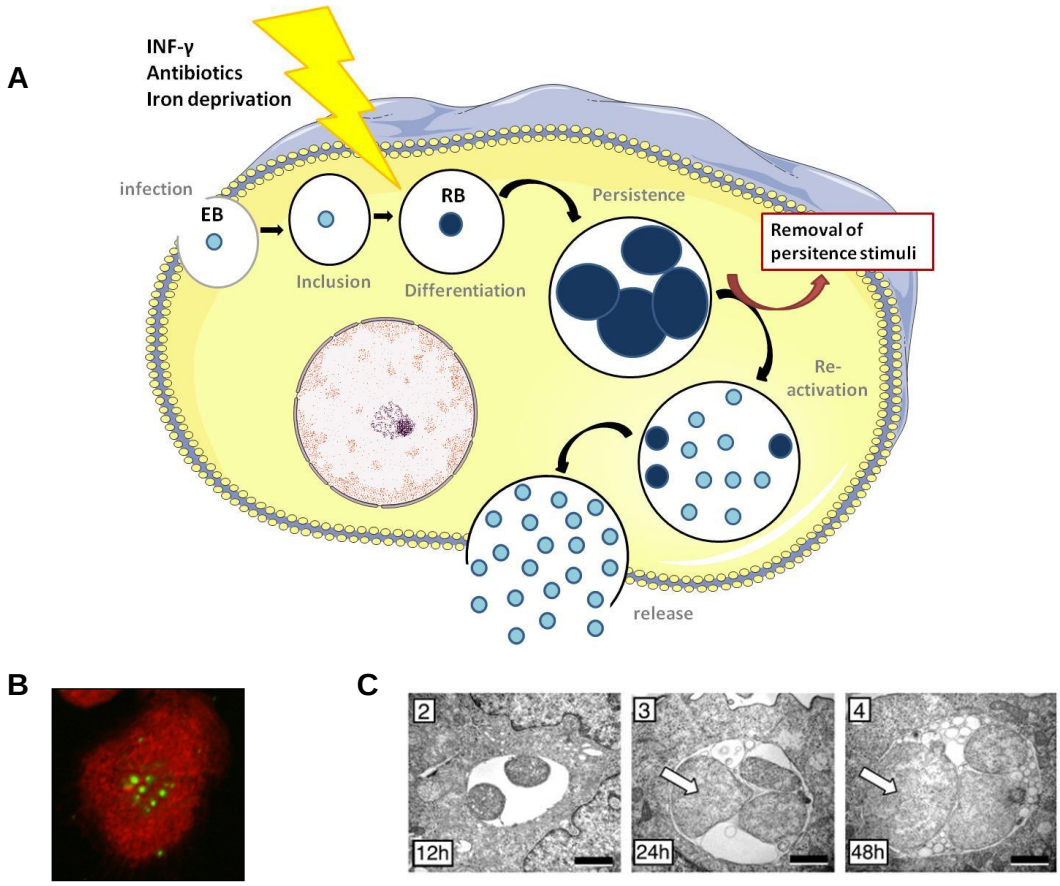

Figure 3: Persistent chlamydiae infection. A persistent chlamydiae infection is schematically outlined in **A**) and can be induced by treatment with IFN-γ, certain antibiotics, iron deprivation or poor nutrient conditions. The inclusions remain small and aberrant and harbor only a few but large an atypical RBs. Removal of the persistence stimuli reactivates chlamydial development and results in the return to replication. **B)** Typical persistent infection in an hMDM with small inclusions stained in green with a specific antibody against chlamydial LPS. **C)** Electron micrograph of an INF-γ induced persistence in an epithelia cell. Initially, RBs appear similar to untreated cultures

at 12 hpi (C2) however, at 24 hpi (B3) and 48 hpi (C4) the RBs exhibit an aberrant morphology and appear as large aberrant non- infectious forms (**adopted and modified from Belland et al. (Belland et al., 2003)**.

1.5 Chlamydiae host cell interactions

Chlamydiae modulate and manipulate various host cell pathways and processes to ensure optimal growth and to acquire nutrients and energy from the host cell as well as for evasion of host defense mechanisms (Mehlitz and Rudel, 2013). Chlamydial modulation starts already upon uptake and is present during EB attachment and internalization as well as for inclusion modifications, such as for protection against lysosomal degradation (Carebeo et al., 2004, Clifton et al., 2004; Grieshaber et al., 2003; Jewett et al., 2006; Rzomp et al., 2003; Scidmore et al., 2003). To avoid immune responses, chlamydiae also interfere with several important host cell signaling pathways, for instance inhibit NF-KB signaling and down-regulate MHC class I and II antigen presentation (Lad et al., 2007a, 2007b; Le Negrate et al., 2008; Zhong et al., 2000). In addition, chlamydiae are well known to modulate host cell apoptosis. They are able to block host cell apoptosis to ensure intracellular survival. On the contrary they trigger their release at later time points by induction of apoptotic blebs (Carabeo et al., 2002; van Zandbergen et al., 2004a). To accomplish the complex manipulation of their host cell, chlamydiae are able to interact with numerous cellular factors, such as transcription factor HIF-1 (Le Negrate et al., 2008; Rupp et al., 2007).

1.5.1 Transcription factor AP-1

A known key player in various regulatory processes of the host cell is the transcription factor AP-1 (activator protein-1). AP-1 is involved in proliferation, differentiation, apoptosis, cell metabolism, migration and neoplastic transformation and inflammation (**Figure 4**) (Angel and Karin, 1991; van Dam and Castellazzi, 2001; Eferl and Wagner, 2003; Kozlovsky et al., 1997; Santalucía et al., 2003; Schonthaler et al., 2011; Shaulian and Karin, 2001, 2002). The involvement of AP-1 in such diverse and partially contradicting processes can be explained by the diversity of induction stimuli and the dependence on several basic conditions. In more detail, AP-1 can be regulated by a large variety of stimuli, such as growth factors, cytokines, UV radiation and other stress signals, in addition to infections and oncoproteins (Shaulian and Karin, 2001, 2002). The influence of AP-1 is determined by the individual AP-1 composition, type of stimulus, species and cell type, as well as by developmental state and cell cycle phase (Lallemand et al., 1997; Schonthaler et al., 2011; Shaulian and Karin, 2001, 2002).

AP-1 is a generic term for dimeric transcription factors which is composed of proteins of the Jun- (c-Jun, JunB and JunD), Fos- (c-Fos, FosB, Fra-1 and Fra-2) or activating transcription factor (ATF-) (ATF-2, ATF-3 and BH-ATF) family members (Zenz et al., 2008). These proteins can form homodimers, except for the c-Fos family, as well as different heterodimers through a bZIP-motif (*basic region leucine zipper*) influencing the fate of the cell (Angel and Karin, 1991; Karin et al., 1997; Kouzarides and Ziff, 1988; Shaulian and Karin, 2001, 2002; Wagner, 2001). As a result of the variety of possible heterodimer constellations, the ability to induce transcriptional activity is variable (Ryseck and Bravo, 1991). However, dimerization is a prerequisite for DNA binding and AP-1 regulates transcription of genes by binding at the consensus sequence (TRE; 5′-TGAG/CTCA-3′). This sequence is called TRE (TPA (12-O-tetradecanoylphorbol-13-acetate) responsive element) and was identified as an AP-1 binding site for many cellular but also viral genes (Angel et al., 1987, 1988; Landschulz et al., 1988; Tseng and Verma, 1995; Turner and Tjian, 1989).

AP-1 activity is regulated on multiple levels. The expression of AP-1 proteins is controlled by differential transcription rates as well as by differential mRNA stabilities and by posttranslational modifications e.g. phosphorylation or ubiquitination (Eferl and Wagner, 2003; Hess et al., 2004). AP-1 regulation on the transcriptional level modulates the availability of the different AP-1 subunits depending on cell type, differentiation status and cell context and therefore influencing the AP-1 composition (Vesely et al., 2009). Posttranscriptional modulation can occur for example by phosphorylation via different kinases belonging to the mitogen activated protein kinase (MAPK) pathway, such as c-Jun N terminal Kinase (JNK) or ERK (Doehn et al., 2009; Karin et al., 1997; Young and Colburn, 2006).

The two major subgroups of AP-1 are the Jun- and Fos-families, which are characterized by a high degree of homology. The Jun-Fos heterodimers exhibit higher stability and stronger DNA binding affinities than Jun-Jun homodimers based on the higher thermostability of heterodimers (Hess et al., 2004; Karin et al., 1997; Smeal et al., 1989). On a functional level, Jun proteins are involved in the regulation of genes which are implied in cellular proliferation and apoptosis, whereas Fos proteins are frequently associated with genes that contribute to angiogenesis and tumor invasion (Karin et al., 1997).

Human c-Jun consists of 334 amino acids and the *jun* gene belongs to the immediate-early genes, meaning it is activated rapidly and transiently upon stimulation (Angel et al., 1988). The most important regulation of c-Jun activity is mainly influenced by phosphorylation and ubiquitination which affect the DNA-binding, stability, interaction with other proteins and transcriptional regulatory activity (Boyle et al., 1991; Franklin et al., 1992; Pulverer et al., 1991). c-Jun protein induces its own transcription in a positive mediated autoregulation of the j*un* gene (Angel and Karin, 1991; Angel et al., 1988; Berry et al., 2001; Mechta-Grigoriou et al., 2001). c-Jun is expressed in proliferating and differentiating cells suggesting that it is

involved in both, cell proliferation and differentiation. It was shown that c-Jun is capable of regulating the activation of the cell cycle promoting gene cyclin D1 transcription, whereas it represses cell cycle inhibiting genes, such as p53 and INK4A (Bakiri et al., 2000; Passegué and Wagner, 2000; Schreiber et al., 1999; Shaulian and Karin, 2001; Shen et al., 2006, 2008).

c-Fos protein is composed of 381 amino acids and the *fos* gene is similar to the *jun* gene an immediate early gene. In contrast to Jun proteins, the Fos proteins cannot homodimerize with other Fos proteins, but form heterodimers preferentially with Jun proteins with varying affinities (Hai and Curran, 1991; Halazonetis et al., 1988). c-Fos protein expression is in most cell types at low or undetectable levels, but its amounts and transcriptional activity increases upon phosphorylation, like those of c-Jun (Distel and Spiegelman, 1990; Karin et al., 1997; Pulverer et al., 1991; Smeal et al., 1994). c-Fos is involved in important biological processes, including cell proliferation, differentiation and survival, as well as cell transformation and tumorigenesis (Shaulian and Karin, 2001; Tulchinsky, 2000).

Transcription factor AP-1 can contribute to both prevention of apoptosis resulting in cell survival and also to induction of apoptosis, leading to cell death (Ameyar et al., 2003; Hess et al., 2004; Shaulian and Karin, 2001). As AP-1 is involved in various host cell processes, chlamydiae may misuse this transcription factor for their

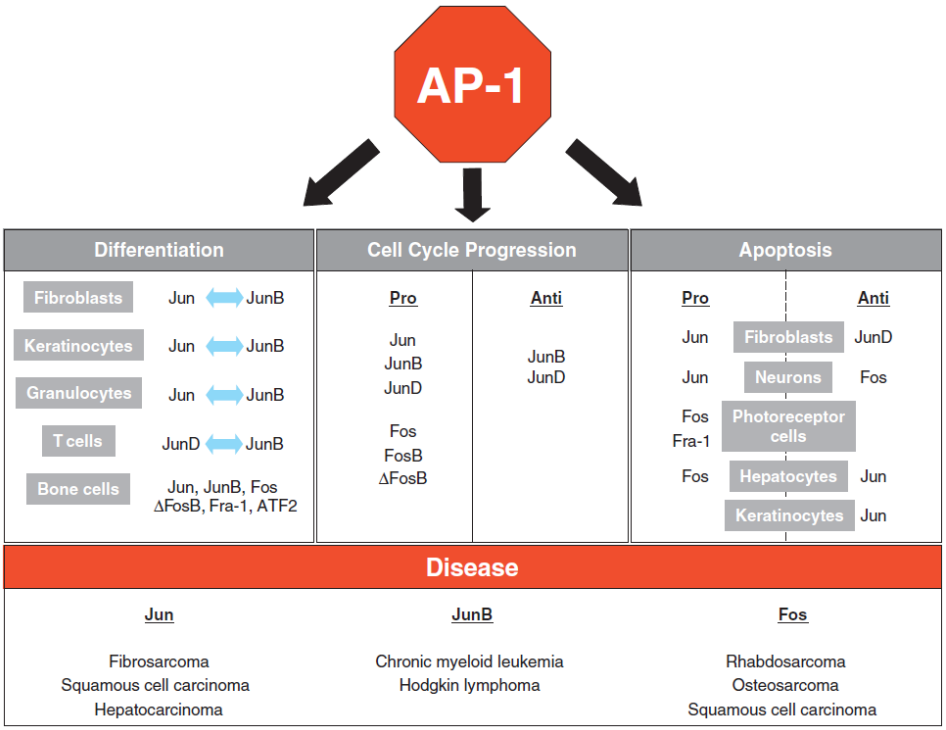

Figure 4: AP-1 regulates various host cell processes and is also involved in some diseases. AP-1 function depends on the subunit of AP-1 which can have a positive, negative or even a dual influence on essential cellular processes. Deregulation of these processes due to AP-1 alterations can lead to grave diseases. Blue double-headed arrow points out antagonists **(adopted from Hess et al. (Hess et al., 2004**).

1.5.2 Chlamydiae modulate host cell apoptosis

Chlamydiae have evolved strategies to regulate apoptosis pathways of their host cell, by either actively blocking of apoptosis or by its induction (Clifton et al., 1998; Fan et al., 1998; Fischer et al., 2001; Ojcius et al., 1998a; Perfettini et al., 2003; Rajalingam et al., 2001; Ying, 2007). The inhibition of apoptosis ensures the completion of the chlamydial development and secures a viable, nutrient-producing host cell alongside with protection for instance from the action of cytotoxic T cells (Byrne and Ojcius, 2004; Fling et al., 2001; Gervassi et al., 2004; Miyairi and Byrne, 2006). The prevention of their clearance thereby promotes a persistent infection. This is strengthened by the fact that chlamydiae infected cells, which were treated with persistence inducer IFN-γ, resist apoptosis (Dean and Powers, 2001). As premature induction of host cell apoptosis was shown to impair the chlamydial development, chlamydiae infected cells are able to block both chemically and spontaneously induced apoptosis (Dean and Powers, 2001; Fan et al., 1998; Fischer et al., 2001, 2004; Greene et al., 2004; Rajalingam et al., 2001; Ying et al., 2008). In contrast to apoptosis inhibition chlamydiae are also able to induce apoptosis which is connected to chlamydial release and dissemination (Byrne and Ojcius, 2004; Maass et al., 2000; Rupp et al., 2009; Shio et al., 2012). Several hypotheses have been suggested about how the chlamydiae are released from their host cell. As for most intracellular pathogens, it is suggested that chlamydial release is accomplished by lysis of the host cell, as chlamydiae infection in productive cell culture was shown to eventually result in host cell lysis (AbdelRahman and Belland, 2005; Campbell et al., 1989; Neeper et al., 1990; Patton et al., 1988; Rockey et al., 1996). This biological process was initially assumed to be a physical consequence as the inclusion expands and captures a majority of the intracellular space. Recent findings demonstrate that lysis is actively induced and orchestrated by the chlamydiae from within the bacteria-containing vacuole (Campbell et al., 1989; Hybiske and Stephens, 2007b; Neeper et al., 1990). In contrast to lysis another strategy for chlamydial release, called extrusion, was described (Hybiske and Stephens, 2007b). Extrusion is a packaged release mechanism which leaves the host cell intact, while some or all of the chlamydial inclusion pinches out of the host cell with viable chlamydiae inside (Hybiske and Stephens, 2007b). Extrusions were supposed to be involved in chlamydial dissemination as the uptake of extrusions by macrophages could distribute the chlamydiae to systemic sites, such as the lymph nodes (Hybiske and Stephens, 2008; Moazed et al., 1998).

Similar to extrusion an additional way of cell exit is provided by induction of host cell apoptosis (Ojcius et al., 1998b; Perfettini et al., 2003). The initiation of apoptosis at the end of chlamydial development could trigger or enhance release of EBs from which chlamydiae would benefit by facilitating their subsequent uptake by macrophages and therefore propagate infection without provoking an inflammatory response (Rupp et al., 2009).

Apoptosis occurs in infected cells at later stages of infection and is accompanied by nuclear morphological changes or nuclear damage during infection, in the absence of classical caspase activation (Dumrese et al., 2005; Ojcius et al., 1998b; Perfettini et al., 2002a, 2002b; Schöier et al., 2001). This caspase-independent induction of apoptosis could be explained by activation of the pro-apoptotic protein Bax as a possible result of the chlamydiae-mediated increase of mitochondrial metabolism and oxidative stress (Azenabor and Mahony, 2000; Hatch and McClarty, 1998; Ojcius et al., 1998b; Perfettini et al., 2002a, 2003). Furthermore, pro-apoptotic stimuli like tumor necrotic factor α (TNF-α) have been connected to chlamydiae induced apoptosis (Jendro et al., 2004). Moreover, a chlamydial effector protein associated with death domain (CADD) interacts with TNF receptor death domains and induces Fas-related apoptosis upon ectopic expression (Schwarzenbacher et al., 2004; Stenner-Liewen et al., 2002). Chlamydiae induced apoptosis may not only cause their release but also facilitate the subsequent transfer to new cells.

1.6 Silent transfer of chlamydiae between potential host cells

During the course of infection, human neutrophils are among the first cells to be present and to react on inflammation. They are naturally short-lived cells and have a life span between 6 – 10 hours in the circulation after which they normally undergo spontaneous apoptosis (Payne et al., 1994; Rupp et al., 2009; Tak et al., 2013; Zandbergen et al., 2004). During apoptosis neutrophils show typical apoptotic characteristics like decondensation of the nuclei, cell shrinkage, membrane blebbing followed by formation of apoptotic bodies as well as phosphatidylserine exposure (Payne et al., 1994; Squier et al., 1995; Zandbergen et al., 2004). In contrast, chlamydiae infection prolonged the life span of the neutrophils up to 90 hpi as the chlamydiae actively delayed apoptosis (Zandbergen et al., 2004). The infected neutrophils did not become apoptotic until 66 hpi, when the chlamydiae had finished their development cycle. In addition, the delay in apoptosis allowed the infiltration of macrophages to the site of infection which are crucial for systemic dissemination (Blasi et al., 2004; Shio et al., 2012). Subsequently, the macrophages internalize the apoptotic neutrophils and blebs which contain viable chlamydiae. The chlamydiae use this as “Trojan horse” strategy to benefit from an unrecognized uptake which generates a productive infection (**Figure 5**) (Byrne and Ojcius, 2004; Zandbergen et al., 2004). Furthermore, the interaction of phosphatidylserine on the surface of the apoptotic blebs with its receptor on the phagocytic cell reduces the inflammatory response (Byrne and Ojcius, 2004). Apoptosis may therefore be utilized by chlamydiae to achieve their transfer to macrophages ((Byrne and Ojcius, 2004; Rupp et al., 2009). In general, decoding the chlamydial transfer mechanisms is of fundamental importance to understand chlamydiae pathogenesis.

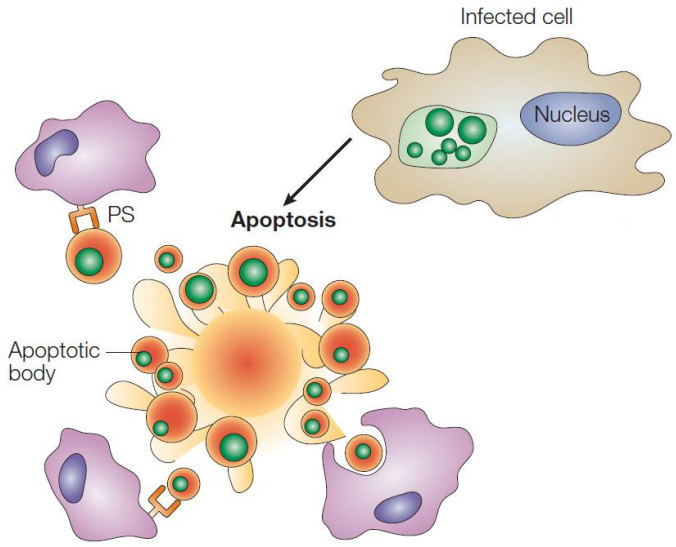

Figure 5: Infected cells can die by apoptosis and thereby reduces the inflammatory response. Chlamydiae-infected cells might induce apoptosis to be released from the host cell. They then may hide in the apoptotic blebs to be silently taken up by avoiding an inflammatory response. This mechanism might benefit chlamydial propagation (**adopted and modified from Byrne and Ojcius (Byrne and Ojcius, 2004)**.

1.6.1 Macrophages as host cells for chlamydiae

The first cells that are affected during chlamydiae infection are epithelial cells of the lung (*C. pneumoniae*) or the urogenital tract (*C. trachomatis*). However, additional host cells, involved in disease propagation, are macrophages. Macrophages (MFs) are white blood cells and are like dendritic cells and neutrophilic granulocytes professional phagocytes. They play a central role in the innate immunity as well as in initiating adaptive immune responses. MFs reside at strategic locations, in almost all tissues or develop from immature monocytes upon inflammation, to form the first line of defense against infections and infiltrating pathogens. The monocytes circulate through the bloodstream until they are recruited to the site of infection via chemotaxis. While they infiltrate into the inflamed tissue stimulation by various cytokines leads to differentiation into tissue resident MFs, such as alveolar MF (Adams and Hamilton, 1984; Nathan, 1987; Stout and Suttles, 2004). Mature human MFs can be characterized by the expression of specific markers, like pattern recognition receptors CD14 for detection of LPS and scavenger receptor CD68 and are responsible for engulfment and killing of invading microorganisms as well as for the removal of apoptotic and necrotic cells (Holness and Simmons, 1993; Leenen et al., 1994; Solovjov et al., 2005). Therefore they are equipped with mannose-receptors, scavenger-receptors and pattern recognition receptors (PRRs) for example Toll-like-receptors (TLRs) which recognize invading pathogens followed by elimination in the course of trigging phagocytosis. Subsequent to phagocytosis an intracellular endocytic compartment, called the phagosome, is formed. The modification of

the phagosome leads to the fusion with the lysosomes resulting in digest and destruction of the pathogen in the phagolysosome. Once pathogens were eradicated, scavenger receptors are involved in the clearance of apoptotic cells by inducing phagocytosis and inhibition of pro-inflammatory cytokine production, switching off previously activated macrophages (Fadok et al., 1998). This deactivation process is important to avoid destruction of tissues and persistence of inflammation (Gordon, 2003). Macrophages are relatively long-lived cells and the secretion of signaling proteins like cytokines and chemokines during inflammation leads to the activation and the recruitment of other immune cells.

1.6.2 Pro-inflammatory and anti-inflammatory macrophages

Two different macrophage phenotypes have been studied predominantly, whose differentiation depends on lineage-determining cytokines. These phenotypes differ in their morphology and effector functions causing opposite immune functions with either a Th1 or a Th2 response and therefore resulting in a different disease outcome (Mills et al., 2000). During inflammation monocytes differentiate into pro-inflammatory type I MFs which are responsible for host defense against pathogens, anti-tumor responses and autoimmunity (Neu et al., 2013; Xu et al., 2013). These pro-inflammatory type I MFs secrete the pro-inflammatory cytokines tumor necrosis factor alpha (TNF-α), Interleukin-1 (IL-1), IL1B, IL-6, IL-12(p40) and IL-23 and are therefore also termed “classically activated macrophages” (Goerdt et al., 1999; Mosser and Edwards, 2008; Verreck et al., 2004, 2006). Pro-inflammatory type I MFs are characterized by a round, fried egg-shaped morphology and they are positive for LPS receptor CD14, but negative for scavenger receptor CD163. In addition to production of pro-inflammatory cytokines they kill microorganisms by release of antimicrobial effector molecules like reactive oxygen and nitrogen intermediates and prime the adaptive immune cells towards a Th-1 phenotype (Mantovani et al., 2004; Mills et al., 2000; Mosser and Edwards, 2008). Moreover, type I MFs are found to express high levels of MHC class I and class II antigens (Cassol et al., 2010; Martinez and Gordon, 2014; Mosser and Edwards, 2008). *In vitro* pro-inflammatory type I monocyte derived macrophages (MDM) can be generated by incubation of human blood derived monocytes in the presence of granulocyte-macrophage colony-stimulating factor (GM-CSF) (Mantovani et al., 2004; Verreck et al., 2004).

In contrast to inflammation, during the steady state, monocytes differentiate to “alternatively activated macrophages”, the anti-inflammatory type II MFs (Chapuis et al., 1997; Martinez et al., 2006; Smith et al., 1998). These type II MFs dampen the adaptive immune responses (Th2 response) by producing high levels of anti-inflammatory cytokines such as IL-10 and transforming growth factor beta (TGF-β) and low levels of IL-12 (Verreck

et al., 2004, 2006). Type II MFs exhibit a wide stretched morphology with a spindle-like shape. In contrast to type I MFs, the type II MFs are known to possess a higher phagocytic capacity (Neu et al., 2013; Zizzo et al., 2012). Furthermore, type II MFs lack microbicidal activity and show only a low antigen presentation (Ehrt et al., 2001; Savage et al., 2008). Because of their involvement in homeostatic processes and their ability to clear dead cells and cell debris without releasing inflammatory mediators as well as by expression of the scavenger receptor CD163 they are called general scavenger cells (Buechler et al., 2000; Kharkrang, 2010; Mosser, 2003; Savage et al., 2008). Upon uptake of apoptotic cells they retain their anti-inflammatory status by secretion of anti-inflammatory TGF beta (Ehrt et al., 2001; Savage et al., 2008; Xu et al., 2006, 2007). In addition to the involvement in phagocytosis of apoptotic cells the type II MF are also responsible for tissue remodeling, repair and wound healing, as well as for allergy and elimination of pathogens (Mantovani et al., 2004; Martinez et al., 2009). *In vitro* incubation of blood derived human monocytes with macrophage colony-stimulating factor (M-CSF) leads to the differentiation into anti-inflammatory hMDM type II (Goerdt and Orfanos, 1999; Goerdt et al., 1999; Mills et al., 2000; Smith et al., 1998; Verreck et al., 2004).

1.7 Hypotheses and Aims of this study

Chlamydiae are obligate intracellular bacteria which can infect a variety of different cells causing replicative or persistent infections. The trigger, which determines the development of a persistent infection phenotype in vivo, remains unknown. Initially chlamydiae infect the lung or genital epithelium. After replication they leave the epithelial cells in order to infect new cells, such as macrophages. How the chlamydiae are transferred from one cell to another is still unclear.

To address these specific questions we used different chlamydiae species and cell types in this thesis. In the first part we investigated chlamydial persistence focusing on *C. pneumoniae* infection in an epithelial cell model, using a HEp-2 cell line. In the second part, the focus was put on chlamydial transfer, in which we concentrated on infection with *C.trachomatis* or its transgenic variant eGFP-*C. trachomatis*. Furthermore, as host cells we exclusively used primary human monocyte derived macrophages (hMDM).

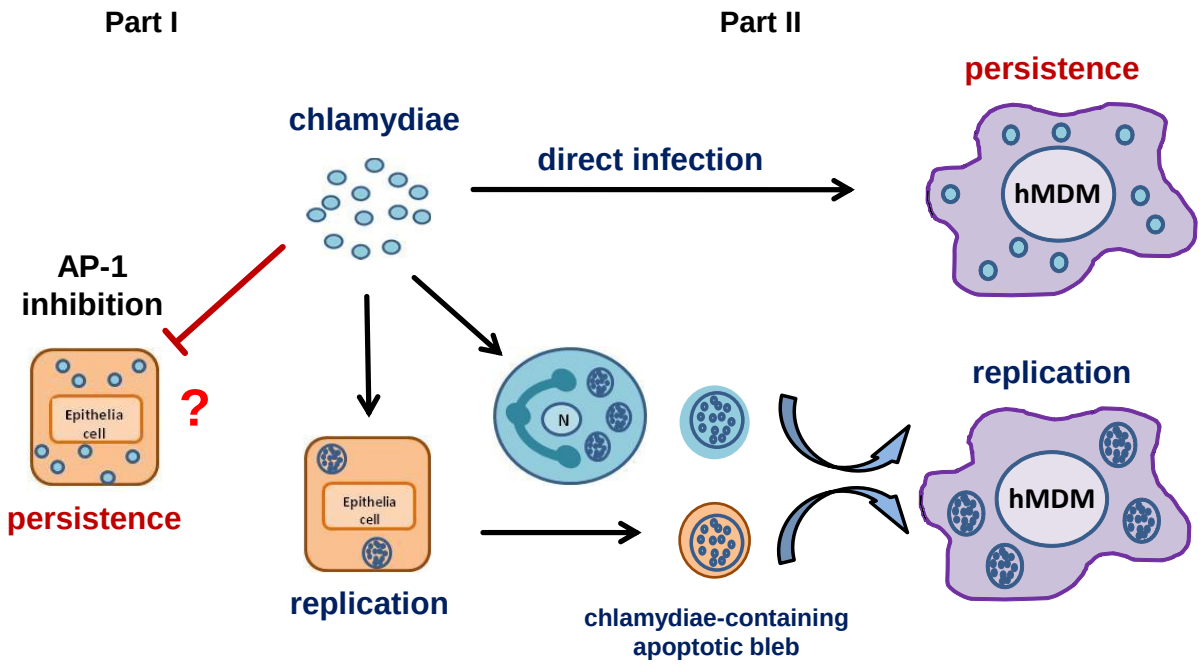

Figure 6: Hypotheses of this thesis. After infection chlamydiae usually replicate within their epithelial host cell, but they can also enter a persistent state. **A**) In part I of this thesis we focused on Hypothesis I: **Transcription factor AP-1 plays an important role in the induction of persistence in HEp-2 cells**. Direct infection of macrophages results in a persistent chlamydiae infection. In contrast, the uptake of apoptotic and infected cells or blebs leads to a replicative infection. **B**) In part II of the thesis we concentrated on Hypothesis II - **Chlamydiae hide inside apoptotic blebs to ensure a silent uptake without being visible for the innate immune system**.

Part I:

After infection chlamydiae usually replicate within their epithelial host cell. However, infection with *C. pneumoniae* is often associated with severe sequelae due to chronic and persistent infections. Why the chlamydiae enter a persistent state during the course of infection is still not completely clear. As obligate intracellular pathogens, chlamydiae efficiently manipulate host cell processes and pathways to ensure their intracellular development. The universal transcription factor AP-1 is involved in a number of these cellular processes and pathways and therefore a potential target for chlamydial manipulation (**Figure 6**).

We hypothesize that: "Transcription factor AP-1 is a key regulator of persistence during *C. pneumoniae* infection in HEp-2 cells"

To investigate this hypothesis, we have the following aims:

Aim 1: Investigate if AP-1 is regulated during *C. pneumoniae* infection by analyzing the protein and mRNA level of the AP-1 components c-Jun, c-Fos and ATF-2 using Western Blot analysis and qRT-PCR.

Aim 2: Establish a siRNA knockdown of AP-1 components c-Jun and c-Fos and assess its consequences on *C. pneumoniae* development using immunofluorescence microscopy, qRT-PCR and Western Blot analysis.

Aim 3: Analyze the requirement of AP-1 mediated transcription for chlamydial development by using an AP-1 specific inhibitor, Tanshinone IIA, and assess the inhibitory effect for infection by using immunofluorescence microscopy, qRT-PCR and Western Blot analysis.

Aim 4: Characterization of the infection phenotype (replicative vs. persistence) after Tanshinone IIA treatment and the underlying mechanism preceding this phenotype.

Part II:

In previous studies we observed that a direct infection of macrophages leads to a persistent infection phenotype, whereas the uptake of an apoptotic, chlamydiae-containing cell or bleb resulted in the formation of a productive infection (**Figure 6**). We suggest that the way of cell entry, e.g. direct infection or indirect infection via bleb transfer, is decisive for the outcome of infection. In chlamydiae research it is common to centrifuge the chlamydiae elementary bodies onto the host cells to achieve optimal infection. As this approach stands far from *in vivo* conditions, we decided to investigate the bleb macrophage interaction in a more physiological setting, using state of the art live cell microscopy.

We hypothesize that: "Chlamydiae hide inside apoptotic blebs to ensure a silent uptake without being visible for the innate immune system".

To investigate this hypothesis, we have the following aims:

Aim 5: Characterization of chlamydiae infection in pro-inflammatory hMDM I and anti-inflammatory hMDM II comparing their suitability as host cell for different chlamydiae species (*C. trachomatis* and *C. pneumoniae*).

Aim 6: Investigation of the importance of AP-1 for *C. trachomatis* development in hMDM I and hMDM II.

Aim 7: Visualization of the transfer of eGFP-*C. trachomatis*-containing apoptotic blebs to hMDM by using high speed live-cell imaging.

2 Material and Methods

2.1 Material

2.1.1 Chemicals and compounds

Chemical/compound	manufacturer
2-propanol	VWR, Bruchsal, GER
β-Mercaptoethanol	Sigma-Aldrich, Deisenhof, GER
Acrylamide / Bisacrylamide solution 30%	Serva Electrophoresis, Heidelberg, GER
Agarose, LE	Biozym Scientific GmbH, Oldendorf, GER
Ammonium chloride (0.15 M)	in-house facility, PEI, Langen GER
Ammoniumpersulfat (APS)	Serva Electrophoresis, Heidelberg, GER
Aqua bidest.	in-house facility, PEI, Langen, GER
ATP, 100 mM Solution	Fermentas, Thermo Scientific, Dreieich, GER
AZD-8055	Selleckchem, Houston, USA
Bovine Serum Albumin (BSA)	Sigma-Aldrich, Deisenhof, GER
CASYton	Roche Innovatis AG, Reutlingen, GER
Cycloheximide	Sigma-Aldrich, Deisenhof, GER
Diethyl pyrocarbonate (DEPC)	AppliChem, Darmstadt, GER
Developer G153 A+B	AGFA, Mortsel, BE
Dimethylsulfoxid (DMSO)	Sigma-Aldrich Chemie, Steinheim (GER)
dNTP-Mix (10 mM each)	NEB, Frankfurt am Main, GER
Dithiothreitol (DTT)	Sigma-Aldrich, Steinheim, GER
Dulbecco´s Modified Eagle Medium (DMEM)	Lonza, Basel, CH
ECL Western Blotting Detection Reagents	GE Healthcare, Buckinghamshire, UK
EDTA (Ethylenediaminetetraacetic acid)	in-house facility, PEI, Langen, GER
Ethanol (EtOH), absolute	VWR, Bruchsal, GER
Fetal Calf Serum (FCS)	Sigma-Aldrich, Deisenhof, GER
gentamycin	Sigma-Aldrich, Taufkirchen, GER
HEPES (1 M)	AppliChem, Darmstadt, GER in-house facility, PEI, Langen, GER
High-purity water	in-house facility, PEI, Langen, GER
Human recombinant Granulocyte Macrophage Colony Stimulating Factor (GM-CSF)	Bayer Healthcare Pharmaceutical, Leverkusen, GER
Human recombinant Macrophage Colony Stimulating Factor (M-CSF)	R&D Systems, Minneapolis, USA

Human Serum Type AB	Lonza, Walkersville, USA
Hydrochloric acid (HCl), 1 N	AppliChem GmbH, Darmstadt, GER
Hydrochloric acid	in-house facility, PEI, Langen, GER
Immersion oil (Immersol™ 518F)	Carl Zeiss, Jena, GER
L-glutamine	Biochrom AG, Berlin, GER
Lymphocyte Separation Medium (LSM) 1077	PAA, Pasching, AUT
Magnesiumchlorid ($MgCl_2$)	Merck, Darmstadt, GER
Methanol	Merck, Darmstadt, GER
Milk powder Sucofin	TSI GmbH & Co. KG, Zeven, GER
Natrium chloride (NaCl)	Sigma-Aldrich, Deisenhof, GER
Nuclease free water	Promega Corporation, Madison, USA
Paraformaldehyde (PFA)	Sigma-Aldrich, Deisenhof, GER
Penicillin/Streptomycin	Biochrom AG, Berlin, GER
Phosphate buffered saline (1x PBS) wo/ Ca2+, Mg2+; pH 7.1	in-house facility, PEI, Langen, GER
PI-103	Selleckchem, Houston, USA
Rapamycin	Selleckchem, Houston, USA
Rapid Fixer	AGFA, Mortsel, BE
RNase AWAY	VWR, Darmstadt, GER
RNase-free water	in-house facility, PEI, Langen, GER
Roswell Park Memorial Institute (RPMI) 1640 Medium	Sigma-Aldrich, Deisenhof, GER
Saponin from *Quillaja bark*	Sigma-Aldrich, Steinheim, GER
Sodium azide (NaN_3)	Sigma-Aldrich, Steinheim, GER
Sodium chloride (NaCl)	Merck, Darmstadt, GER
Sodium Dodecyl Sulfate (SDS)	Merck, Darmstadt, GER
Spautin-1	Sigma-Aldrich, Deisenhof, GER
Sucrose	Sigma-Aldrich, Deisenhof, GER
Tanshinone IIA	Sigma-Aldrich, Deisenhof, GER
TEMED	Serva, Heidelberg, GER
Tris(hydroxylmethyl)-aminomethan (Tris)	in-house facility, PEI, Langen, GER
Trypsin 250	in-house facility, PEI, Langen, GER
Tween 20	Sigma-Aldrich, Steinheim, GER
Western Blot Detection Substrate	GE Healthcare, Buckinghamshire, UK

2.1.2 Buffers and solutions

Buffer/solution	Composition
Ammoniumchloride solution	0.15 M Ammoniumchloride
	Aqua bidest.
Antibody - immunofluorescence application	
PFA fixation solution	4 %
Buffer A (washing)	PBS
	1 % FCS
	1 % BSA
	1 % Human serum
Buffer B (permeabilization)	PBS
	1 % FCS
	1 % BSA
	1 % Human serum
	0.5 % Saponin
	Sterile filtrated
Blocking solution	TBS/T + 5% milk powder (w/v)
WB Blotting buffer	50 mM Tris
	40 mM Glycin
	0.0375% SDS (w/v)
	2.5% Methanol (v/v)
	Aqua bidest.
DEPC-H_2O	0.1% DEPC
	Aqua bidest.
DNA loading dye (6x)	25 mM EDTA
	20% glycerol (v/v)
	0.025% bromphenol blue dye (w/v)
HEPES buffer (1M) pH 7.4	1M HEPES
	Aqua bidest.
	pH 7.4 adjust with NaOH

Laemmli-Buffer (6x)	500 mM Tris/HCl pH 6.8 38% Glycerol (v/v) 10% SDS (w/v) 600 mM DTT 0.01% bromphenol blue dye (w/ v) Aqua bidest.
PBS without Ca^{2+} and Mg^{2+} pH 7.1 (1x)	136.9 mM sodium chloride 2.68 mM kalium chloride 1.47 mM potassium dihydrogen orthophosphate 8.1 mM sodium dihydrogen phosphate Aqua bidest.
SDS-PAGE Running buffer (5x)	125 mM Tris 1.25 M Glycine 0.5% SDS (w/v) Aqua bidest.
Separating gel buffer pH 8.8 (4x)	1.5 M Tris-HCl pH 8.8 0.4% SDS (w/v) Aqua bidest.
SPG buffer	219,1 mM Sucrose/ Saccharose 17,39 mM Na_2HPO_4 2,6 mM $NaH_2PO_4xH_2O$ 4,89 mM glutamic acid pH 7.3 with NaOH, sterile filtered
Stacking gel buffer pH 6.8 (4x)	0.5 M Tris-HCl pH 6.8 0.4% SDS (w/v) Aqua bidest.
TBS buffer (10x)	50 mM Tris-HCl pH 7.4 150 mM NaCl Aqua bidest.

	pH 6.8 adjusted with HCl
TBS/T solution	1x TBS buffer 0.5% Tween 20 (v/v)
Tris-HCl (0.5 M) pH 6.8	460 mM Tris(hydroxymethyl)-aminomethan hydrochlorid 40 mM Tris(hydroxymethyl)-aminomethan Aqua bidest. pH 6.8 adjusted with 1 N HCl
Tris-HCl (1.5 M) pH 8.8	1.5 M Tris(hydroxymethyl)-aminomethan Aqua bidest. pH 8.8 adjusted with 25% HCl
Trypsin/EDTA solution	1x PBS without Ca^{2+} and Mg^{2+}pH 7.1 0.05% Trypsin 0.7 mM EDTA
Washing buffer	1x PBS without Ca^{2+} and Mg^{2+}pH 7.1 5% complete medium (v/v)

2.1.3 Media and supplements

Medium	**Composition**
Culture medium (HEp-2)	500 mL DMEM 10% FCS (v/v) 2 mM L-glutamine 33,2 mM HEPES 10 µg/mL Gentamycin
Infection medium (HEp-2)	500 mL DMEM 10% FCS (v/v) 2 mM L-glutamine 33,2 mM HEPES 10 µg/mL Gentamycin 1 µg/mL cycloheximide

Complete Medium (hMDM)	500 mL RPMI-1640 10% v/v FCS 2 mM L-glutamine 50 µM β-Mercaptoethanol 100 U/mL Penicillin 100 µg/mL Streptomycin 10 mM HEPES buffer
Infection medium (hMDM)	500 mL RPMI-1640 10% v/v FCS 2 mM L-glutamine 50 µM β-Mercaptoethanol 10 mM HEPES buffer 10 µg/mL Gentamycin

2.1.4 Chlamydiae organisms

Chlamydia pneumoniae	ATCC-Nr. VR-1310™
Chlamydia trachomatis	Serovar L2 (kindly provided by Jan Rupp)
eGFP-*Chlamydia trachomatis*	kindly provided by Thomas Rudel in cooperation with Ian Clarke

2.1.5 Primary cells and cell lines

Human primary cells
Human peripheral blood mononuclear cells (PBMCs) were obtained from buffy coats of healthy donors from the DRK-Blutspendedienst in Frankfurt/Main. Subsequently, cells were isolated as described in 2.2.1.6

Cell lines	
HEp-2	human epithelial cells derived from a larynx carcinoma ATCC CCL-23

2.1.6 Ready-to-use kits and enzymes

kit	Manufacturer
Amersham ™ ECL ™ Western Blotting Analysis System	GE Healthcare, Buckinghamshire, UK
PhosphoWorks™ Luminometric ATP Assay Kit	Biomol, Hamburg, GER
IMAGEN™ Chlamydia Kit	Oxoid, Wesel (GER)
ImPromII™ Reverse Transcription System	Promega, Mannheim, GER
MESA Blue qPCR MasterMix Plus for SYBR Assay No Rox	Eurogentec, Colone, GER
RNeasy Plus Mini Kit	Qiagen, Hilden, GER
Stemfect™ RNA Transfection Kit	Stemgent, San Diego, USA
Venor®GeM-OneStep-mycoplasma Detection Kit	Minerva Biolabs, Berlin, GER

Enzyme	Manufacturer
Recombinant RNasin® Ribonuclease Inhibitor (20-40 U/µL)	Promega, Mannheim, GER
Taq-polymerase (5U/µL)	NEB, Frankfurt am Main, GER

2.1.7 Oligonucleotides

All primers were obtained from Eurofins MWG Operon (Ebersberg, GER) with HPSF purified grade and a synthesis scale of 0.01 µmol.

Primer	5´-3´ sequence
C. pneumoniae 16S rRNA fwd	TCG CCT GGG AAT AAG AGA GA
C. pneumoniae 16S rRNA rev	AATGCTGACTTGGGGTTGAG
C. trachomatis 16S rRNA fwd	CGG TAA TAC GGA GGG TGC TA
C. trachomatis 16S rRNA rev	CTA CGC ATT TCA CCG CTA CA
cHsp60 fwd	AGGACGTCACGTAGTTATAGATAA
cHsp60 rev	AGTTTTGCTGGCGACTTCT
c-Jun fwd	ATCGACATGGAGTCCCAG
c-Jun rev	CGATTCTCTCCAGCTTCC
c-Fos fwd	AACCTGTCAAGAGCATCAGC
c-Fos rev	CCCAGTCTGCTGCATAGAAG

GAPDH fwd	GAG TCA ACG GAT TTG GTC GT
GAPDH rev	TTG ATT TTG GAG GGA TCT CG
glut-1 fwd	GGT TGT GCC ATA CTC ATG ACC
glut-1 rev	CAG ATA GGA CAT CCA GGG TAG C
MOMP fwd	GCCACAGCATTGTCTACTACTGAT
MOMP rev	AATCTGAACTGACCAGATACGTGA

siRNAs	**Manufacturer**
AllStars Negative Control siRNA SI03650318	Qiagen, Hilden, GER
JUN siRNA SI00034664	Qiagen, Hilden, GER
JUN siRNA SI00034671	Qiagen, Hilden, GER
JUN siRNA SI00034678	Qiagen, Hilden, GER
JUN siRNA SI00300580	Qiagen, Hilden, GER
FOS siRNA SI00074543	Qiagen, Hilden, GER
FOS siRNA SI00074564	Qiagen, Hilden, GER
FOS siRNA SI02781429	Qiagen, Hilden, GER
FOS siRNA SI02781464	Qiagen, Hilden, GER

2.1.8 Dyes and markers

Dye	**Manufacturer**
AnnexinV Fluos 586	Invitrogen Molecular Probes, Eugene, USA
Bromphenol blue dye	Serva, Heidelberg, GER
DAPI (5 µg/mL)	Molecular Probes, California, USA
Ethidium bromide solution (1% in water)	Merck, Darmstadt, GER
Cell Mask™ Deep Red Plasma membrane stain C10046	Invitrogen Molecular Probes, Eugene, USA
Trypan Blue staining solution	Lonza, Basel, CH

Marker	**Manufacturer**
1 kb DNA ladder	NEB, Frankfurt am Main, GER
100 bp DNA ladder	NEB, Frankfurt am Main, GER
Full-Range Rainbow Molecular Weight Marker	GE Healthcare, Buchinghamshire, UK
PageRuler Prestained Protein Ladder	Fermentas, Thermo Scientific, Dreieich, GER

2.1.9 Antibodies

All primary Western Blot (WB) antibodies were diluted in TBST/5% BSA + 0.01% NaN_3 and were incubated overnight. Secondary HRP-coupled Western Blot antibodies were diluted in 5% milk powder/TBST for 1h at RT. Immunofluorescence antibodies (IF) were diluted in PBS + 0.5% saponin/1% BSA/1% FCS/1% human serum (Buffer B).

Primary Antibodies	**Use**
α-c-Jun, rabbit monoclonal, Cell Signaling (60A8)	WB 1:1000 IF 1:50
α-phospho-c-Jun, rabbit monoclonal, Cell Signaling (D47G9)	WB 1:1000
α-c-Fos, rabbit monoclonal, Cell Signaling (9F6)	WB 1:1000
α-phospho-c-Fos, rabbit monoclonal, Cell Signaling (D82C12)	WB 1:1000
α-ATF-2, rabbit monoclonal, Cell Signaling (20F1)	WB 1:1000
α-phospho-ATF-2, rabbit monoclonal, Cell Signaling (11G2)	WB 1:1000
α-MOMP, mouse monoclonal, hybridoma supernatant, generated and kindly provided by G. Zhong, partly described in (Wolf et al., 2001)	WB 1:25
α-chlamydial Hsp60, mouse monoclonal, hybridoma supernatant, generated and kindly provided by G. Zhong	WB 1:500
α-β-actin, mouse monoclonal, Sigma (AC-15)	WB 1:1000
α-LC3B, rabbit polyclonal, Cell Signaling (2775)	WB 1:1000
α-SQSTM1/p62, mouse monoclonal, Santa Cruz Biotechnology (sc-28359)	WB 1:100
Isotype controls	
Rabbit serum isotype control, Roland Plesker, PEI, 5-10 mg/mL	IF 1:10
Secondary antibodies	
goat α-rabbit IgG AF568 conjugated, Invitrogen (A-11036)	IF 1:100
goat α-rabbit IgG HRP conjugated, Santa Cruz Biotechnology (sc-2004)	WB 1:1000 - 5000
goat α-mouse IgG HRP conjugated, Santa Cruz Biotechnology (sc-2005)	WB 1:1000 - 20000

2.1.10 Laboratory supplies

Consumable	Manufacturer
CASY cups	Roche Innovatis AG, Reutlingen, GER
Cell culture flasks with filter (25 cm^2 and 75 cm^2)	Greiner Bio-One, Kremsmünster, AT BD labware Europe, Le Pont de Claix, FRA
Cell culture petri dish (10 cm diameter)	BD labware Europe, Le Pont de Claix, FRA
Cell culture plates (6-well, 24-well)	Sarstedt, Nümbrecht, GER
Cell Scraper, 16 cm	Sarstedt, Nümbrecht, GER
Centrifuge tubes (0.2 mL)	PE Applied Biosystems, Norwalk, USA
Reaction tubes (1.5 mL, 2.0 mL)	Eppendorf, Hamburg, GER
Centrifuge tubes PCR Tube Multiply® Pro (0.5 mL)	Sarstedt, Nümbrecht, GER
Chamber slide™, 12-well, ibidi-treat	ibidi GmbH, Planegg / Martinsried, GER
Chamber slide™ 8 well	Thermo Scientific, Bonn, GER
Cover Slide (24x50 mm)	VWR, Darmstadt, GER
Cryogenic vial, internal thread (2 mL)	Greiner Bio-One GmbH, Frickenhausen, GER
Cryogenic vial, external thread (1 mL)	Nunc, Thermo Scientific, Dreieich, GER
ECL films (Hyperfilm™ ECL)	GE Healthcare, Buckinghamshire, UK
Falcons (15 mL, 50 mL)	BD labware Europe, Le Pont de Claix, FRA
glass beads	Glaswarenfabrik Karl Hecht, Sondheim, GER
Ibidi µM dish	ibidi GmbH, Planegg / Martinsried, GER
Light Cycler 96-well plates with foil, white	Roche Applied Science, Darmstadt, GER
Nalgene™ Mr. Frosty Freezing Container	Thermo Scientific, Dreieich, GER
Nitril gloves	Ansell Healthcare, Brussels, BE
Nitrocellulosemembrane (Hybond ECL blot membrane)	GE Healthcare, Buchinghamshire, UK
Neubauer improved cell counting chamber (depth 0.1 mm)	VWR, Darmstadt, GER
white Nunclon™ Surface plates	Fisher Scientific, Schwerte, GER
Oak-Ridge Centrifuge tubes	Fisher Scientific, Schwerte, GER
Paseur pipette, plastic	Sarstedt, Nümbrecht, GER

Pipette controller (accu-jet® pro)	BRAND, Wertheim, GER
Pipette filter tips (1-10 µL; 10-200 µL, 100-1000 µL)	Nerbe plus, Winsen/Luhe, GER
Pipettes (Research® plus: 0.5-10 µL; 10-100 µL, 20-200 µL, 100-1000 µL)	Eppendorf, Hamburg, GER
Pipette tips (0.5-10 µL; 2-200 µL; 50-1000 µL)	Eppendorf, Hamburg, GER
Cover glasses, round, 0,18 mm	VWR, Darmstadt, GER
Serological pipettes, sterile (5 mL; 10 mL; 25 mL)	Greiner Bio-One, Kremsmünster, AT
Sterile filter (0.22 µm, 0.45 µm)	VWR, Darmstadt, GER
Syringe (20 mL, 50 mL)	BD labware Europe, Le Pont de Claix, FRA
Whatman paper gel blotting	VWR, Darmstadt, GER

2.1.11 Instruments

Device	**Manufacturer**
Centrifuges	
Beckman J6-HC + JA-14	Beckman Coulter, Krefeld, GER
BIOLiner Buckets (75003670; 7500368)	Thermo Scientific, Dreieich, GER
Bench top centrifuges 5430 and 5430R	Eppendorf, Hamburg, GER
Heraeus Megafuge 40R	Thermo Scientific, Dreieich, GER
Sprout Mini-Centrifuge	Biozym, Hamburg, GER
Electrophoresis and Blotting	
Development machine Curix 60	AGFA, Mortsel, BE
Horizontal electrophoresis equipment	Biotec-Fischer, Reiskirchen, GER
Mini-PROTEAN® Tetra Cell	Bio-Rad, München, GER
Power Supply “PowerPac™ 200/2.0”	Bio-Rad, München, GER
Semi-Dry Transfer Unit TE 77 PWR	Amersham Biosciences, Freiburg, GER
UV-Transilluminator GenoView	VWR International, Darmstadt, GER
Imaging	All Carl Zeiss, Jena, GER
Microscope Primo Star	
Microscope Axio Vert.A1	
Microscope Observer Z.1	equipped with an ApoTome, an AxioCam

	MRM, an illuminator HXP120C, reflectors DIC TL, 38 HE GFP, 43 HE DsRed, 49 DAPI, 50 Cy5, 64 HE mPlum, objectives LD Achro Pln 20x/0.4 Ph2 DICIII, LD Achro Plan 40x/0.6 Ph2, Pln Apo 20x/0.8 DICII, PlnN 10x/0.3 Ph1 DICI, EC PlnN 40x/1.3 Oil DICIII, Pln Apo 63x/1.4 Oil DICIII
Microscope LSM7 *Live* Observer Z.1	equipped with a line scanner; four laser lines (405 nm, 488 nm, 561 nm and 635 nm), an AxioCam MRM, an illuminator HXP120C, a piezo z-controller 24V80CAP (piezo system jena), an incubation chamber (PECON), reflectors Pol TL, 26 AF660, 38 HE GFP, 43 DsRed, 49 DAPI, objectives Pln Apo 63x/1.4 Oil DICIII, Pln Apo 40x/0.95 DICIII
EM 109 transmission electron microscope	Zeiss, Jena, GER

Incubators

CO_2-Incubator Forma Series II Water Jacket	Thermo Scientific, Marietta, USA
Heracell 240i CO_2 Incubator	Thermo Scientific, Marietta, USA

Lamina air flow

Workbench MSC-Advantage	Thermo Scientific, Dreieich, GER
Steril Gard III Advance	The Baker Company, Sanford, USA
Steril Gard Hood	The Baker Company, Sanford, USA

PCR Thermo Cycler

LightCycler® 480 System	Roche Applied Science, Mannheim, GER
Personal Cycler	Biometra, Göttingen, GER
S1000™ Thermal Cycler	Bio-Rad, München, GER

Others

Autoclave Systec vx-150	Systec, Wettenberg, GER
Analytical balance KB BA 100	Sartorius, Göttingen, GER
CASY Modell TT	Roche Innovatis AG, Reutlingen, GER
Ice machine AF 1000	Scotsman, Pogliano Milanese, IT
Freezer (-20°C)	Bosch, Stuttgart, GER
Freezer U725-G (-80°C)	New Brunswick, Eppendorf, Hamburg, GER
Nalgene™ Mr. Frosty Freezing Container	Thermo Scientific, Dreieich (DE)

Nitrogen container “Chronos”	Messer, Bad Soden, GER
Magnetic stirrer IKA® C-MAG HS7	IKA®-Werke, Staufen (DE)
Microwave	Bosch, Gerlingen, GER
pH Meter PB-11	Sartorius, Göttingen, GER
Refrigerator	Bosch, Stuttgart, GER
Tecan Infinite M200PRO microplate reader	Tecan, Crailsheim, GER
Thermomixer comfort (1.5 mL)	Eppendorf, Hamburg, GER
Thermomixer 5437 (1.5 ml)	Eppendorf, Hamburg (DE)
UV-Vis Spectrophotometer NanoDrop 2000c	PeqLab, Erlangen, GER
Vortex mixer VV3	VWR International, Darmstadt, GER
Water bath	Köttermann VWR International, Darmstadt, GER

2.1.12 Software

Software	Manufacturer
Axio Vision Rel. 4.8	Carl Zeiss, Jena, GER
GraphPad Prism 6	GraphPad Software, Inc., La Jolla, USA
ImageJ and FiJi	Open Source
Light Cycler software LC480 (v1.5.0 SP4)	Roche Applied Science, Mannheim, GER
Mendeley Desktop	Mendeley Ltd., London, UK
Microsoft® Office 2010	Microsoft, Redmont, US
Zen 2012 (blue edition, black edition)	Carl Zeiss, Jena, GER

2.2 Methods

Cell culture work and infection experiments were performed under sterile conditions in a laminar air flow workbench under endotoxin free conditions. Human cells (HEp-2 and hMDM) were cultivated in humidified incubators at 37°C and 5% CO_2.

2.2.1 Cell culture

For experiments the adherent human epithelial (HEp-2) cell line was grown in 75 cm^2 culture flasks in culture medium, Dulbecco's Modified Eagle's Medium (DMEM) supplemented with 10% fetal calf serum (FCS), 2 mM L-glutamine, 33 mM HEPES and gentamicin 10 µg/mL. Cells were passaged every 3 - 4 days, when they had reached a confluence of 70 - 90%. Therefore the medium was discarded and cells were washed with 10 mL prewarmed PBS, to remove the dead cells and medium leftovers and after that proteolytically detached through incubation with 2 mL of trypsin-EDTA (ethylenediaminetetraacetic acid) for 5 min at 37°C with 5% CO_2. Afterwards 8 mL of warm culture medium was used to stop the reaction and to dilute the cells. The cells were then centrifuged at 1024 xg for 5 min at room temperature (RT). The pellet was resuspended in 10 mL of fresh medium. Subsequently the cells were counted using a hemocytometer (see 2.2.1.3) and then seeded for experiments or transferred to a new culture flask with fresh medium for further cultivation.

2.2.1.1 Long-time storage of HEp-2 cells

Prior to long-time storage the cells were tested for *Mycoplasma* contamination with PCR using a VenorGeM kit (Minerva Biolabs) according to the manufacturer´s instructions. The HEp-2 cells were harvested and counted as described (see 2.2.1 and 2.2.1.3). After centrifugation at 1024 xg for 5 min at RT the cells were resuspended in DMEM containing 20% FCS and 10% DMSO to a concentration of $2.5x10^6$ cells per 0.5 mL medium. The cells were then transferred to cryo tubes and pre-cooled in a Mr. Frosty freezing container at -80°C over night. The next day the tubes were transferred to a liquid nitrogen tank.

2.2.1.2 Thawing of HEP-2 cells

For thawing a cryo tube was taken out of the liquid nitrogen tank and warmed at 37°C in a water bath. The cells were then transferred drop wise to 10 mL pre-warmed culture medium. To remove the DMSO the cells were centrifuged at 1024xg for 5 min at RT and the pellet

was afterwards resuspended in fresh culture medium and transferred to a culture flask for further incubation.

2.2.1.3 Cell counting with using a hemocytometer

HEp-2 cells were counted using a neubauer improved counting chamber with a depth of 0.1 mm. To distinguish between live and dead cells, the cell suspension was mixed with trypan blue, which stains the dead cells blue, in a ratio of 1:1. Then 10 µL of the stained cell suspension was added to the neubauer chamber. Afterwards at least 3 of the 4 big squares (each contains of 16 small squares) were counted. Concentration of cells per mL was calculated by the following formula:

$$\text{cells/mL} = \frac{\text{amount of the counted cells x dilution factor x chamber factor } (x10^4)}{\text{amount of counted big squares}}$$

2.2.1.4 Inhibitor treatment

Tanshinone IIA (Sigma) was resuspended in DMSO and used parallel to infection with a final concentration of 25 µM.

2.2.1.5 Autophagy modulation

For autophagy modulation the HEp-2 cells were treated with different compounds. For autophagy inhibition spautin-1 and for induction of autophagy rapamycin, AZD-8055 or PI-103 was used. The compounds were added in different concentrations (0.5, 1, 2, 5 or 10 µM) for 30 min or 2 h. In addition to the autophagy modulators a control comprising cells without any treatment was used. As the infection medium is supplemented with cyclohexemide (C_x, 1 µg/mL) also a C_x control was used. After treatment the supernatant was removed and the cells were centrifuged at 1024 xg for 5 min at RT. Next, they were resuspended and lysed in 1x Laemmli buffer for Western blot analysis (see 2.2.3.1).

2.2.1.6 Isolation of human peripheral blood mononuclear cells (PBMC)

Peripheral blood mononuclear cells (PBMCs) were isolated from buffy coats of healthy donors. 30-50 mL of blood containing the concentrated immune cells was diluted with prewarmed sterile PBS to a final volume of 100 mL. Subsequently 25 mL of diluted blood was layered on 15 ml of prewarmed LSM gradient medium (leukocyte separation medium 1077) in 50 mL tubes and centrifuged at 545 x g for 30 min (20°C) with acceleration and deceleration set at a minimum level. After centrifugation, the blood cells were separated

generating a density gradient and the interphase containing the PBMCs was collected. For removal of remaining LSM, cell debris and small cells like erythrocytes and thrombocytes the PBMCs were distributed into 6 new tubes and subsequently washed with prewarmed washing buffer (PBS without Ca^{2+} and Mg^{2+}+ 5% complete medium) through centrifugation first at 1024 xg, then at 545 xg and finally at 135 xg for 8 min at RT. After each centrifugation step the pellet was resuspended in fresh prewarmed washing buffer. In the last washing step the pellets were pooled into 4 tubes and the washing was repeated until the supernatant was clear. For lysis of residual erythrocytes, the PBMCs were resuspended in 10 mL 0.15 M cold ammonium chloride solution and incubated for 10-15 min at RT. Afterwards the cells were again washed (washing buffer; 135 xg, 8 min), pooled in one tube and the cell number was determined by automatically counting using a CASY cell counter. Subsequently isolation of monocytes was achieved by plastic adherence.

2.2.1.7 Generation of hMDMs by plastic adherence and harvesting of differentiated hMDMs

For monocyte isolation by plastic adherence $40x10^6$/5 mL freshly isolated PBMCs were seeded in a 25 cm^2 culture flask. Cells were incubated in complete medium in the presence of 1% human serum at 37°C and 5% CO_2 for 90 min to allow the monocytes to adhere to the plastic. The supernatant containing the non-adherent cells, mainly lymphocytes, residual erythrocytes and thrombocytes, was discarded by gently washing the flasks two times with prewarmed washing buffer.

For generation of human monocyte derived macrophages (hMDM), the adherent monocytes were cultured in complete medium supplemented with the growth factors GM-CSF (10 ng/mL) for generation of pro-inflammatory macrophages (hMDM type I) or with M-CSF (30 ng/mL) to differentiate monocytes to anti-inflammatory macrophages (hMDM type II). After differentiation for 5 - 7 days at 37°C with 5% CO_2 the hMDMs were harvested. To detach the hMDMs from the plastic the culture flasks were put on ice for 15 - 30 min and afterwards the cells were harvested with a cell scraper. Each culture flask was washed with 3-4 mL cold washing buffer which was added to the cells in a 50 mL tube. Finally the number of hMDMs was counted using a CASY cell counter.

2.2.2 Chlamydiae infections

2.2.2.1 Chlamydiae organisms

Chlamydia pneumoniae (CWL strain 029 (ATCC® VR-1310™), *Chlamydia trachomatis* L2 (kindly provided by Jan Rupp) and eGFP-*Chlamydia trachomatis* L2 (kindly provided by

Thomas Rudel in cooperation with Ian Clarke) were propagated in HEp-2 cells as described previously (Gieffers et al., 2004).

2.2.2.2 Inactivation of *C. pneumoniae*

For heat inactivation a defined amount of *C. pneumoniae* was diluted in 1 or 2 mL of infection medium in reaction tubes. The tubes were then heated at 95°C for 30 min. The heat killed chlamydiae were stored in aliquots at -80°C. For infection experiments the heat killed chlamydiae were handled as the viable chlamydiae.

2.2.2.3 Infection procedure

Cells were seeded 24 hours prior to infection. Directly before infection of HEp-2 cells the medium was removed and prewarmed infection medium (culture medium + C_x 1 µg/mL) was added. For infection of hMDMs the cells were transferred into complete medium without penicillin-streptomycin but containing gentamycin (10 µg/mL) at least 24 hours before infection. Chlamydiae were thawed and vortexed. For infection chlamydiae were added to the cells in different infection doses (1, 10, 15, 25 or 30 IFU per cell) and then centrifuged onto the cells with 896 xg for 1 h and at 37°C with acceleration and deceleration set at a minimum level. Centrifugation was followed by incubation at 37°C and 5% CO_2 until the desired time points were reached. As control cells without infection were used for each time point.

2.2.2.4 Preparation of chlamydiae stock solutions

For generation of chlamydiae stock solutions HEp-2 cells were seeded in a maximum of 8 6-well plates 24 h prior to infection with a density of 1.25 x 10^6 cells per well. Cells were infected with 10 - 15 IFU per cell as described above (see 2.2.2.3). Infected cells were harvested 42 - 45 h post *C. trachomatis* and 64 - 67 h post *C. pneumoniae* infection. The cells were harvested in the medium using a cell scraper. The cells and the medium were transferred in 50 mL tubes containing sterile glass beads. For chlamydial release each tube was vortexed for 10 min. Cellular debris was pelleted by centrifugation for at least two times by 1024 xg for 5 min at 4°C. This was followed by high speed centrifugation at 30100 xg for 90 min at 4°C to pellet the chlamydiae. The supernatant was removed and the chlamydial pellet was strongly resuspended in 1 – 2 mL cold SPG buffer (sucrose-phosphate-glutamate buffer, ph 7.3). Small aliquots of the chlamydiae stock solution were stored at -80°C. After at least 24 h of storage the infectious titer was determined. For each infection, a fresh aliquot of chlamydiae was thawed.

2.2.2.5 Determination of infectious stock solution titer

HEp-2 cells with a density of 0.3 x 10^5 cells per well were seeded 24 hours before infection in a 24-well plate with glass cover slips in each well. For infection the medium was removed and 1 mL prewarmed infection medium was added to each well. Different serial dilutions (1:5 or 1:10 in infection medium) of the 1:50 pre-diluted chlamydiae stock solution were used for infection as described above (see 2.2.2.3). After 30 h post *C. trachomatis* and 48 h post *C. pneumoniae* infection the medium was removed and the cells were methanol fixed for 10 min at RT. After removal of the methanol the cells were stained using an IMAGEN^{TM} Chlamydia kit (see 2.2.5.1). The developed inclusions of 10 microscopic fields of view were counted using a Zeiss Observer with a 20x oil-immersion for *C. trachomatis* and a 40x oil-immersion for *C. pneumoniae*. The counting was performed in the appropriate dilution with 10 - 20 inclusions per field of view. Each inclusion represented one *inclusion forming unit* (IFU). The total number of IFUs per mL was calculated with the following formula:

$$\text{IFUs/mL} = \frac{\text{amount of counted inclusions x diameter of one well (200 mm}^2\text{)}}{\text{amount of counted fields of view x used volume of chlamydiae x diameter field of view}}$$

The diameter of a field of view for 20x oil-immersion is 0,557 mm^2 and 0,139 mm^2 for 40x oil-immersion. The diameter of one well from a 24-well plate was taken into account with 200 mm^2. At the end the calculated number had to be multiplied with the dilution factor (x50), as the stock solution was pre-diluted.

2.2.2.6 Chlamydial recovery

Chlamydial recovery assays are used to determine the amount of infectious chlamydiae after a full developmental cycle in order to compare the bacterial development under different conditions, for example chemical treatment or knockdown of host cell gene products. The amount of newly produced infectious elementary bodies is assessed by titration experiments as described (Beatty et al., 1993). Therefore, cells (HEp-2 or hMDM) were seeded in 6-well plates 24 h prior to infection and subsequently treated as desired or left untreated. After infection with chlamydiae in infection medium for 45 h – 48 h (*C. trachomatis*) or 65 h - 72 h (*C. pneumoniae*) the cells were harvested with a cell scraper and the supernatant was transferred into tubes containing glass beads. For chlamydial release each tube was vortexed for 5 min, followed by several centrifugation steps (1024 xg, 5 min, RT) to remove cellular debris. The chlamydiae-containing supernatant was then used for re-infection. Thereby, the lysates were diluted serially and titrated onto fresh HEp-2 cells. 0.3 x10^5 cells per well were seeded 24 h prior to infection in either a 24-well plate with glass cover slips in

each well or in chamber slides. After centrifugation (only possible with 24-well plate) and species-specific time of incubation, the cells were methanol fixed and stained as described before (see 2.2.5.1), followed by quantification of the inclusion amounts. The quantity of newly developed EBs was determined by comparing the number of inclusions of treated against those of untreated infected cells.

2.2.3 Protein techniques

2.2.3.1 SDS-PAGE and Western Blot analysis

Sample preparation

For generation of Western Blot samples cells were pelleted and lysed by resuspending in 1x Laemmli buffer ($1x10^5$ cells/ 100 µL). The samples were strongly vortexed and stored at -20°C. Before using in Western Blot analysis the samples were heated at 95°C for 5 – 10 min followed by vortexing.

SDS-PAGE (Sodium **D**odecyl **S**ulfate **– P**oly **A**crylamide **G**el **E**lectrophoresis**)**

The expression of host cell and chlamydial proteins was analyzed by SDS-PAGE and immunoblotting. SDS-PAGE is a standard method to analyze denatured proteins which are separated according to their electrophoretic mobility depending on their molecular weight. The proteins are first collected in a stacking gel (~ 4%) and then separated in a separation gel which differs in its pH conditions to improve the sharpness. 12% or 15% separation gels were prepared following a standard protocol (see 2.1.2). In each gel lane 20 µL of sample was loaded. Besides, one lane was loaded with a prestained marker ladder as size reference and empty lanes were filled with 1x Laemmli buffer. Proteins were electrophoretically separated in a Mini-PROTEAN® Tetra cell (Bio-Rad) in 1x SDS running-buffer (see 2.1.2) at constant 80 Volt for protein passage through the stacking gel. When the samples reached the separating gel the voltage was increased to 100 V and the gel was stopped when the bromophenol blue line approached the bottom line of the gel. SDS-PAGE gels were then used for Western Blot.

Western Blot and band detection

For immunoblotting the separated proteins were transferred on a nitrocellulose membrane using a semi-dry blot system and Western Blot blotting buffer (see 2.1.2) at a constant 1.5 mA/cm^2 for 60 min. After blotting the membranes were shortly washed in tris buffered saline supplemented with tween (TBST) and subsequently incubated in TBST + 5 % skimmed milk for 1 h at RT by gentle agitation on a shake table. This is required

in order to prevent unspecific binding of the antibody during the following incubation steps. Before incubation with the primary antibody milk leftovers were removed by a washing step in TBST. The membrane was then exposed to the primary antibody at 4°C overnight with gentle shaking. Primary antibodies are listed above (see 2.1.9). Equal loading and blotting efficiency were verified by the use of antibody against a housekeeping gene of eukaryotic cells. After overnight incubation the membranes were washed 3 times for 10 min in TBST followed by incubation with a species specific horseradish peroxidase (HRP)-coupled secondary antibody for 1 h at RT with gentle shaking (see 2.1.9). After additional 3 washing steps for 10 min at RT, protein bands were visualized using enhanced chemiluminescence (ECL) substrate according to the manufacturer´s protocol. Turnover of the substrate by the horseradish peroxidase leads to generation of chemiluminescence which can be detected by exposure of high performance ECL films to the membrane in the dark. The films were developed in an Agfa Citrix 60 developer and scanned on a Hewlett Packard Scanjet G4050 flatbed scanner for digitalization. For subsequent antigen detection the membrane was again blocked and prepared as described above. Protein amounts were quantified by densitometry using ImageJ software.

2.2.4 ATP assay

For ATP measurement PhosphoWorks™ Luminometric ATP Assay Kit was used following the manufacturer's instructions. Cells were seeded 24 hours before infection and treatment in white Nunclon™ Surface plates. Cells were infected with 10 and 30 IFUs and treated with (w/) or without (w/o) Tanshinone IIA as described above. As control uninfected and untreated cells were used. Directly after infection and treatment (0 hpi), 6 and 12 hours post infection ATP amounts were measured. For ATP measurement 50 µL medium per well were removed. To the remaining 50 µL medium within the well 50 µL of ATP solution was added. ATP solution was prepared according to the manufacturer's protocol and stored in aliquots to avoid repeated thawing. Every step involving the ATP Assay Kit or its compounds was performed in the dark, as the procedure is light sensitive. After adding the ATP solution, the plate was wrapped up in aluminium foil and incubated for 15 min at RT. The developing bioluminescence was then measured with a Tecan Infinite M200PRO microplate reader.

2.2.5 Microscopic techniques

2.2.5.1 Immunofluorescence analysis

For different analyses such as determination of the infection rate, infectious titer, the chlamydial recovery or inclusion morphology 0.25 x10^5 cells per well were seeded 24 hours prior to infection in either chamber slides or 24-well plates with a glass cover slips in each well. Cells were infected as described and fixed with methanol after the desired infection time. After removal of the methanol the cells were air dried and stained. For immunofluorescence staining IMAGEN^{TM} Chlamydia kit was used, containing an FITC-labeled monoclonal antibody against chlamydia-LPS and a red staining for cytoplasm. Before usage, 1 mL PBS was added to the staining solution. For each well 15 µL staining solution was mixed with 10 µL PBS. Cells were counterstained with 0.5 µL DAPI per well to visualize nuclei and chlamydial DNA. The mixed staining solution was added to the cells and was incubated for 20 min at 37°C with 5% CO_2. To avoid the staining solution to dry on the cells, the surrounding of wells was kept wet with PBS. After incubation the wells were washed at least twice with PBS and afterwards air dried. The glass cover slips were put on a microscope slide in a drop of mountain fluid with the cell side downwards. The incubation chambers of the chamber slides were removed and some drops of mountain fluid were added before a glass cover slip was put onto the chamber slide. The slides were analyzed using a Zeiss Observer with a 20x or 40x oil-immersion and a Zeiss LSM7 Live with a 63x oil-immersion. Quantification of infection was assessed by counting at least 300 cells randomly. Inclusion size was measured using ImageJ analysis. Briefly, a threshold algorithm was run over FITC/DAPI images following area measurement of the inclusions. The slides were stored at 4°C in the dark and could be used several weeks.

2.2.5.2 Immunofluorescence staining of c-Jun protein in hMDMs

Expression of c-Jun protein in infected and uninfected hMDM was assessed by indirect antibody staining. Therefore, 0.3 x10^5 hMDM per well were seeded in a chamber slide. After infection or incubation for the desired time the medium was removed and the cells were fixed with 100 µL 4% paraformaldehyde (PFA) for 10 min on ice. Subsequently, cells were washed with 100 µL buffer A (PBS + 1% BSA, 1% FCS, 1% human serum) and permeabilized using 100 µL of a saponin containing buffer B (PBS + 0.5% saponin, 1% BSA, 1% FCS, 1% human serum). The primary antibody c-Jun and the isotype control (see 2.1.9) were diluted in 100 µL buffer B, added to the cells and incubated for 30 min on ice in the dark. Washing with buffer B removed unbound antibody and was followed by incubation with a secondary fluorochrome-conjugated antibody for 30 min on ice in the dark. Additionally, the cells were

counterstained with DAPI. Afterwards the cells were again washed with 100 µL buffer and subsequently with 100 µL buffer A. The incubation chamber was removed and the slide was air dried. The slide was then mounted in ProLong® Gold Antifade Reagent to suppress photobleaching and preserve the signals of target molecules and the cover slip was sealed with nail polish. The slides were then analyzed with a Zeiss Observer. For storage the slides were put in the dark at 4°C.

2.2.5.3 Live cell imaging

To investigate dynamic infection processes, such as chlamydial transfer, in a physiological surrounding live cell imaging experiments were performed using a LSM 7 *Live* (Zeiss) confocal laser scanning microscope with an incubation chamber. The incubation chamber provided optimal culturing conditions for the cells with 37°C and 5% CO_2. For experiments cells were seeded in ibidi imaging dishes. For proper visualization hMDM were stained with a Deep Red plasma membrane stain (see 2.1.8). Therefore the cells were incubated for at least 30 min in presence of the plasma stain at 37°C. Afterwards 1% FCS was added and the cells were washed by centrifugation (135 xg, 8 min, RT). The cells were then resuspended in fresh medium and seeded in the imaging dishes. For visualization of apoptotic blebs an Annexin V staining was used. Annexin V binds the apoptosis marker phosphatidylserine in a Ca^2+-dependent way with high affinity. For the staining a fluorophore-conjugated Annexin V was added to the cells. Live cell imaging data was analyzed with Zen Black 2012 or Zen Blue 2012 Software.

2.2.5.4 Electron microscopy

For transmission electron microscopy *C. trachomatis* infected hMDM were prepared as described previously (van Zandbergen et al., 2004b). Briefly, infected hMDM were incubated for 48 h. Afterwards cells were fixed using 5% glutaraldehyde in PBS (pH 7.4) for 1 h at 4°C. Samples were then treated with 1% osmium tetroxide followed by block contrasting with tannin (0.1 % in 50 mM HEPES). The samples were dehydrated in graded ethanol series, infiltrated with propylenoxide and finally embedded in Epon. Epon polymerization was performed at 60°C for 48 h. Samples were analyzed with a transmission electron microscope Zeiss EM 109.

2.2.6 Molecular biology methods

2.2.6.1 siRNA transfection of HEp-2

For siRNA transfection the Stemfect™ RNA Transfection Kit (Stemgent) was used. Prior to the knockdown (KD) experiments HEp-2 cells were seeded in 6-well plates 24 hours before transfection. For the siRNA KD approach the medium was removed and the cells were washed with sterile PBS to remove the medium leftovers. This was followed by another washing step with 1 mL DMEM without supplements and afterwards 1 mL DMEM without supplements per well was added. For transfection c-Jun or c-Fos siRNA smart pool, transfection reagent (mock control), non-target siRNA (allstar control, siRNA AllStars Negative Control) was used according to the manufacturer's instructions or cells were left untreated (medium control). Briefly, for each well 20 µM of each siRNA was mixed with 20 µM of Stemfect Buffer to prepare solution A and 4.6 µl of Stemfect Reagent was mixed with 20 µl Stemfect Buffer to prepare solution B. In a timeframe of 5 min, both solutions were mixed and the siRNA transfection complex was incubated for 20 min at RT. Afterwards, the siRNA transfection complex solution was added drop wise to the cells. By gently shaking of the plate an even distribution within the well was ensured. Next, cells were incubated at 37°C with 5% CO_2, harvested 24 hours post transfection (24 hpt) using trypsin-EDTA (see 2.2.1) and counted with a CASY cell counter. Knockdown efficacy was assessed by qRT-PCR and Western Blot analysis. Furthermore, cells were seeded for infection (10 IFU) experiments either in 24-well plates (for qRT-PCR and Western Blot analysis) or in chamber slides (for immunofluorescence analysis) for the desired incubation time. For data analysis normalization was performed against mock control.

2.2.6.2 RNA isolation

Eukaryotic and bacterial RNA was isolated using the RNeasy Plus Mini Kit according to the manufacturer's instructions. Briefly, 0.3 - 1 x 10^6 HEp-2 or 0.5 – 1.5 x 10^6 hMDM were pelleted and afterwards washed by resuspending in cold PBS followed by another centrifugation. The supernatant was discarded and the pellet was then either stored at -80°C or directly used for RNA isolation. For RNA isolation the pellet was lysed in 350 µL RLT-buffer by repeatedly resuspending. The lysate was then transferred to a gDNA Eliminator spin column to remove genomic DNA which gets caught in the column by centrifuging at 15300 xg for 30 sec at RT. The flow-through containing the RNA was mixed in a ratio of 1:1 with 350 µL 70% ethanol and subsequently loaded on a RNeasy spin column. To precipitate the RNA onto the column it was centrifuged at 15300 xg for 30 sec at RT. The flow-through was discarded and the column was washed once with 700 µL buffer RW1 and

twice with 500 µL RPE buffer (15300 xg, 30 sec, RT). The column was then dried by centrifugation in a fresh collection tube at 15300 xg for 1 min at RT. For RNA elution, 30 µL RNase-free water were added to the column and centrifuged at 15300 xg for 1 min at RT. The eluted RNA was put on ice for further use or stored at -80°C for a later use.
RNA concentration was measured in duplicates using a NanoDrop 2000c UV-Vis spectrophotometer. Before cDNA synthesis RNA was used as template in a Test-PCR.

2.2.6.3 Test-PCR

To assure that the RNA is free of genomic DNA a Test-PCR using GAPDH primer (see 2.1.7) was performed. Amplification leading to a detectable product can only occur if DNA is present in the samples, because the primers do not bind to RNA. As positive control cDNA and as negative control water was used as template instead of the RNA. A master mix was prepared, distributed to PCR tubes and the templates were added. For each reaction the following master mix was pipetted:

volume [µL]	reagent	concentration
X	RNA / cDNA / ddH_2O	≥ 100ng
5	NEB Taq-buffer [10x]	1x
1	forward primer [10 µM]	0.2 µM
1	reverse primer [10 µM]	0.2 µM
5	dNTP-Mix [2 mM each]	0.2 mM
0.25	NEB Taq-polymerase [5 U/µL]	1.25 U
ad 50	ddH_2O	-

The PCR tubes were gently mixed and centrifuged at 800 xg for a few seconds. Subsequently the PCR was performed according to the following program:

steps	temp [°C]	time
initial denaturation	95	30sec
amplification 30 cycles		
denaturation	95	30 sec
annealing	60	30 sec
elongation	68	30 sec
final elongation	68	10 min
cooling	4	∞

PCR products were separated on a 2% TAE agarose gel which was supplemented with ethidium bromide and DNA bands were visualized with ultraviolet light.

2.2.6.4 cDNA synthesis by reverse transcription

To generate complementary DNA (cDNA) the ImProm-II Reverse Transcription System™ was used according to the manufacturer's instructions. Briefly, 100 ng of HEp-2 RNA or 50 ng of hMDM RNA was used for the reaction. As negative control water was added instead of RNA to one sample. For one reaction the following mix was prepared:

volume [µL]	reagent	concentration
1	ImProm-II™ Random Primer Mix	5 µg
x	RNA template	50 ng (hMDM) / 100 ng (HEp-2)
ad 5	ddH_2O	-

The PCR tubes were gently mixed and centrifuged at 800 xg for a few seconds. The mix was thermally denatured for 5 min at 70°C and subsequently cooled down for at least 5 min. A reverse transcription reaction mix was added with the following reagents for one reaction:

volume [µL]	reagent	concentration
6.5	Nuclease-free H_2O	-
4	ImProm-II™ 5x Reaction Buffer	1x
2	$MgCl_2$(25 mM)	2.5 mM
1	dNTP Mix (10 mM each)	0.5 mM
0.5	recombinant RNasin® Ribonuclease Inhibitor (20-40 U/µL)	10 – 20 U
1	ImProm-II™ Reverse Transcriptase	
15 µL		

Again the PCR tubes were gently mixed and shortly centrifuged at 800 xg. Reverse transcription was performed using the following program:

step	temp [°C]	time
annealing	25	5 min
cDNA synthesis	42	60 min
inactivation	70	15 min
cooling	4	∞

The cDNA could now be used for quantitative real-time PCR or had to be stored at -20°C until usage.

2.2.6.5 Quantitative real-time PCR

For determination of target gene expression cDNA was analyzed via quantitative real-time PCR (qRT-PCR) using a Light Cycler 480 and a master mix which contains the fluorescent dye *SYBR Green* (*MESA BLUE qPCR Master Mix Plus*) according to the manufacturer's instructions. The fluorescent *SYBR Green* intercalates into double-strand DNA and the arising fluorescence signal is thereby proportional to the amount of amplified DNA. As the quantification can be followed during the reaction progress the PCR is called "real-time" PCR. Determination of the target gene expression was achieved by the use of specific primers as listed above (see 2.1.7). Prior to usage in qRT-PCR the primer efficacy was tested for each primer pair.
For one reaction the following mix was prepared:

volume [µL]	reagent	concentration
10	*MESA BLUE qPCR Master Mix*	1x
6	(2x)ddH_2O	-
1	forward primer [10µM]	0.5 µM
1	reverse primer [10µM]	0.5 µM
2	cDNA / H_2O	undiluted
15 µL		

The mix for one reaction was transferred to one well of a white 96-well plate in duplicates for each condition. As negative control 2 µL water was added instead of 2 µL cDNA template. The following qRT-PCR program was used:

steps	temp [°C]	time	°C/sec
activation	95	10 min	4.4
amplification 45 cycles			
denaturation	95	10 sec	4.4
annealing	60	5 sec	2.2
elongation	72	10 sec	4.4
melting curve	95	1 sec	4.4
	50	30 sec	2.2
	95	0 sec	0.11
cooling	40	15 sec ∞	2.2

For data analysis the applied software LC480 (version 1.5.0 SP4) was used. Relative gene expression was calculated by using the CT-value (cycle threshold) and the $2^{-\Delta\Delta CT}$ method as previously described (Livak and Schmittgen, 2001). The CT-value specifies the cycle in which the fluorescence signal exceeded the background signal for the first time.

2.2.7 Statistical analysis

Numerical data are presented as the mean ± standard deviation (SD) or standard error of the mean (SEM). All data were assumed to be distributed normally. Data were consequently analyzed by paired Student´s *t*-test (two tailed distribution) using Microsoft Excel 2010 and GraphPad Prism4 software. Values of $p< 0.05$ (*), $p< 0.01$ (**) and $p< 0.001$ (***) were considered significant.

3 Results

3.1 Part I

3.1.1 AP-1 proteins are regulated during *C. pneumoniae* infection

To investigate if AP-1 is regulated during *C. pneumoniae* infection, we first determined the protein expression of the AP- 1 components c-Jun, c-Fos and ATF-2 over time by using Western Blot analysis. We therefore infected HEp-2 cells with either a low dose (10 IFUs) or a high dose (30 IFUs) of *C. pneumoniae* or stimulated the cells with heat killed *C. pneumoniae* (**Figure 7**). Protein expression of c-Jun was not found to be regulated at early time points (4 and 24 hpi) after infection. At later time points (48 hpi and 72 hpi) the expression of c-Jun clearly increased upon infection with either a low or high dose of *C. pneumoniae* infection, but remained unchanged upon stimulation with heat killed *C. pneumoniae*. The expression of c-Fos protein after 4 h was up-regulated after infection with a high dose or stimulation with heat killed *C. pneumoniae*, whereas after infection with a low dose the expression decreased. After 24 h the c-Fos expression remained reduced after infection with a low dose or after stimulation with heat killed *C. pneumoniae*, but infection with a high dose did not alter c-Fos expression level. After 48 h only the c-Fos expression in cells infected with a low dose was changed and showed a decrease.

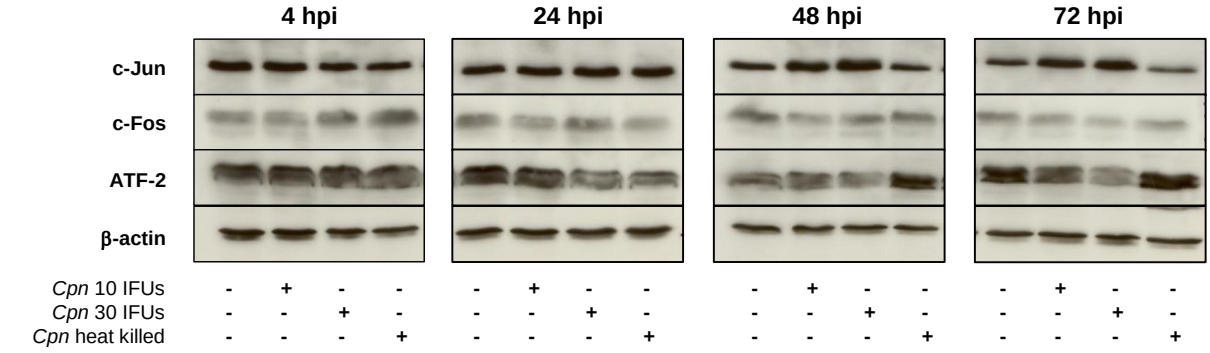

Figure 7: AP-1 proteins are differentially regulated after *C. pneumoniae* infection. Lysates from uninfected HEp-2 cells or HEp-2 cells infected with 10 IFU (low dose), 30 IFU (high dose) or stimulated with heat killed *C. pneumoniae* (*Cpn*) were prepared at various time points after infection (4 hpi, 24 hpi, 48 hpi and 72 hpi). Using Western Blot analysis protein expression of c-Jun, c-Fos, ATF-2 and ß-actin was analyzed at the indicated time points. Immunoblots are representative for six independent experiments (n = 6).

At late time points (72 hpi) c-Fos expression was reduced upon infection with a low or high dose, while the stimulation with heat killed *C. pneumoniae* did not result in changes of the c-Fos expression. Regarding ATF-2 protein expression no clear differences could be observed after 4 h of infection. However, protein expression decreased after 24 h in cells infected with high dose or stimulated with heat killed *C. pneumoniae.* After 48 hours the

expression of ATF-2 was not altered in infected cells, but increased after stimulation with heat killed *C. pneumoniae*. At late time points (72 hpi) the ATF-2 expression was reduced after infection with both infection doses, however the decrease was more pronounced in cells which were infected with a high dose of *C. pneumoniae*.

Subsequently, we quantified protein expression using densitometry analysis. We did not observe a difference in c-Jun protein expression after 4 h (**Figure 8 A**). However, 24 h after infection the protein level of c-Jun increased with a low dose of infection and the increase was significant with a high dose of infection. At later time points, 48 and 72 hours after infection, c-Jun protein expression remained significantly up-regulated. Of note, stimulation with heat killed *C. pneumoniae* did not alter AP-1 protein expression over time. When we focused on c-Fos and ATF-2 protein expression we found no significant differences in expression level in comparison to the uninfected control at 4 hpi, 24 hpi and 48 hpi (**Figure 8 B-C**). In contrast, after 72 hpi the protein expression of c-Fos and ATF-2 was significantly down-regulated in infected cells (low or high dose), but did not significantly change upon stimulation with heat killed *C. pneumoniae*.

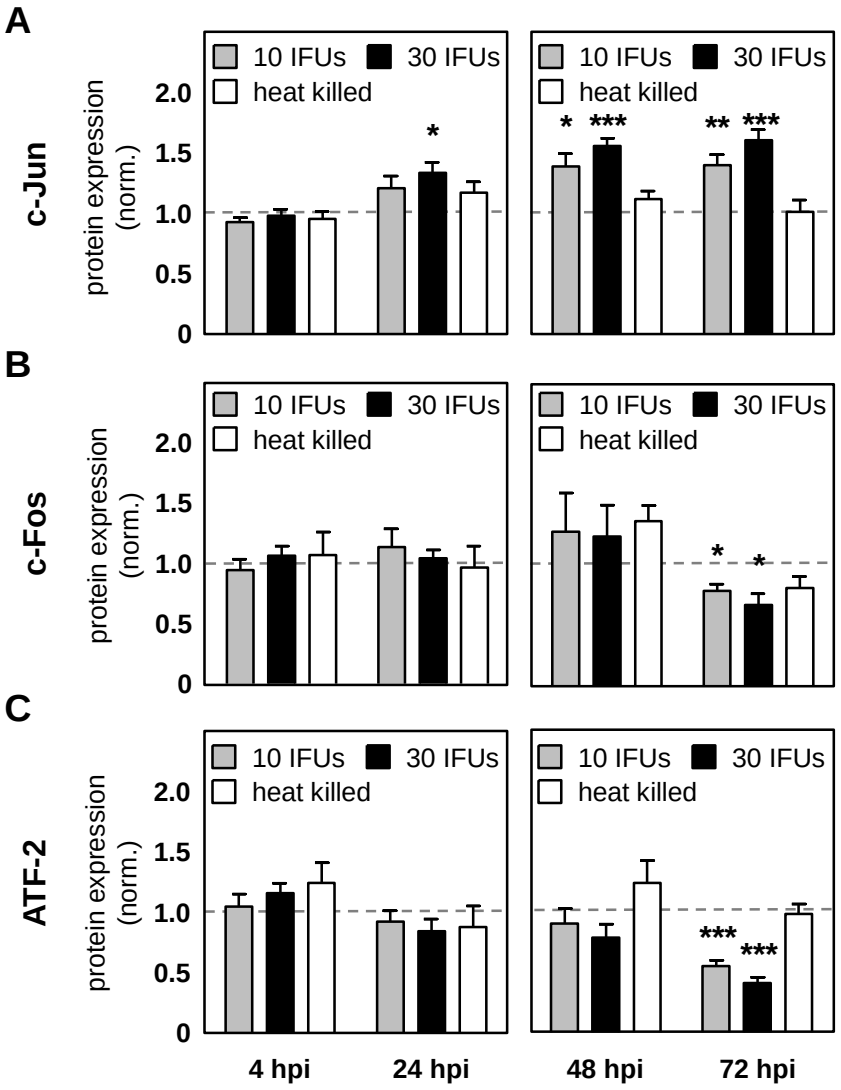

Figure 8: After *C. pneumoniae* infection AP-1 protein expression is regulated in a time and dose dependent manner. Lysates from uninfected or infected HEp-2 cells with 10 IFU (low dose), 30 IFU (high dose) or stimulated with heat killed *C. pneumoniae* were prepared at various time points after infection (4 hpi, 24 hpi, 48 hpi and 72 hpi) (**A-C**) Quantification of protein expression over time of (**A**) c-Jun, (**B**) c-Fos and (**C**) ATF-2 using densitometry. Data were normalized against control and presented as mean ± SD. Data are representative for six independent experiments (n = 6). *p<0.05, **p<0.01, *** p<0.001

In addition to protein expression, we assessed the mRNA levels of c-Jun and c-Fos using qRT-PCR. Similar to protein expression we found that gene expression of c-Jun was significantly up-regulated 48 hours after infection with low or high dose of *C. pneumoniae* (**Figure 9 A**). Regarding c-Fos, mRNA levels were elevated which contradicts the data observed for c-Fos protein expression (**Figure 9 B**). In all, we find that *C. pneumoniae* regulates AP-1 protein expression and activity levels, both in a time and dose dependent manner.

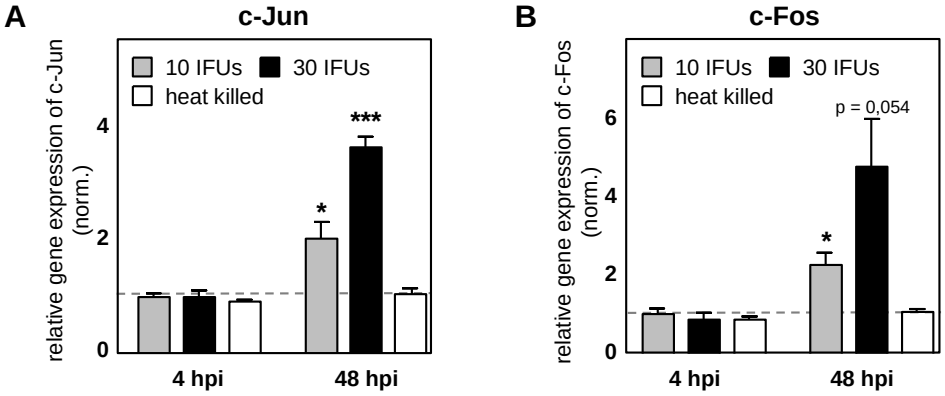

Figure 9: *C. pneumoniae* infection leads to up-regulation of c-Jun and c-Fos gene expression over time. mRNA of uninfected or HEp-2 cells infected with 10 IFU (low dose), 30 IFU (high dose) or stimulated with heat killed *C. pneumoniae* was isolated 4 hpi and 48 hpi. Relative gene expression of (**A**) c-Jun and (**B**) c-Fos 4 hpi and 48 hpi was assessed using qRT-PCR. Data were normalized against the uninfected control and presented as mean ± SD. Data are representative for four independent experiments (n = 4). *p<0.05, *** p<0.001

In a next step we used Western Blot analysis to assess the phosphorylation status of the AP-1 proteins which was in complete accordance with the regulation of the c-Jun, c-Fos or ATF-2 protein expression (**Figure 10**). Densitometry analysis revealed that phosphorylation of c-Jun was up-regulated 4, 48 and 72 hpi and the up-regulation was significant for infection with both, low and high dose of *C. pneumoniae*, after 4 and 72 hpi (**Figure 11 A**). While phosphorylation levels of c-Jun increased over time, the quantity of phosphorylated c-Fos and ATF-2 significantly decreased. Regarding c-Fos protein, phosphorylation was not changed 4 hpi, but started to decrease significantly 24 hours after infection with a high dose of *C. pneumoniae* and remained significantly reduced up to 72 hpi (**Figure 11 B**). During infection with a low dose of *C. pneumoniae* we also observed a significant reduction of phosphorylation at this late time point (72 hpi). In addition, also for ATF-2 protein a decline of

the phosphorylation level was detectable. Infection with a high dose of *C. pneumoniae* resulted in significant less phosphorylation of ATF-2 at 48 and 72 hpi (**Figure 11 C**).

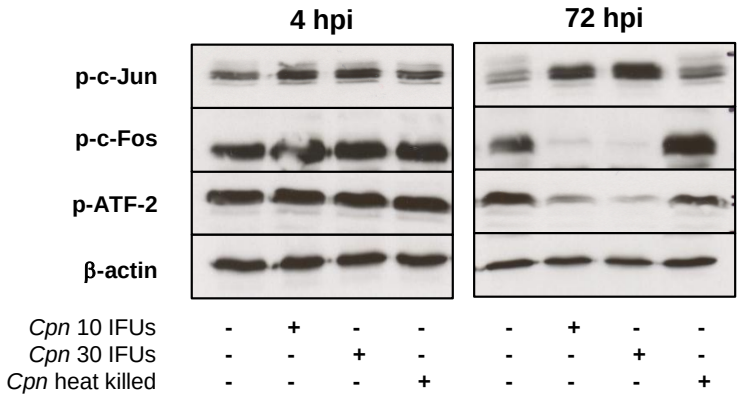

Figure 10: *C. pneumoniae* infection regulates phosphorylation of AP-1 proteins. Lysates from uninfected HEp-2 cells or HEp-2 cells infected with 10 IFU (low dose), 30 IFU (high dose) or stimulated with heat killed *C. pneumoniae* (*Cpn*) were prepared at various time points after infection (4 hpi, 24 hpi, 48 hpi and 72 hpi). By Western Blot analysis protein phosphorylation of c-Jun, c-Fos, ATF-2 and expression of β-actin were analyzed at the indicated time points (4 hpi and 72 hpi). Immunoblots are representative for at least three independent experiments (n = 3 - 6).

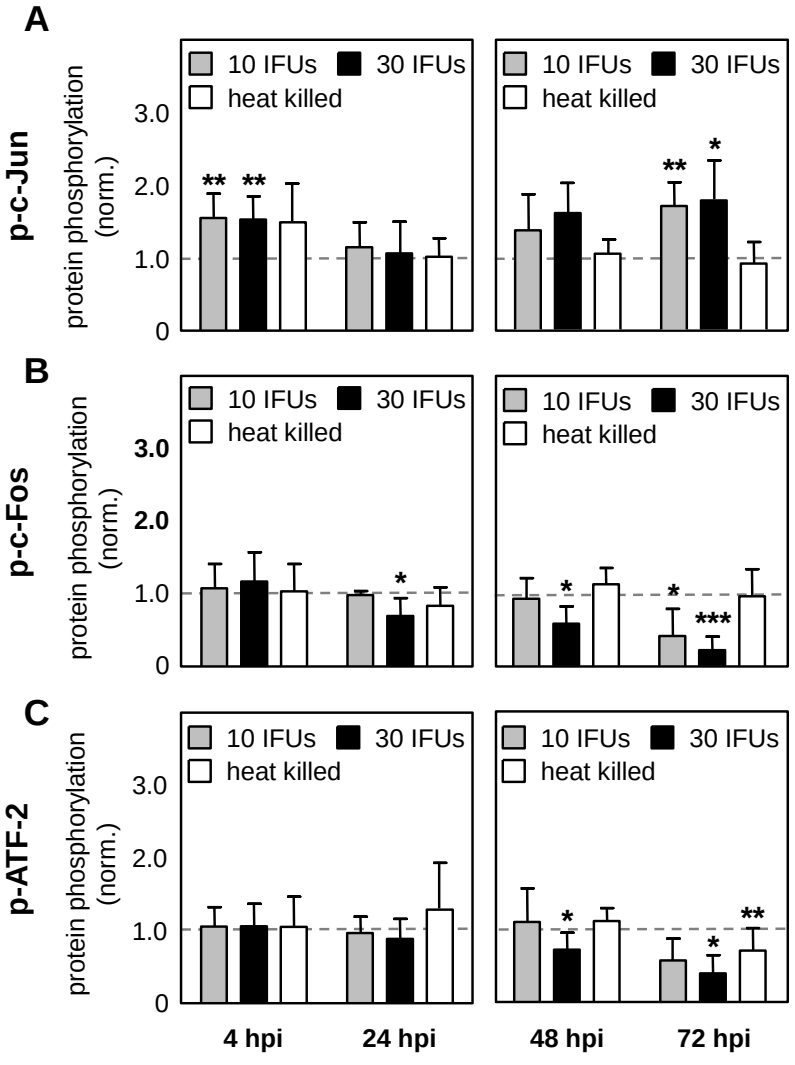

Figure 11: Phosphorylation of AP-1 proteins is regulated in a time and dose dependent manner during *C. pneumoniae* infection. Lysates from uninfected or HEp-2 cells infected with 10 IFU (low dose), 30 IFU (high dose) or stimulated with heat killed *C. pneumoniae* (*Cpn*) were prepared at various time points after infection (4 hpi, 24 hpi, 48 hpi and 72 hpi). (**A-C**) Using densitometry, protein phosphorylation of (**A**) c-Jun, (**B**) c-Fos and (**C**) ATF-2 was quantified during *C. pneumoniae* infection of HEp-2 cells. Data were normalized against the uninfected control (dashed grey line). Data are presented as mean ± SD. Data and immunoblots are representative for at least four independent experiments (n = 4 - 6). *p<0.05, **p<0.01, *** p<0.001

3.1.2 Establishment of a siRNA knockdown approach

We could demonstrate that infection with *C. pneumoniae* results in a significant up-regulation of c-Jun protein expression and phosphorylation. Subsequently we investigated whether an increased expression of c-Jun would be beneficial for intracellular growth and progeny of *C. pneumoniae*. Therefore we performed c-Jun specific siRNA knockdown experiments in HEp-2 cells.

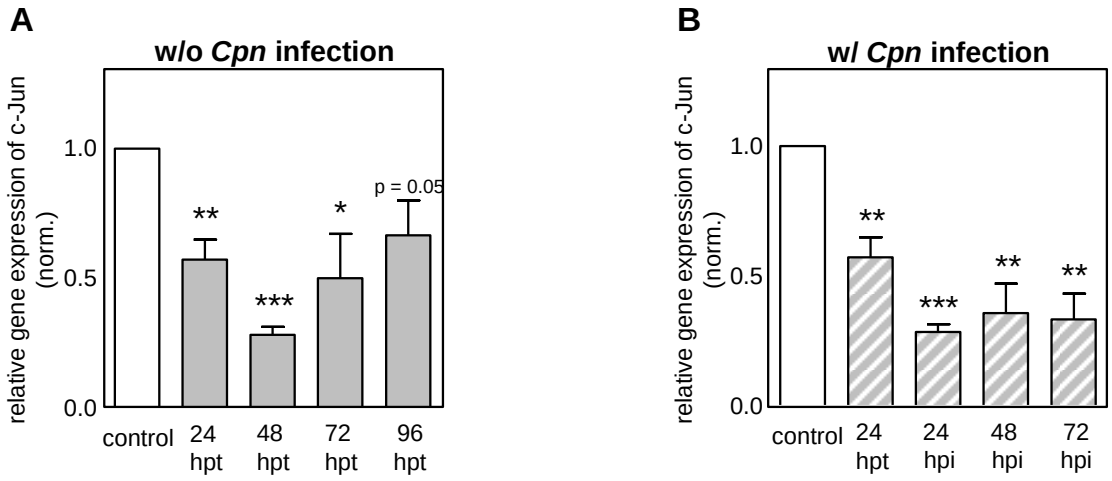

Figure 12: c-Jun siRNA treatment leads to reduced c-Jun mRNA expression. HEp-2 cells were treated with c-Jun siRNA (c-Jun KD) or transfection reagent (control) for 24 hours. After transfection (24 hpt) cells were infected with 10 IFU of *C. pneumoniae*. mRNA was isolated 24 hpt as well as after 24 hpi, 48 hpi and 72 hpi. Relative gene expression of c-Jun (**A**) in uninfected KD cells and (**B**) *C. pneumoniae* (*Cpn*) infected KD cells was assessed using qRT-PCR. Data were normalized against the mock control (control; dashed line). Data, presented as mean ± SD, are representative for seven independent experiments (n = 7). *p<0.05, **p<0.01, *** p<0.001

We assessed c-Jun knockdown efficacy on mRNA level by using qRT-PCR. We determined the c-Jun mRNA expression in absence (**Figure 12 A**) or presence (**Figure 12 B**) of *C. pneumoniae* infection. After 24 hours of transfection (24 hpt) the c-Jun mRNA expression was significantly reduced (0.6 ± 0.2) in comparison to c-Jun mRNA expression of control cells (1.0 ± 0.0) (**Figure 12 A-B**). The c-Jun mRNA level remained significantly reduced up to 72 hpt in uninfected c-Jun KD cells (48 hpt 0.3 ± 0.1; 72 hpt 0.5 ± 0.4; 96 hpt 0.7 ± 0.3) (**Figure 12 A**). In addition, in *C. pneumoniae* infected c-Jun KD cells the mRNA expression decreased even more, being significantly diminished over time (24 hpi 0.3 ± 0.1; 48 hpi 0.4 ± 0.3; 72 hpi 0.3 ± 0.2) (**Figure 12 B**).

We continued to investigate the c-Jun knockdown efficacy on protein level using Western Blot analysis. After 24 h of transfection we could detect less c-Jun protein after siRNA treatment in comparison to untreated or control cells (**Figure 13 A**). We analyzed c-Jun protein levels at later time points in either uninfected or *C. pneumoniae* infected cells (**Figure 13 B**). In c-Jun siRNA treated cells the amount of c-Jun protein was always strongly reduced compared to the untreated or control cells. Of note, in the *C. pneumoniae* infected cells c-Jun expression was up-regulated as already seen in our initial experiments depicted in **Figure 7**.

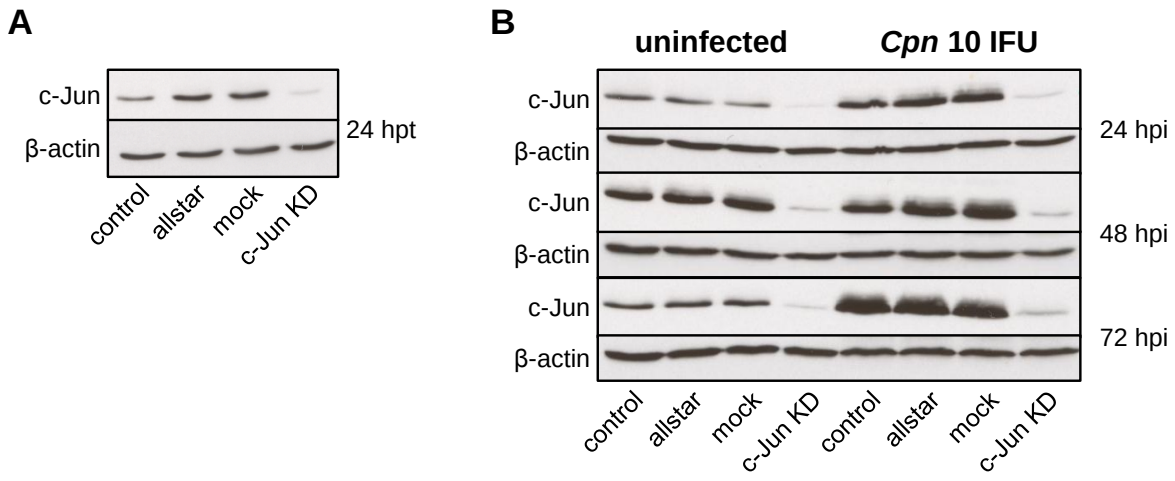

Figure 13: Establishment of a stable c-Jun siRNA knockdown on protein level. HEp-2 cells were treated with c-Jun siRNA (c-Jun KD), allstar siRNA, transfection reagent (mock) or left untreated (control). Lysates were prepared 24 hours after transfection (24 hpt) and 24 hpi, 48 hpi and 72 hpi. (**A-B**) Western Blot analysis was used to determine c-Jun knockdown efficacy in HEp-2 cells (**A**) 24 hours post transfection (24 hpt) and (**B**) 24, 48 and 72 hours post *C. pneumoniae* (*Cpn*) infection (hpi). Immunoblots are representative of seven independent experiments (n = 7).

We proceeded to quantify c-Jun protein levels using densitometry. We discovered that the c-Jun siRNA treated cells expressed only low amounts of c-Jun protein. Already 24 hpt a significant decrease in c-Jun protein amount was detectable. Expression of c-Jun protein was reduced to 30.4% (± 22.1%) compared to the amount of c-Jun expressed in control cells (100% ± 0.0%) (**Figure 14 A+B**). Without infection the c-Jun protein continued to be expressed significantly lower, with 44.7% (± 23.6%) of c-Jun protein 48 hpt, 19.1% (± 8.6%) of c-Jun protein 72 hpt and 23.4% (± 10.7) of c-Jun protein after 96 hpt (**Figure 14 A**). Also during *C. pneumoniae* infection the c-Jun protein expression was significantly decreased with 34.6% (± 21.6%) c-Jun 24 hpi, 29.1% (± 24.7%) c-Jun 48 hpi and 24.7% (± 25%) of c-Jun 72 hpi compared to control cells without c-Jun siRNA treatment (**Figure 14 B**).

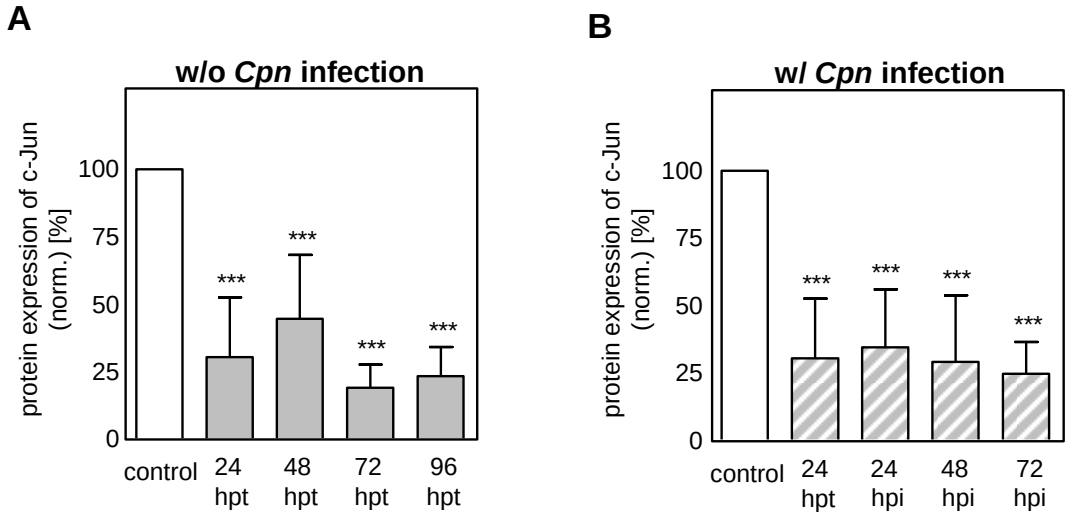

Figure 14: Protein level of c-Jun are significantly decreased after siRNA knockdown independent of *C. pneumoniae* infection. Lysates from HEp-2 cells treated with c-Jun siRNA (c-Jun KD) or transfection reagent (control) were used to determine c-Jun knockdown efficacy 24 hours after transfection (24 hpt) and 24, 48 and 72 hours post *C. pneumoniae* (*Cpn*) infection (hpi). Using densitometry protein expression of (**A**) uninfected c-Jun KD cells and (**B**) infected with 10 IFU of *Cpn* was quantified. Data were normalized against the control. Data are presented as mean ± SD. Data are representative for seven independent experiments (n = 7). *** p<0.001

The Jun/c-Fos heterodimer represents the predominant variant of transcription factor AP-1. To strengthen our hypothesis that the c-Jun protein is critical for chlamydiae development, we wanted to establish c-Fos knockdown as a control. Therefore we treated the cells with c-Fos specific siRNA. We determined c-Fos knockdown efficacy first on mRNA level with qRT-PCR. Similar to the c-Jun siRNA knockdown, the treatment with c-Fos siRNA resulted in a significant reduction of the c-Fos mRNA levels 24 hpt (**Figure 15 A**). The analysis of c-Fos protein expression using Western Blot showed, that c-Fos protein expression in these cells was not affected and remained stable (**Figure 15 B**).

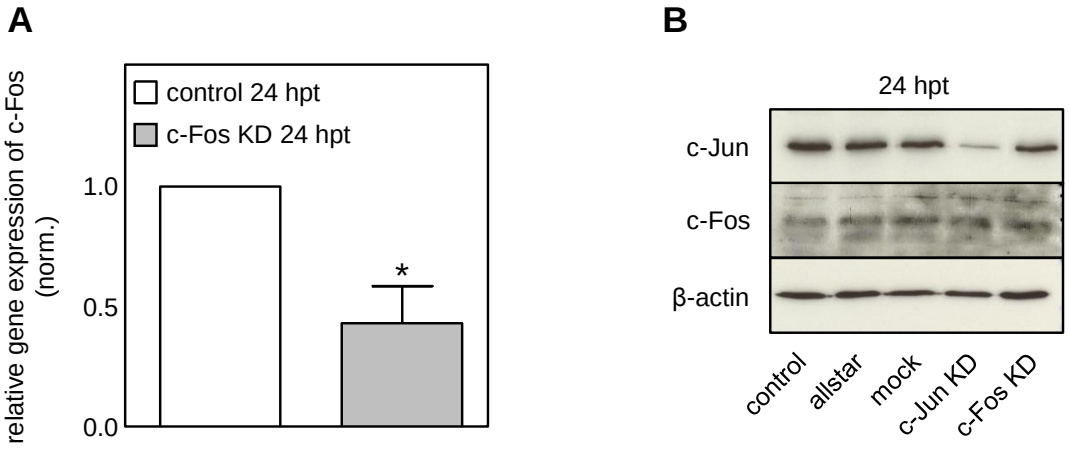

Figure 15: c-Fos siRNA treatment reduces c-Fos mRNA but not c-Fos protein expression. HEp-2 cells were treated with c-Jun or c-Fos siRNA (c-Jun KD/c-Fos KD), allstar siRNA, transfection reagent or left untreated. After 24 hours of transfection (24 hpt) lysates were prepared and mRNA was isolated. (**A**) Relative gene expression of

c-Fos was assessed using qRT-PCR. (**B**) Western Blot analysis of the indicated proteins 24 hpt. Data were normalized against the control and are presented as mean ± SD. Data and immunoblots are representative of three independent experiments (n = 3). *p<0.05

3.1.3 Knockdown of c-Jun protein impairs *C. pneumoniae* infection

To assess the consequence of the decreased c-Jun mRNA and protein level on *C. pneumoniae* infection we analyzed the infection using a chlamydiae specific staining and immunofluorescence microscopy (**Figure 16 A+B**). We infected untreated and c-Jun KD HEp-2 cells with *C. pneumoniae* and compared their infection morphology 48 hpi. Infection of untreated cells resulted in the development of typical chlamydiae inclusions, characterized by a large and round shaped morphology (**Figure 16 A**), while the inclusions in the siRNA treated cells were found to be smaller (**Figure 16 B**). In addition, we observed that more inclusions (5.1% ± 7.6%) were present in the control cells as compared to the cells treated with c-Jun specific siRNA (**Figure 16 C**). Quantification of the inclusion size revealed that in the c-Jun KD cells the inclusion size was reduced by 20% (± 13.7%) compared to the size of the inclusions in the control cells (**Figure 16 D**).

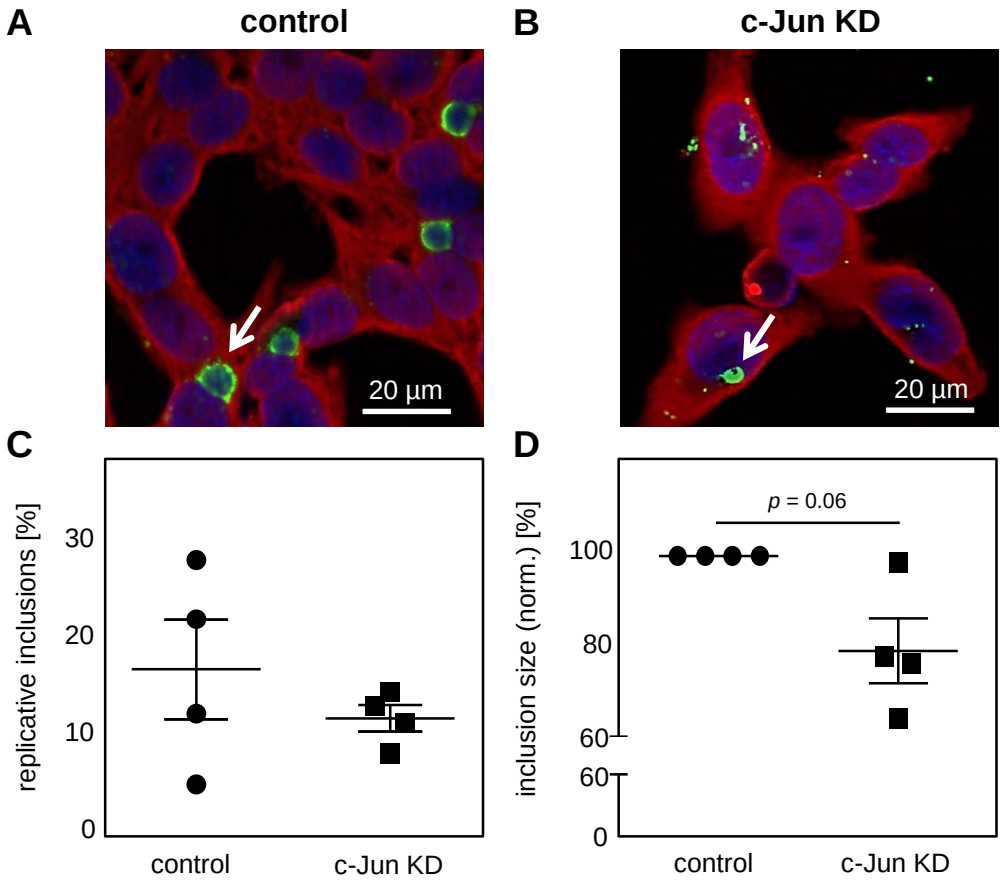

Figure 16: c-Jun siRNA knockdown leads to formation of smaller *C. pneumoniae* inclusions. *C. pneumoniae* (*Cpn*) infected HEp-2 cells (**B**) with and (**A**) without c-Jun knockdown were methanol fixed 48 hpi and immunostained with IMAGEN Chlamydia kit (chlamydiae-LPS green; cytoplasm red) and counterstained with

DAPI (blue). The white arrows point to *C. pneumoniae* inclusions. (**C-D**) From immunofluorescence images the (**C**) amount of replicative inclusions and the (**D**) size of control and c-Jun KD cells were quantified during *Cpn* infection. Data were normalized against the control. Data represent the mean ± SD. Data and immunofluorescence images are representative of four independent experiments (n = 4).

To further investigate this decrease in inclusion size, we used Western Blot analysis. We checked protein expression of *C. pneumoniae* major outer membrane protein (MOMP) to gain information about the chlamydial development. Indeed, the shrinkage of the inclusions was accompanied by a reduction of MOMP protein expression, as we detected less MOMP in the c-Jun KD cells compared to untreated or control cells (**Figure 17 A**). With Western Blot analysis MOMP protein was only detectable 48 and 72 hpi, but not 24 hpi. Quantification with densitometry showed that in the c-Jun KD cells 74.6**%** (± 24.6%) of the MOMP protein was expressed compared to the amount of MOMP expressed in the infected control cells (100%) (**Figure 17 B**).

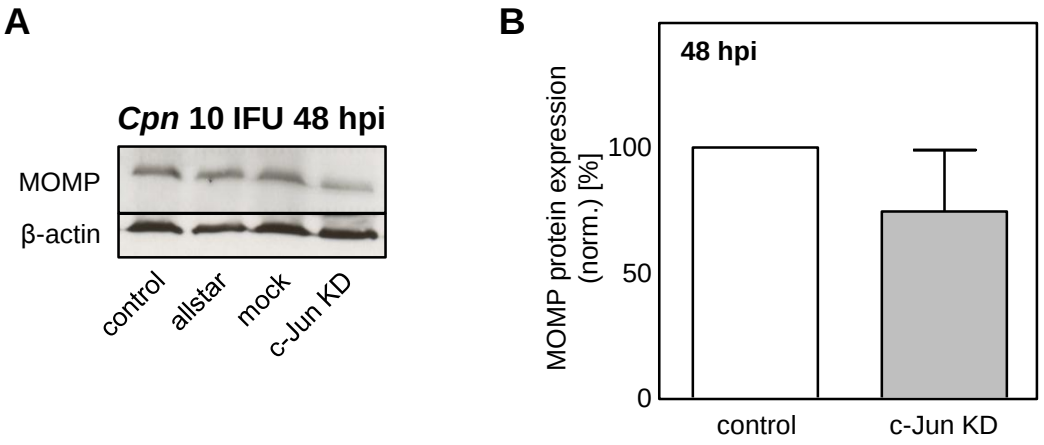

Figure 17: Loss of c-Jun protein results in a reduction of the MOMP protein. HEp-2 cells were treated with c-Jun siRNA (c-Jun KD), allstar siRNA or transfection reagent (mock) or left untreated. (**A**) Western Blot analysis of MOMP protein 48 hpi. (**B**) Quantification of protein MOMP expression 48 hpi using densitometry, normalized to control. Data represent the mean ± SD. Data and immunoblots are representative of four independent experiments (n = 4).

To further characterize the effect of the c-Jun knockdown on *C. pneumoniae* infection we analyzed the chlamydial load in either control or c-Jun KD cells via qRT-PCR. In concordance with the smaller inclusions and decreased MOMP expression, we detected a reduction of *C. pneumoniae* 16S RNA in the c-Jun knockdown cells over time (**Figure 18**).

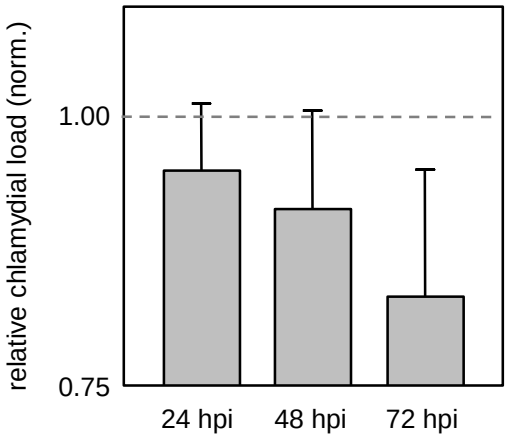

Figure 18: c-Jun siRNA knockdown reduces *C. pneumoniae* load. HEp-2 cells treated with c-Jun siRNA (c-Jun KD) or transfection reagent (control) were infected with 10 IFU of C. pneumoniae. mRNA was isolated 24, 48 and 72 hpi and relative *Cpn* load was assessed using qRT-PCR. Data were normalized against control and represent the mean ± SD. Data are representative of seven independent experiments (n = 7).

Additionally, we assessed the impact of the c-Jun knockdown on the ability of chlamydial recovery. Interestingly, the recovery after c-Jun KD was significantly reduced and resulted in the formation of fewer inclusions (85.1% ± 7.3%) as compared to control cells (100% ± 0.0%) (**Figure 19**).

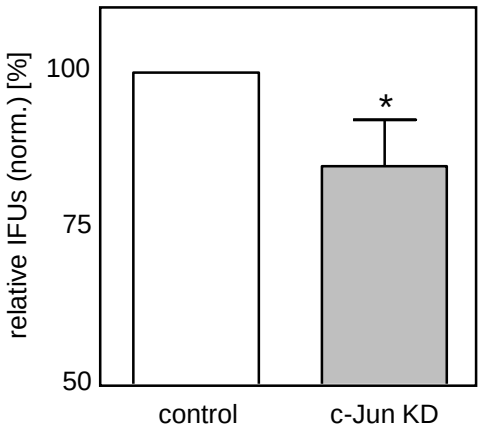

Figure 19: Reduction of c-Jun protein impairs *C. pneumoniae* recovery. HEp-2 cells were infected for 48 hours with *C. pneumoniae* extracted from infected control cells or c-Jun siRNA KD cells. Afterwards (48 hpi) cells were methanol fixed and immunostained. To determine chlamydial recovery the relative IFUs were quantified by randomly counting the inclusions of at least 300 cells. Data were normalized against the control and represent the mean ± SD. Data are representative of three independent experiments (n = 3). *p<0.05

3.1.4 Blocking AP-1 mediated transcription results in chlamydiae growth restriction

We showed that c-Jun knockdown had a negative effect on C. pneumoniae development. As c-Jun is part of the AP-1 complex, we next investigated if the role of c-Jun in the AP-1 mediated transcription is essential for chlamydial development. Therefore we used Tanshinone IIA as a specific inhibitor of c-Jun/cFos AP-1 complexes, which prevents AP-1 DNA binding (Park et al., 1999). In our experiments we applied Tanshinone IIA (25 µM) in parallel to C. pneumoniae infection. To assess the effect of Tanshinone IIA treatment on chlamydial development we first determined the C. pneumoniae load (expression of chlamydial 16S rRNA) with qRT-PCR. We observed that after Tanshinone IIA treatment the chlamydial load of C. pneumoniae inside the HEp-2 cells strongly decreased (1 IFU: 157-fold; 10 IFU: 62-fold; 25 IFU: 46-fold) (**Figure 20**)

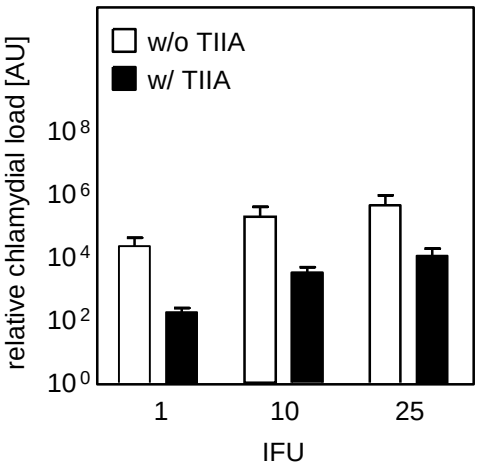

Figure 20: Tanshinone IIA treatment decreases *C. pneumoniae* load. HEp-2 cells were infected with *C. pneumoniae* (1, 10 or 25 IFUs) and in parallel treated with (w/) or without (w/o) Tanshinone IIA (TIIA, 25 µM). After 48 hours the cells were harvested followed by mRNA isolation. Quantification of relative chlamydial load was assessed using qRT-PCR. Data, presented as mean ± SD, and immunofluorescence images are representative of three independent experiments (n = 3).

Subsequently, we checked the effect of Tanshinone IIA on infection morphology by the use of chlamydiae specific immunofluorescence staining. We observed that in comparison to control cells (w/o Tanshinone IIA, **Figure 21 A**), which exhibit a typical replicative infection phenotype, the inclusions were smaller with an aberrant shape (**Figure 21 B**). We quantified the aberrant inclusions and found that after Tanshinone IIA treatment, the majority (98.4% ± 0.6%) of all inclusions exhibited an aberrant shape, while in the untreated cells only few inclusions had such an aberrant morphology (4.1% ± 0.6%) (**Figure 21 C**).

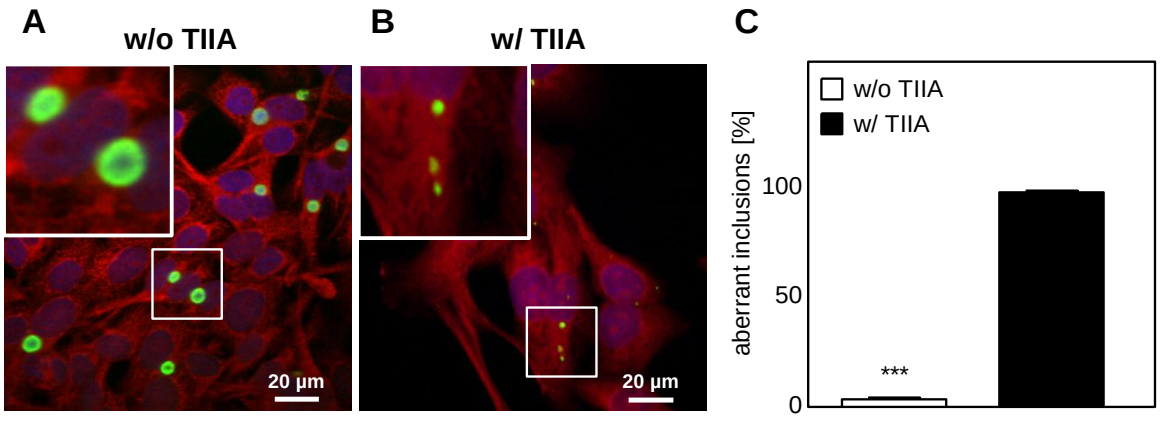

Figure 21: Tanshinone IIA treatment limits inclusion development. HEp-2 cells were infected with *C. pneumoniae* (1, 10 or 25 IFUs) and in parallel treated with (w/) or without (w/o) Tanshinone IIA (TIIA, 25 µM). After 48 hours the cells were fixed with methanol, immunostained with IMAGEN Chlamydia kit (chlamydiae-LPS green; cytoplasm red) and counterstained with DAPI (blue). (**A**) Untreated cells with typical *C. pneumoniae* inclusions and (**B**) aberrant *C. pneumoniae* inclusions after TIIA treatment. (**C**) Aberrant inclusions were quantified in *C. pneumoniae* infected cells w/ and w/o TIIA. Data, presented as mean ± SD, and immunofluorescence images are representative of four independent experiments (n = 4). *** p<0.001

Since Tanshinone IIA treatment had such a strong effect on *C. pneumoniae* development, we assessed the effect of the inhibitor on other chlamydiae species. For that reason we used *C. trachomatis* and eGFP-*C. trachomatis* in the same experimental setting. First we quantified the chlamydial load of untreated and Tanshinone IIA treated HEp-2 cells which were infected with *C. trachomatis*. Preliminary data suggest a decrease in chlamydial load (16S rRNA) after Tanshinone IIA treatment (1 IFU: 87-fold; 10 IFU: 8-fold; 25 IFU: 17-fold; n = 1) (**Figure 22 A**) which was not as strong as in *C. pneumoniae* infected cells (see **Figure 20**). Moreover, in comparison to the large inclusions of untreated cells (**Figure 22 B**), the inclusions in the Tanshinone IIA treated cells also seemed to decrease in size (**Figure 22 C**). Nevertheless, the reduction of inclusion size for *C. trachomatis* was not as pronounced as observed for *C. pneumoniae* (see **Figure 21 A+B**).

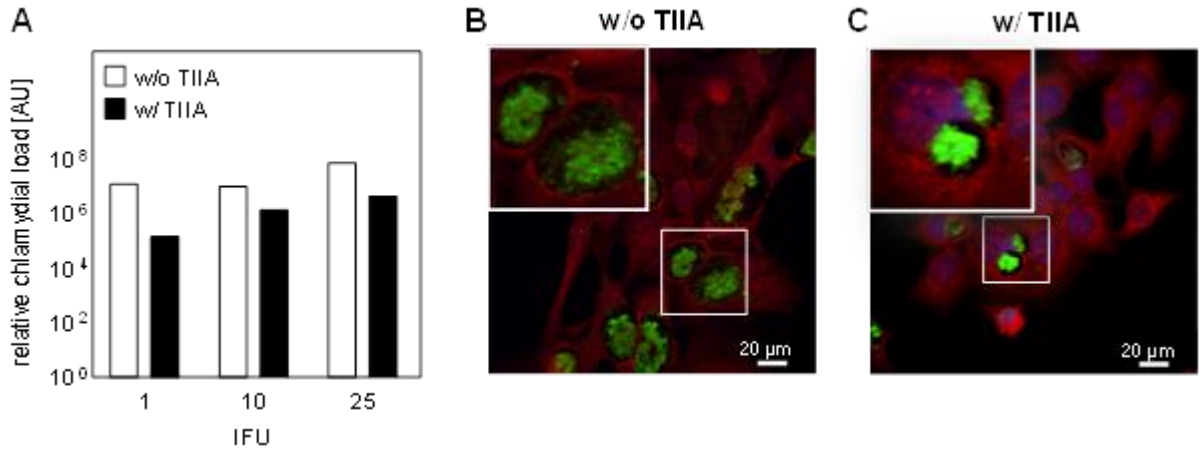

Figure 22: Tanshinone IIA treatment reduces C. trachomatis load and inclusion size. HEp-2 cells were infected with C. trachomatis (1, 10 or 25 IFUs) and in parallel treated with (w/) or without (w/o) Tanshinone IIA (TIIA, 25 µM). After 48 hours the cells were harvested followed by mRNA isolation. (**A**) Quantification of relative chlamydial load was assessed using qRT-PCR. (**B-C**) Infected cells (10 IFU) (**B**) w/o and (**C**) w/ TIIA were fixed

after 48 hours with methanol, immunostained with IMAGEN Chlamydia kit (chlamydiae-LPS green; cytoplasm red) and counterstained with DAPI (blue). Data is presented as mean ± SD. Immunofluorescence images are representative of three independent experiments (n = 1 - 3).

In addition, preliminary data suggest similar effects of Tanshinone IIA treatment in eGFP-*C. trachomatis* infected cells. The chlamydial load decreased upon Tanshinone IIA treatment (1 IFU: 10-fold; 10 IFU: 24-fold; 25 IFU: 19-fold; n = 1) (**Figure 23 A**), however to a lesser extent as observed for *C. pneumoniae* (see **Figure 20**). The effect of Tanshinone IIA on infection morphology showed again that, compared to the large inclusions in the untreated cells (**Figure 23 B**), the size of the inclusions after Tanshinone IIA treatment was reduced (**Figure 23 C**). The reduction of inclusion size we observed upon TIIA treatment for eGFP-*C. trachomatis* was comparable to that observed for the wildtype *C. trachomatis*. Of note, the reduction of inclusion size for both, the transgenic and the wildtype *C. trachomatis,* was not as pronounced as seen for *C. pneumoniae*.

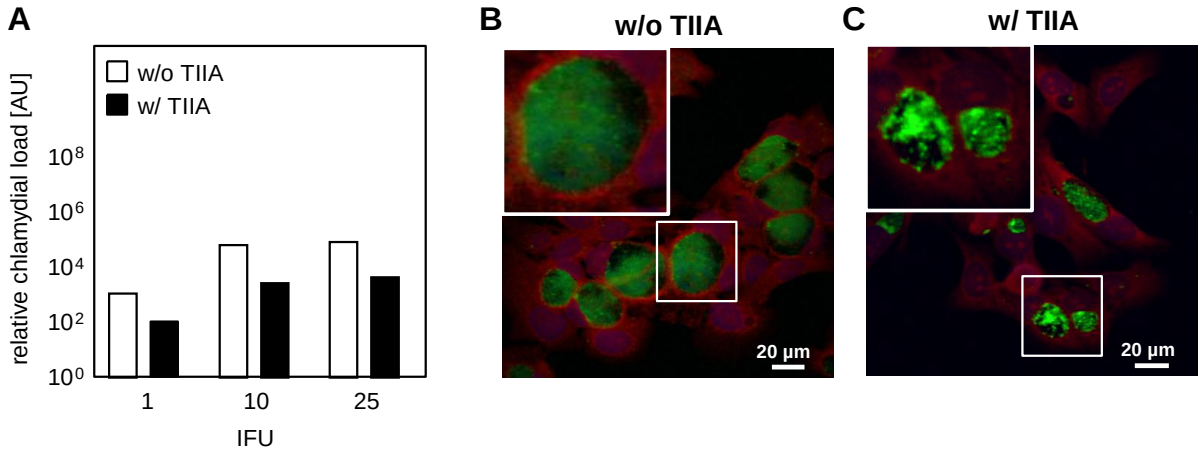

Figure 23: Tanshinone IIA treatment reduces eGFP-*C. trachomatis* load and inclusion size. HEp-2 cells were infected with eGFP-*C. trachomatis* (1, 10 or 25 IFUs) and in parallel treated with (w/) or without (w/o) Tanshinone IIA (TIIA, 25 µM). After 48 hours the cells were harvested followed by mRNA isolation. (**A**) Quantification of relative chlamydial load was assessed using qRT-PCR. (**B-C**) Infected cells (10 IFU) (**B**) w/o and (**C**) w/ TIIA were fixed after 48 hours with methanol, immunostained with IMAGEN Chlamydia kit (chlamydiae-LPS green; cytoplasm red) and counterstained with DAPI (blue). Data is presented as mean ± SD. Immunofluorescence images are representative of three independent experiments (n = 1 - 3).

3.1.5 Tanshinone IIA treatment induces a persistence-like C. pneumoniae phenotype

To investigate if Tanshinone IIA treatment causes a persistent *C. pneumoniae* infection we examined whether this phenotype is reversible, as this is a main characteristic of persistence (Nelson et al., 2005; Wyrick, 2010). We removed the inhibitor by media change and later analyzed inclusion morphology with immunofluorescence microscopy. We found that without removal, all inclusions remained small with an aberrant shape (100% ± 0.0%) (**Figure 24 A+C**). In contrast, 48 hours after removal almost half of all inclusions (43.2% ±15.2%) increased in size, indicating they returned to their replicative developmental cycle (**Figure 24 B+C**).

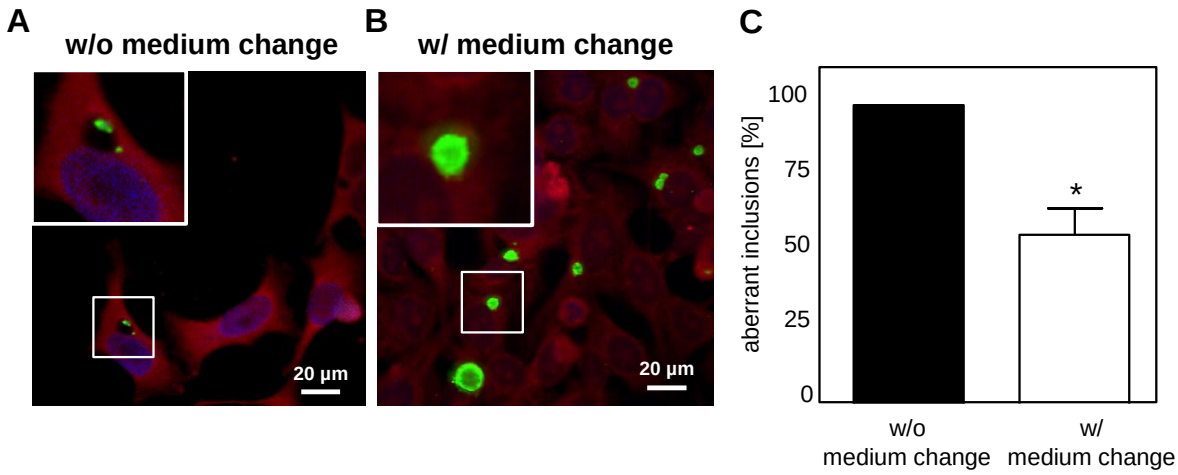

Figure 24: Effect of Tanshinone IIA is reversible as removal results in a return to replicative development cycle. HEp-2 cells were infected with *C. pneumoniae* (10 IFU) and Tanshinone IIA (TIIA, 25µM) was applied in parallel followed by incubation for 48 hours. Cells were cultured w/ or w/o TIIA for additional 48 hours. (**A**) Cells with (w/) and without (w/o) medium change were fixed with methanol and immunostained with IMAGEN Chlamydia kit (chlamydiae-LPS green; cytoplasm red) and counterstained with DAPI (blue). (**B**) Quantification of aberrant inclusions during infection w/o and w/ medium change. Data represent the mean ± SD. Data and immunofluorescence images are representative of three independent experiments (n = 3). *p<0.05

Other indicators for a persistent chlamydiae infection are the chlamydial proteins, MOMP and cHsp60 and their ratio respectively. To confirm if Tanshinone IIA treatment is accompanied by more typical persistence characteristics we assessed the MOMP and cHsp60 mRNA expression after Tanshinone IIA treatment with qRT-PC (**Figure 25 A**). We found that mRNA level of MOMP significantly decreased over time starting at 24 hpi, while cHsp60 mRNA was regulated inversely, increasing significantly already after 4 hpi. Based on these data we calculated the ratio of MOMP:cHsp60 mRNA and found it to decrease significantly over time (4, 24, 48 and 72 hpi) in comparison to that of untreated cells (**Figure 25 B**).

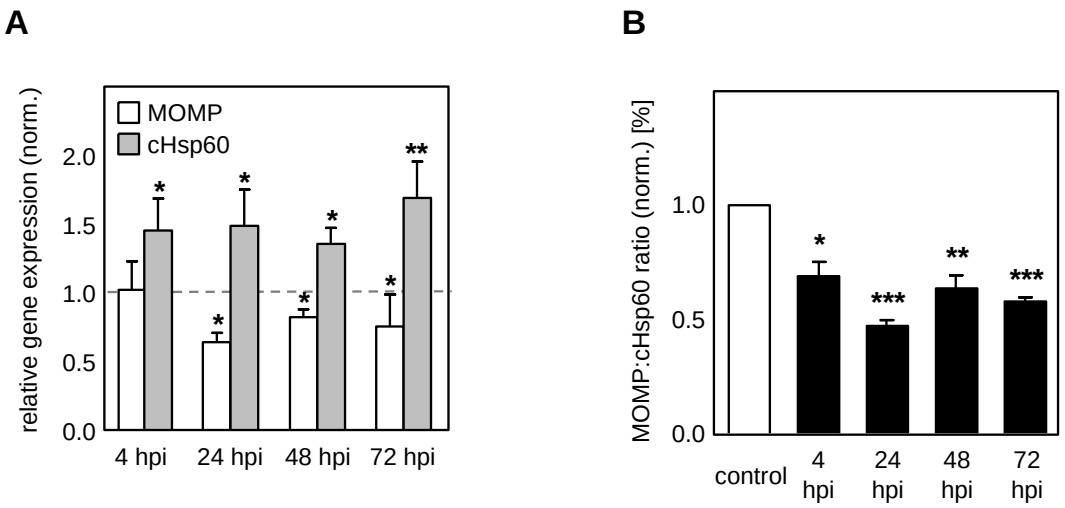

Figure 25: Tanshinone IIA treatment influences MOMP and cHsp60 mRNA expression resulting in lower MOMP:cHsp60 ratio. HEp-2 cells were infected with 10 IFUs of *C. pneumoniae* (*Cpn*) and in parallel treated with (w/) or without (w/o) Tanshinone IIA (TIIA, 25 µM). As control uninfected cells w/ and w/o TIIA treatment were used. (**A**) Relative gene expression of MOMP and cHsp60 4, 24, 48 and 72 hpi, normalized against infected cells w/o TIIA (dashed grey line). (**B**) Quantification of MOMP:cHsp60 ratio based on the mRNA expression data, normalized to control. Data, presented as mean ± SD, are representative of three independent experiments (n = 3). *p<0.05, **p<0.01

Additionally, we determined MOMP and cHsp60 protein expression with Western Blot analysis (**Figure 26 A**). In the presence of Tanshinone IIA the expression of MOMP and cHsp60 was reduced in comparison to that of infected cells in the absence of Tanshinone IIA (**Figure 26 A**). As expected, MOMP and cHsp60 were not detectable in uninfected cells. Using densitometry, we found that Tanshinone IIA treatment strongly altered protein expression of MOMP and consequently cHsp60. After treatment the expression of both proteins was significantly reduced when compared to untreated cells (100% ± 0.0%). After 48 hpi 17.2% (± 7.3%) MOMP and 41.7% (± 13.9%) cHsp60 waere detected. For MOMP the expression remained significantly reduced also after 72 hpi where 19.5% (± 7.9%) MOMP and 67.7% (± 19.0%) cHsp60 were expressed (**Figure 26 B**). Even though MOMP and cHsp60 protein expression decreased, the expression of cHsp60 protein was always significantly higher in comparison to expression of MOMP protein. We again determined the MOMP:cHsp60 ratio, now based on the protein expression data, as indicator for persistence. In Tanshinone IIA treated cells we observed that the MOMP:cHsp60 ratio was significantly decreased (48 hpi 59.9% ± 5.7%; 72 hpi 71.4% ± 5.4%) in contrast to that of the infected but untreated cells (100% ± 0.0%) (**Figure 26 C**).

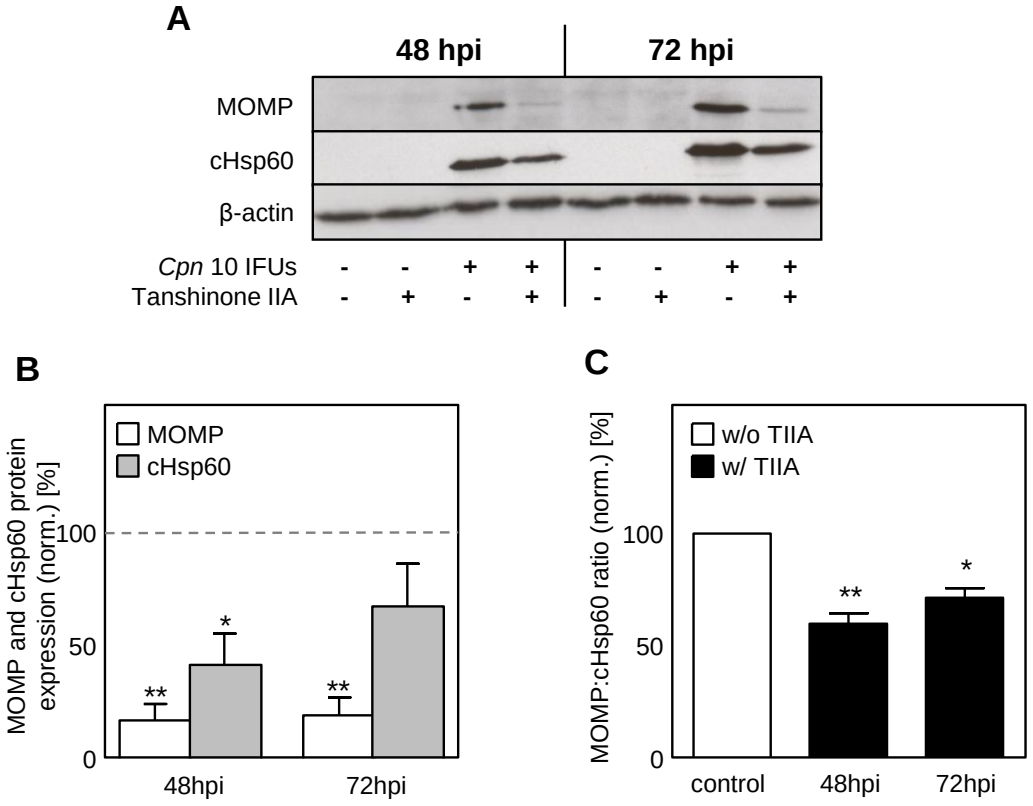

Figure 26: Tanshinone IIA treatment reduces MOMP and cHsp60 protein level and results in a decreased MOMP:cHsp60 ratio. HEp-2 cells were infected with 10 IFUs of *C. pneumoniae* (*Cpn*) and in parallel treated with (w/) or without (w/o) Tanshinone IIA (TIIA, 25 µM). As control uninfected cells w/ and w/o TIIA treatment were used. (**A**) Western Blot analysis of MOMP and cHsp60, 48 and 72 hpi. (**B**) Quantification of MOMP and cHsp60 protein expression using densitometry, normalized against infected cells w/o TIIA (dashed grey line). (**C**) Quantification of MOMP:cHsp60 ratio based on the protein expression data, normalized to control. Data, presented as mean ± SD, are representative of three independent experiments (n = 3). *p<0.05, **p<0.01

3.1.6 Tanshinone IIA treatment interferes with the energy balance of the host cell

Since Tanshinone IIA treatment seems to change the replicate *C. pneumoniae* infection into a persistent one, we wanted to identify an underlying mechanism, uncovering how Tanshinone IIA alters chlamydiae infection. Chlamydiae are hypothesized to be energy parasites and so they are highly dependent on the host cell ATP/glucose supply (Moulder, 1970). Tanshinone IIA inhibits AP-1, which is known to regulate genes responsible for cellular energy balance, such as *glut-1* (Santalucía et al., 2003). With qRT-PCR we quantified *glut-1* gene expression with and without *C. pneumoniae* infection and Tanshinone IIA treatment respectively. We did not find a (significant) change in *glut-1* expression after 4 h (Figure 27). But after 24 h the expression of the *glut-1* mRNA significantly increased, in comparison to the control, when Tanshinone IIA was added to the uninfected or infected cells. After 48 h and 72 h the *glut-1* mRNA expression was up-regulated after chlamydiae infection, Tanshinone IIA treatment or both, but the up-regulation was only significant after 48 h.

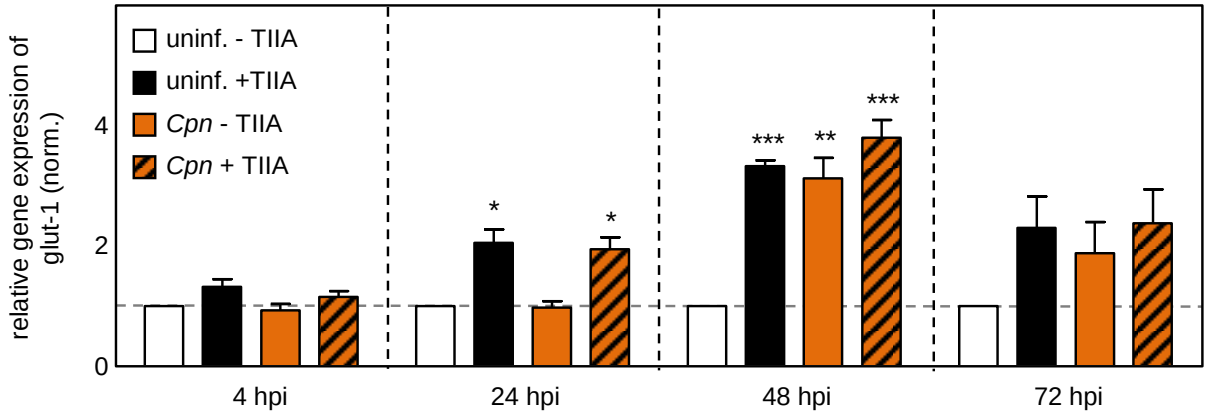

Figure 27: *glut-1* mRNA expression is regulated during *C. pneumoniae* infection and affected upon Tanshinone IIA treatment. HEp-2 cells were infected with 10 IFUs of *C. pneumoniae* (*Cpn*) and in parallel treated with (w/) or without (w/o) Tanshinone IIA (TIIA, 25 µM) for. As control uninfected cells w/ and w/o TIIA treatment were used. mRNA was isolated at 4, 24, 48 and 72 hpi. Relative gene expression of *glut-1* at the indicated time points, normalized against uninfected cells w/o TIIA. Data, presented as mean ± SD, are representative of four independent experiments (n = 4). *p<0.05, **p<0.01, ***p<0.001

We next verified if the influence of Tanshinone IIA on mRNA expression can also be seen for other genes than *glut-1*, such as *c-Jun*. After 4 h we could already detect a significant up-regulation of *c-Jun* mRNA compared to the control when Tanshinone IIA was added to uninfected or infected cells (**Figure 28**). This increase was also observed after 24 h, but was only significant for cells which were infected and Tanshinone IIA treated. After 48 h the up-regulation of *c-Jun* mRNA was significant when cells were infected, Tanshinone IIA treated or both. This significant up-regulation was also observed after 72 h, but was not significant.

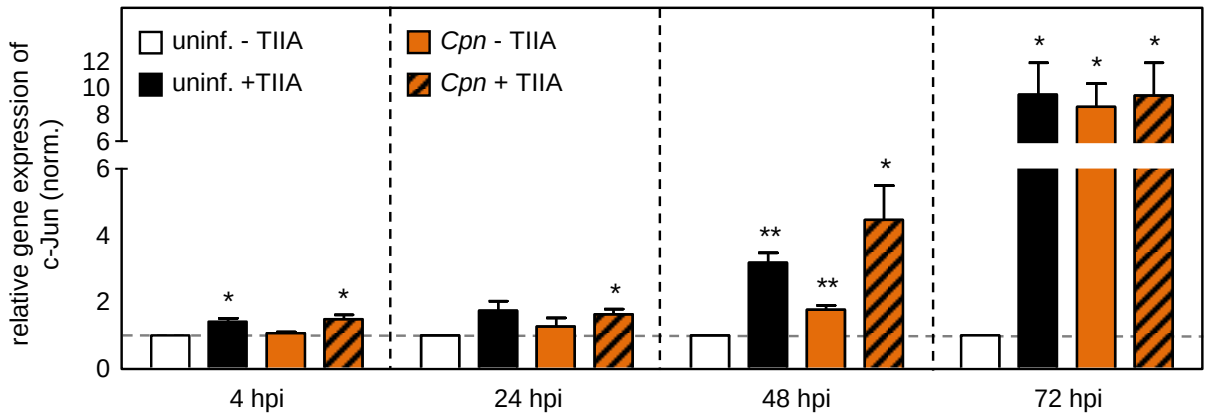

Figure 28: *C. pneumoniae* infection and Tanhinone IIA treatment regulate c-Jun mRNA expression at late time points. HEp-2 cells were infected with 10 IFUs of *C. pneumoniae* (*Cpn*) and in parallel treated with (w/) or without (w/o) Tanshinone IIA (TIIA, 25 µM) for. As control uninfected cells w/ and w/o TIIA treatment were used. mRNA was isolated at 4, 24, 48 and 72 hpi. Relative gene expression of c-Jun at the indicated time points, normalized against uninfected cells w/o TIIA. Data, presented as mean ± SD, are representative of four independent experiments (n = 4). *p<0.05, **p<0.01, ***p<0.001

To further evaluate the role of chlamydiae as energy parasites in our model, we assessed ATP as another possible indicator for changes in energy metabolism. We could observe that with *C. pneumoniae* infection the amount of ATP increased 6 hpi in comparison to ATP levels in cells which were treated with Tanshinone IIA (**Figure 29**). This increase was significant for infection with a low dose (10 IFU) of *C. pneumoniae*. After 12 hours the ATP level in the infected cells dropped and was now comparable to the ATP level of the control cells. In contrast, in the presence of Tanshinone IIA the ATP amount in infected cells (low and high dose) was significantly reduced 6 and 12 hpi compared to the untreated cells.

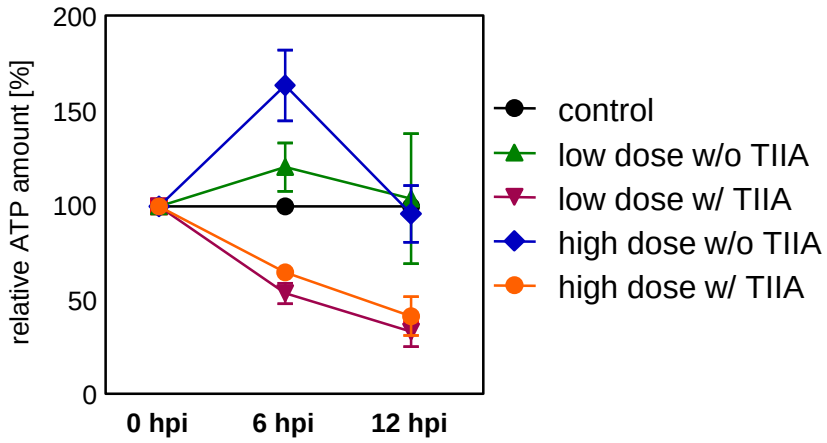

Figure 29: Tanshinone IIA treatment results in decreases ATP level 6 and 12 hpi. Quantification of relative ATP amount. HEp-2 cells were infected with 10 IFU (low dose) or 30 IFU (high dose) of *C. pneumoniae* (*Cpn*) and treated w/ or w/o Tanshinone IIA (TIIA, 25µM). Relative ATP levels were measured directly (0 hpi), 6 hpi and 12 hpi. Data, presented as mean ± SEM, are representative of three independent experiments (n = 3). * $p<0.05$

3.1.7 Autophagy (LC3/p62) is modulated in chlamydiae infection

Since it has been described that autophagy can be involved in chlamydial development and that Tanshinone IIA can modulate autophagy we investigated this pathway additionally (Al-Younes et al., 2011; Al-zeer et al., 2013; Li et al., 2015).

To investigate if chlamydial infection has an influence on autophagy, we used microtubule-associated protein 1A/1B-light chain 3 (LC3) and SQSTM1/p62 (p62) protein as indicators for autophagy activity. LC3 is expressed in two different forms, the cytosolic form LC3-I and the lipidated form LC3-II. When autophagy is induced, LC3-I to LC3-II conversion increases and p62 protein expression decreases. To measure induction of autophagy in *C. pneumoniae* infected cells, with and without Tanshinone IIA treatment, we assessed protein expression of LC3 and p62 after 4 and 48 hours post infection and treatment, using Western Blot and densitometry analysis (**Figure 30**). Using densitometry, we could not observe autophagy induction after 4 h. After 48 h the LC3 conversion significantly increased in infected cells and infected cells which were treated with Tanshinone IIA. However, in uninfected and untreated cells the LC3 conversion was also increased after 48 h. Regarding p62, we observed

a reduced expression after 48 h, which became significant in the infected cells which were Tanshinone IIA treated.

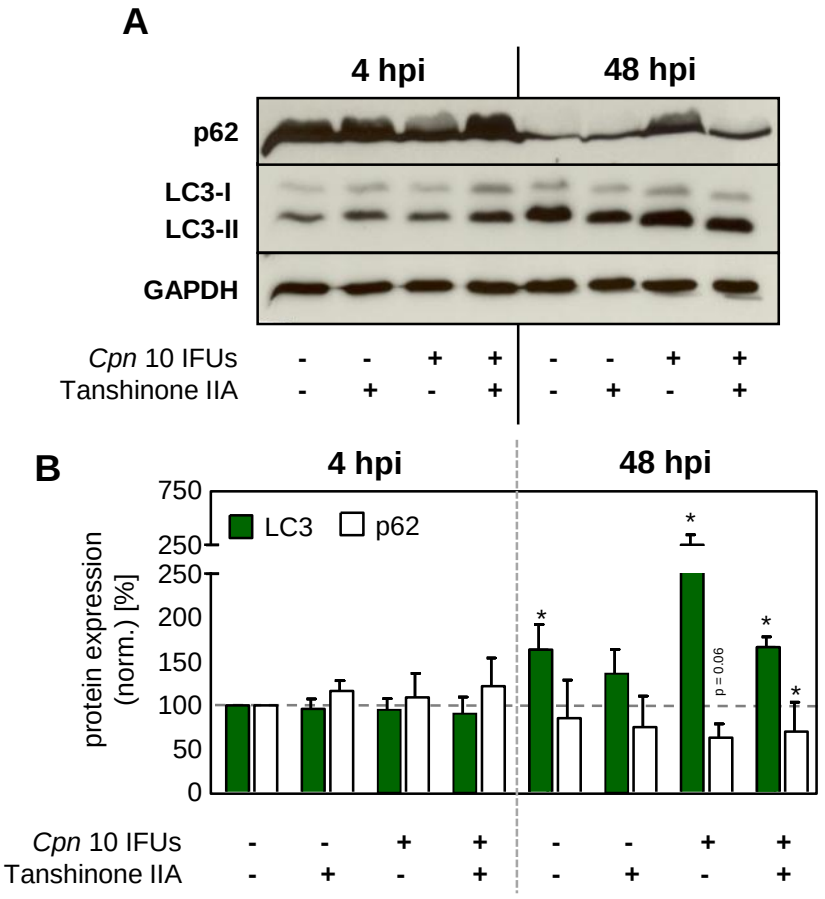

Figure 30: *C. pneumoniae* infection and Tanshinone II treatment induce autophagy 48 hpi. Uninfected or *C. pneumoniae* infected (*Cpn*, 10 IFU) HEp-2 cells were treated with and without Tanshinone IIA (TIIA, 25 µm). Lysates were prepared 4 hpi and 48 hpi. (**A**) Western Blot analysis of the LC3 and p62 at the indicated time points. (**B**) Quantification of protein expression using densitometry. Data were normalized against control (uninfected, untreated, 4h) and presented as mean ± SD. Data and immunoblots are representative of three independent experiments (n = 3). *<p 0.05

In addition, we also investigated autophagy induction during *C. trachomatis* infection using Western Blot and densitometry analysis (**Figure 31**). With densitometry we did not find significant differences in LC3 conversion and p62 expression after 4 h. After 48 h the LC3 conversion increased in all conditions but was only significantly higher in the uninfected, untreated cells. In concordance, the expression of p62 decreased in all conditions, but only significant in the infected cells.

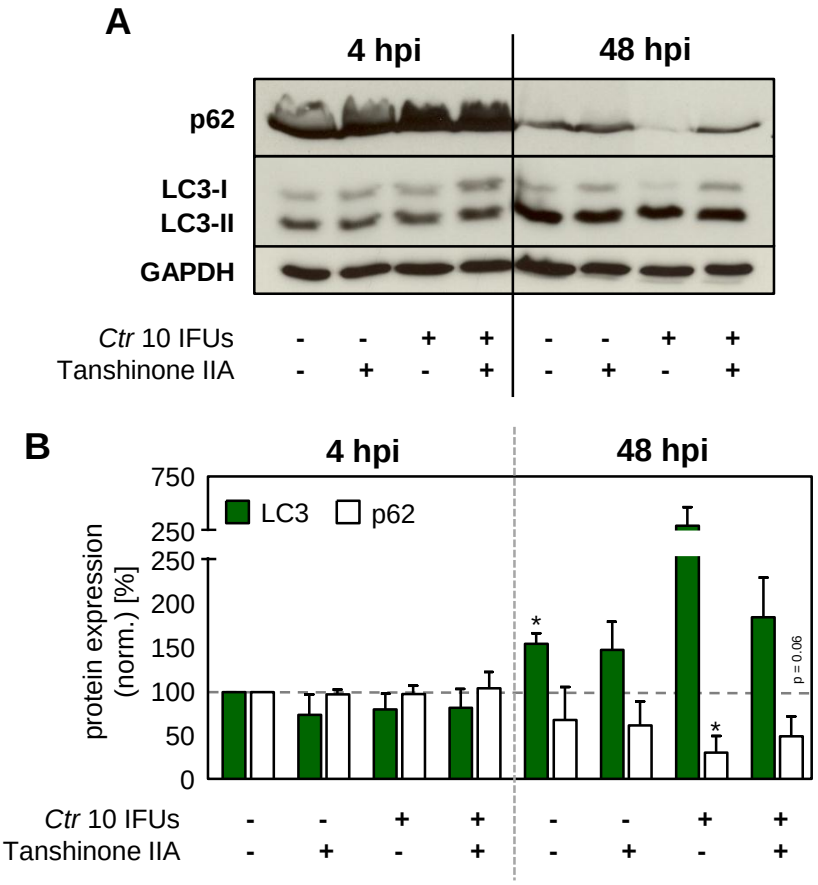

Figure 31: Autophagy induction during *C. trachomatis* infection and Tanshinone II treatment. Uninfected or *C. trachomatis* infected (*Ctr*, 10 IFU) HEp-2 cells were treated with and without Tanshinone IIA (TIIA, 25 µm). Lysates were prepared 4 hpi and 48 hpi. (**A**) Western Blot analysis of the indicated proteins. (**B**) Quantification of protein expression using densitometry. Data were normalized against control (uninfected, untreated, 4h) and presented as mean ± SD. Data and immunoblots are representative of three independent experiments (n = 3). *<p 0.05

These data show that autophagy, 48 hours after *C. pneumoniae* or *C. trachomatis* infection, is induced in the HEp-2 cells. Tanshinone IIA treatment did not result in increased autophagy induction, as the LC3 and SQSTM1/p62 level were comparable to those present in the uninfected and untreated cells.

Next, we modulated autophagy using the autophagy inhibitor spautin-1 and autophagy inducers PI-103, rapamycin and AZD-8055, as established in our group for human macrophages. We applied different concentrations of each autophagy modulator and prepared lysates for Western Blot analysis afterwards (**Figure 32**).

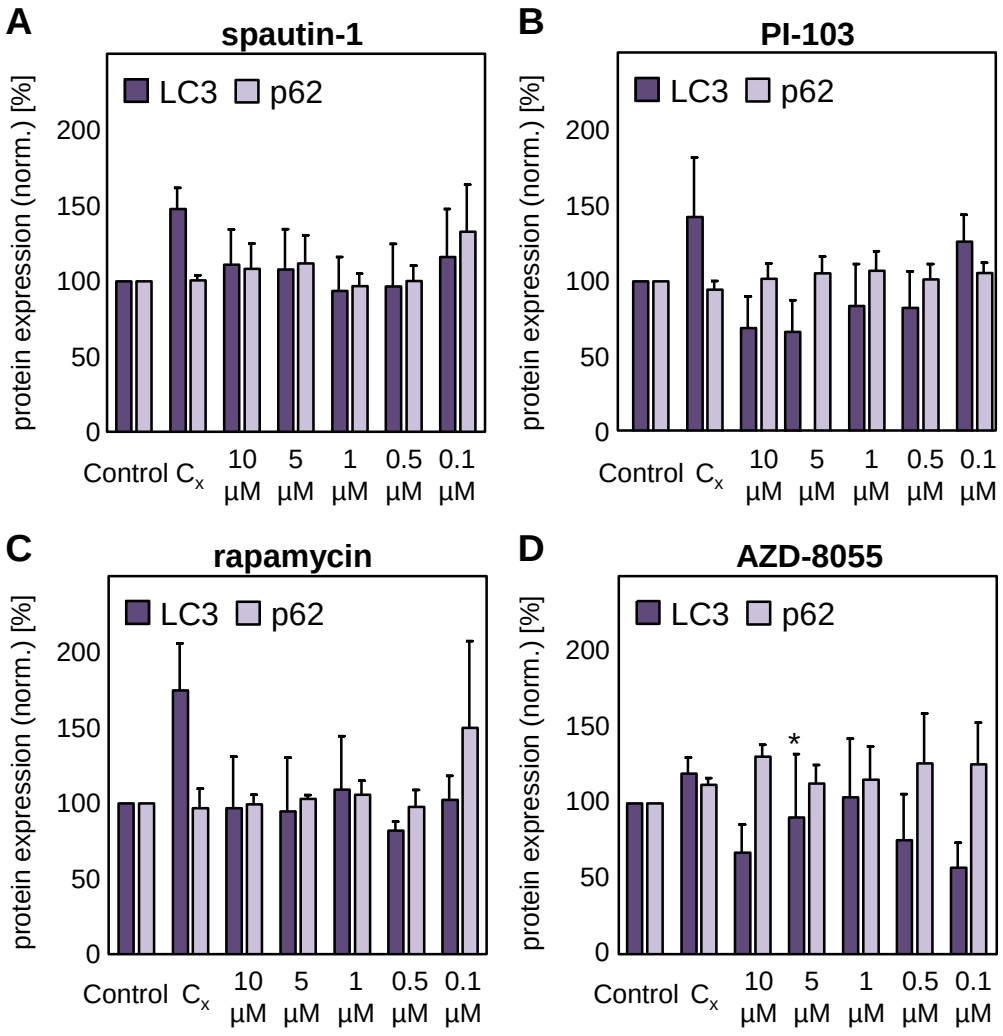

Figure 32: Treatment with autophagy modulators for 30 min does not affect autophagy level in HEp-2 cells. HEp-2 cells were treated with different concentrations of 4 different autophagy modulators, cycloheximide (C_x, 1 µg/ml) or left untreated (control). Lysates were prepared 30 min after treatment and quantified using Western Blot analysis and densitometry. Protein expression of LC3 and p62 after 30 min of (**A**) spautin-1 (**B**) PI-103 (**C**) rapamycin and (**D**) AZD-8055. Data presented as mean ± SD are representative of three independent experiments (n = 3). *p<0.05

Densitometry analysis revealed no significant autophagy modulation after 30 min of treatment with either autophagy inhibitor spautin-1 (**Figure 32 A**) or autophagy inducers PI-103 (**Figure 32 B**), rapamycin (**Figure 32 C**) or AZD-8055 (**Figure 32 D**). As this 30 min pre-treatment with the autophagy modulators had little effect we tested 2 h treatment additionally. Again no classical autophagy induction was detectable (data not shown).

3.2 Part II

3.2.1 Chlamydiae infection of primary human monocyte-derived macrophages

Antibiotic treatment is known to affect chlamydiae infection. The primary human macrophages (hMDM), which are used as our *in vitro* model, are generated in medium supplemented with penicillin-streptomycin (PS). To assess the effect of PS, we performed infection experiments using *C. trachomatis* in pro-inflammatory hMDM I and anti-inflammatory hMDM II with (w/) and without (w/o) PS. Using immunofluorescence microscopy infection rates were quantified. In the absence of PS, we observed both hMDM I and hMDM II to be infected. By applying a higher infection dose (1, 10 or 25 IFU) a higher infection rates was reached, which did not strongly differ over time (24 and 48 hpi). Remarkably, the presence of PS did not significantly alter the course of infection, either in hMDM I or hMDM II (**Figure 33**).

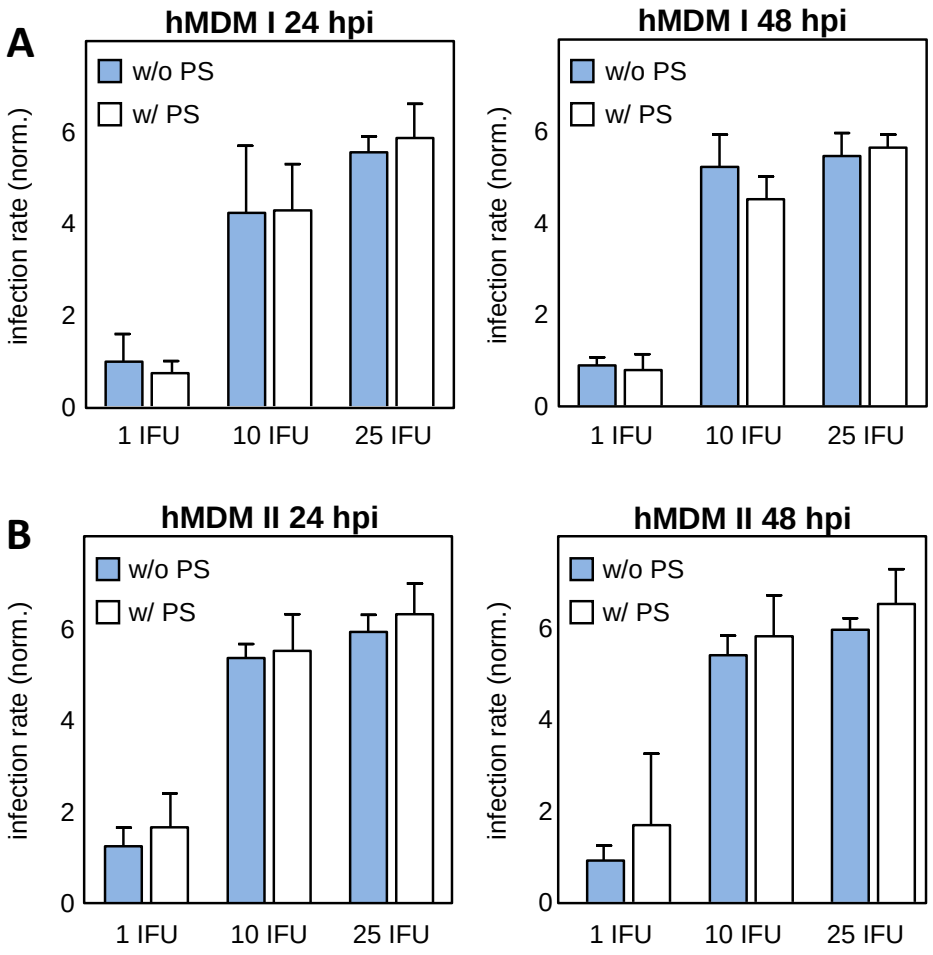

Figure 33: Presence of penicillin-streptomycin does not affect the infection rate of *C. trachomatis* in human primary macrophages. Primary human macrophages type I or type II were generated of human buffy coats and infected with 1, 10 or 25 IFU of *C. trachomatis* in the presence (w/) or absence (w/o) of penicillin-streptavidin (PS). Cells were methanol fixed after 24 or 48 hpi and immunostained. Infection rate was quantified by counting randomly of at least 300 cells. (**A**) Infection rate of hMDM I w/ or w/o PS after 24 or 48 hpi. (**B**) Infection rate of hMDM II w/ or w/o PS after 24 or 48 hpi. Data are presented as mean ± SD and are representative of three independent experiments (n = 3).

Next we characterized chlamydiae infection in type I and type II hMDM using the different chlamydiae species, *C. pneumoniae*, *C. trachomatis* (wildtype) and *C. trachomatis* expressing eGFP (transgenic) for infection and analyzed infection morphology with immunofluorescence microscopy. Infection with the different chlamydiae species resulted in a persistent-like infection of both macrophage phenotypes. More specifically, we observed small and aberrant inclusions, sometimes randomly distributed within the cells (**Figure 34**, white arrows).

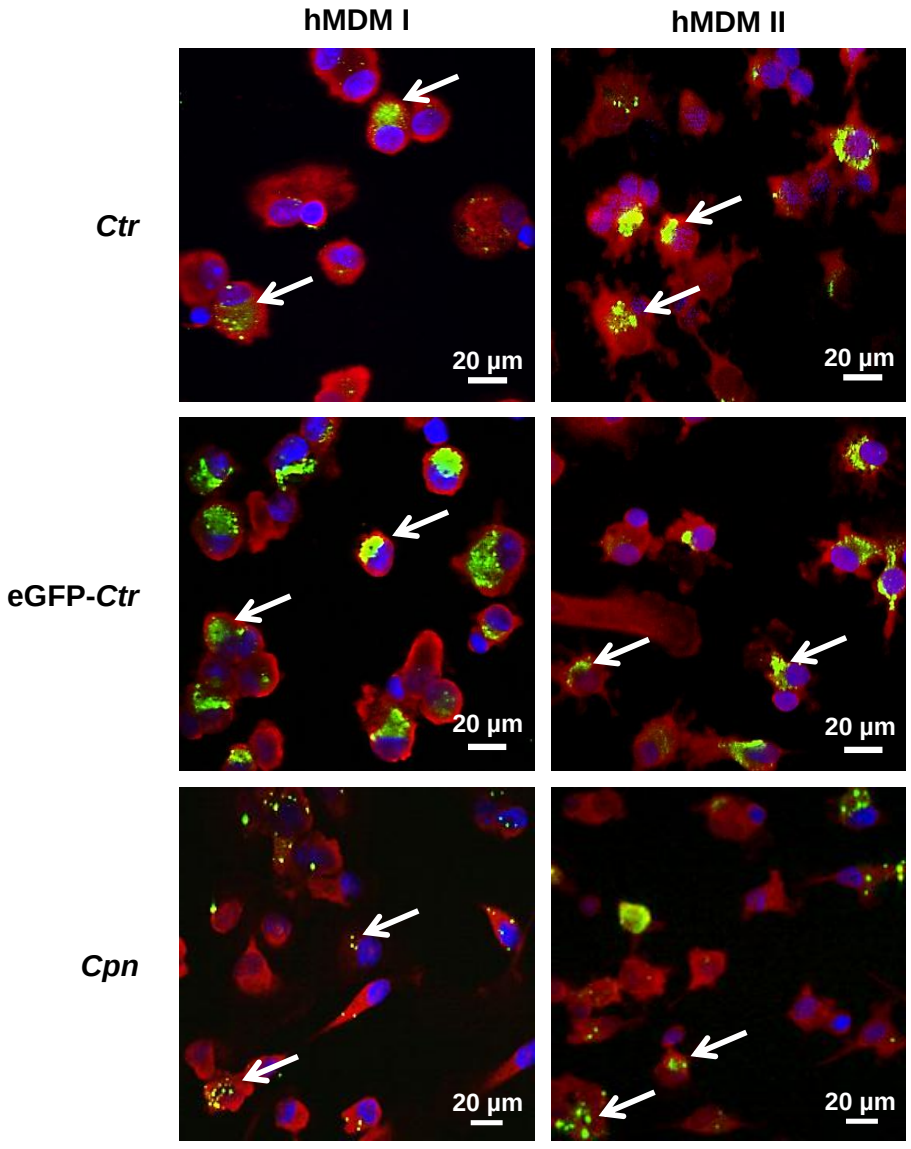

Figure 34: Chlamydiae infection of hMDM leads to a persistent infection phenotype. Human primary macrophages type I or type II were infected with 10 IFU of either *C. trachomatis* (*Ctr*), eGFP-*C. trachomatis* (eGFP-*Ctr*) or *C. pneumoniae* (*Cpn*). Cells were methanol fixed 48 hpi and immunostained with IMAGEN Chlamydia kit (chlamydiae-LPS green; cytoplasm red) and counterstained with DAPI (blue). White arrows indicate persistent chlamydiae inclusions. Immunofluorescence images are representative of three independent experiments (n = 3).

We then determined the chlamydial infection rate after 48 h in both, hMDM I and hMDM II. For all tested chlamydiae species the infection rate increased dose dependently (Figure 35). Infection with *C. trachomatis* wildtype or its transgenic variant resulted in comparable infection rates, whereas the infection rate of *C. pneumoniae* was always the lowest. Interestingly, hMDM II, compared to hMDM I, were found to be more susceptible to infection with *C. trachomatis* and eGFP-*C. trachomatis*, but not to infection with *C. pneumoniae*.. More specifically, infection rates in hMDM II were higher than in hMDM I after infection with 10 or 15 - 25 IFUs (**Figure 35 D + A-C)**.

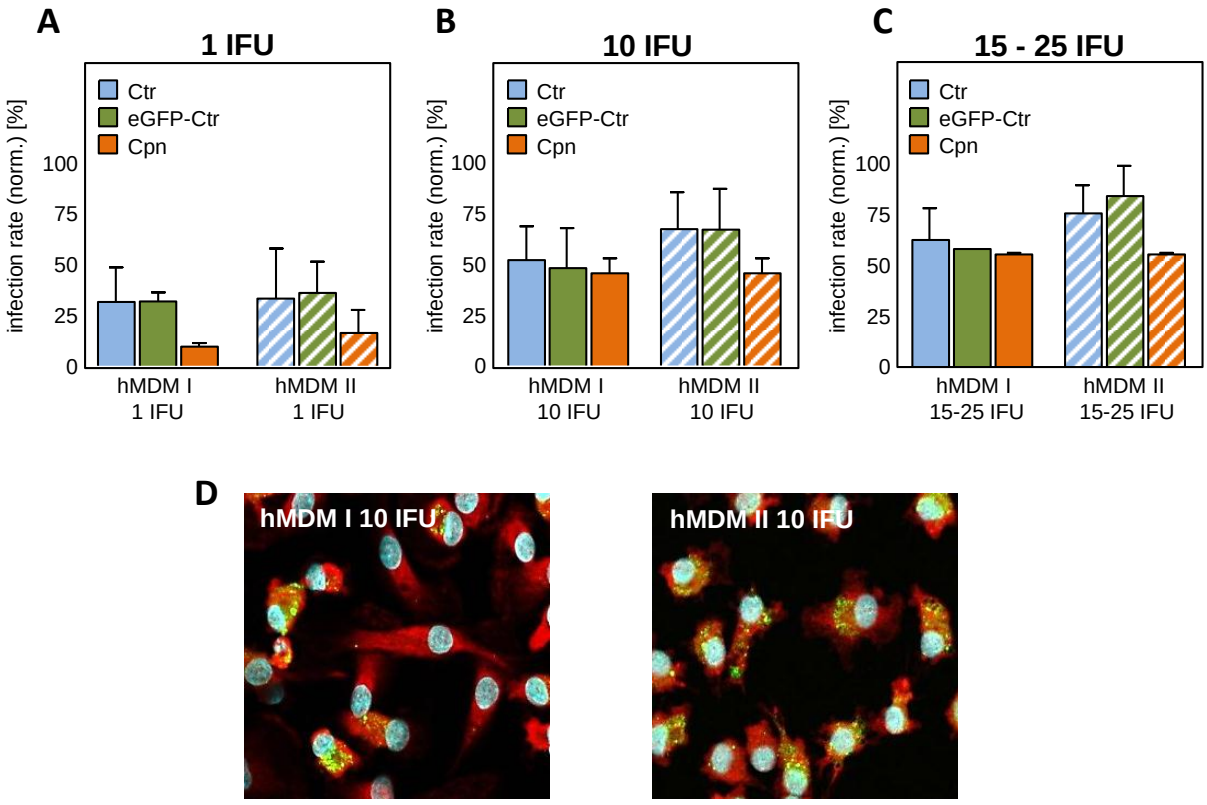

Figure 35: Chlamydial infection rate increased dose dependently and is higher in hMDM II compared to hMDM I. Human primary macrophages type I (filled bars) or type II (dashed bars) were infected with different doses of either *C. trachomatis* (*Ctr*), eGFP-*C. trachomatis* (eGFP-*Ctr*) or *C. pneumoniae* (*Cpn*). Cells were methanol fixed 48 hpi and immunostained. Infection rate was assessed by randomly counting 300 cells after infection with (**A**) 1 IFU (**B**) 10 IFU or (**C**) 15-25 IFU of chlamydiae. (**D**) Representative immunofluorescence image of type I or type II hMDM after infection with 10 IFU of *C. trachomatis.* Data, presented as mean ± SD, and immunofluorescence images are representative of three independent experiments (n = 3).

In addition to infection rates we assessed the chlamydial load in the hMDMs by quantification of chlamydial 16S rRNA with qRT-PCR. Focusing on the different species, we found that an equal infection dose (1, 10 or 15 - 25 IFU) of either *C. trachomatis*, eGFP-*C. trachomatis* or *C. pneumoniae*, resulted in a comparable bacterial load (**Figure 36 A-C**). We observed that a higher infection dose resulted in an increased infection rate, however chlamydial load did not increase dose dependently in either hMDM I or hMDM II (Figure 36). Interestingly the chlamydial load was always higher in hMDM I cells as compared to hMDM II (**Figure 36**).

In contrast to the infection rates being lower for *C. pneumoniae* as compared to wildtype and transgenic *C. trachomatis,* the chlamydial load upon infection between all three species was similar.

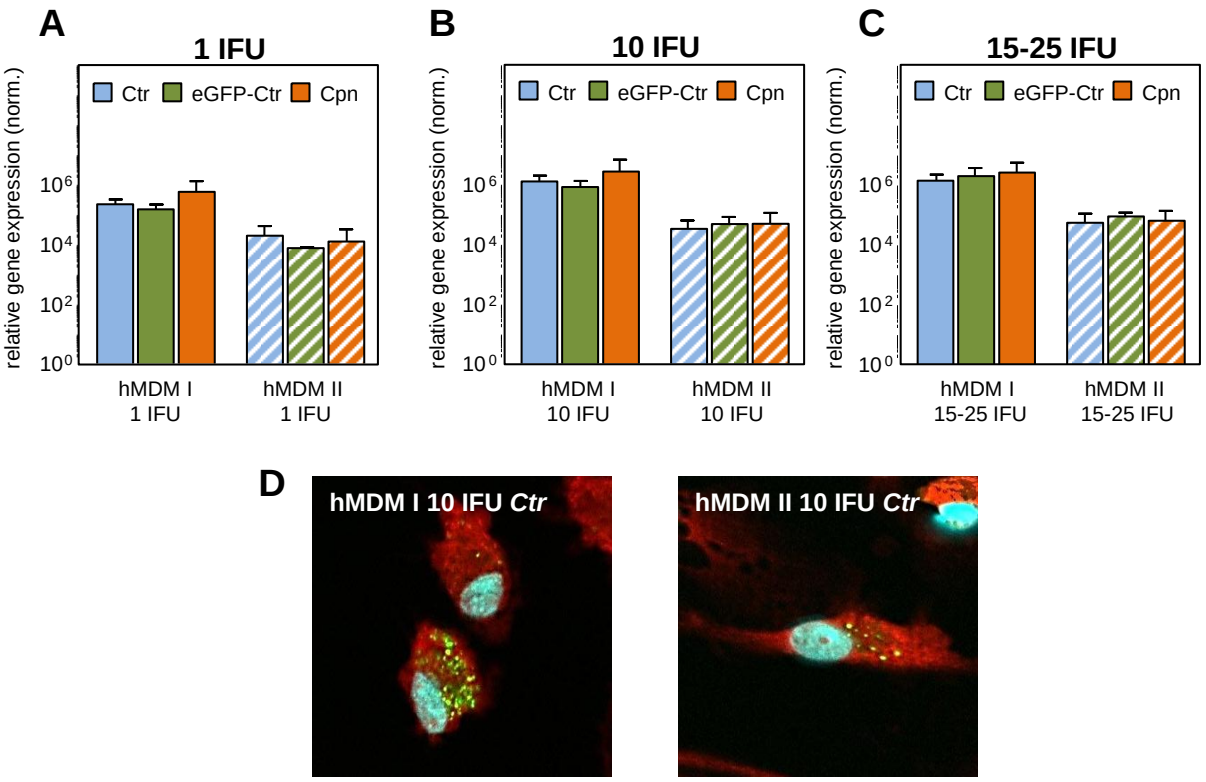

Figure 36: Chlamydial load is higher in hMDM I after infection with different chlamydiae species. Human primary macrophages type I (filled bars) or type II (dashed bars) were infected with different doses of either *C. trachomatis* (*Ctr*), eGFP-*C. trachomatis* (eGFP-*Ctr*) or *C. pneumoniae* (*Cpn*). After 48 hours the cells were harvested followed by mRNA isolation. Quantification of relative chlamydial load after infection with (**A**) 1 IFU (**B**) 10 IFU or **C**) 15-25 IFU was assessed using qRT-PCR. D) Representative immunofluorescence image of type I or type II hMDM after infection with 10 IFU of *C. trachomatis.* Data, presented as mean ± SD, and immunofluorescence images are representative of three independent experiments (n = 3).

As chlamydiae infection of hMDM typically results in a persistent phenotype consequently chlamydial load should not increase over time. Indeed, we did not observe significant differences in bacterial load of the different chlamydiae species over time in either hMDM I or hMDM II (**Figure 37**).

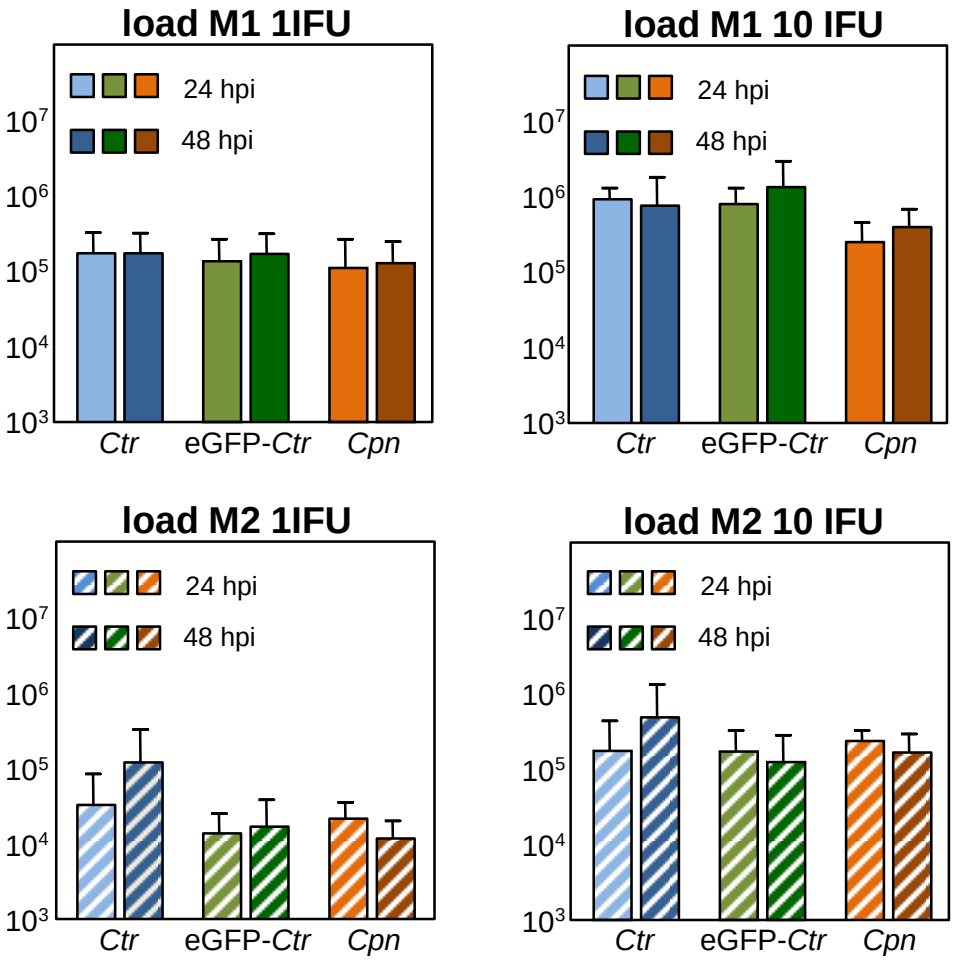

Figure 37: Chlamydial load in type I or type II macrophages does not increase over time. Human primary macrophages type I (filled bars) or type II (dashed bars) were infected with different doses of either *C. trachomatis* (*Ctr*), eGFP-*C. trachomatis* (eGFP-*Ctr*) or *C. pneumoniae* (*Cpn*). After 24 and 48 hours the cells were harvested followed by mRNA isolation. Quantification of relative chlamydial load after infection was assessed using qRT-PCR. Data, presented as mean ± SD, are representative of three independent experiments (n = 3).

In summary, more hMDM II get infected with *C. trachomatis* or eGFP-*C. trachomatis*, although chlamydial load is higher in hMDM I . The chlamydial load inside the hMDM did not significantly change over time, what confirms the mainly persistent infection morphology we observed with immunofluorescence microscopy. Of note, wildtype *C. trachomatis* and transgenic eGFP-*C. trachomatis* show comparable infection rates and chlamydial loads.

3.2.2 Replicative chlamydiae infection of hMDM

Upon infection of hMDM we predominantly found a persistent infection phenotype, however occasionally we observed larger inclusions, which resemble a replicative infection (**Figure 38 A**). Subsequently, we quantified the occurrence of these replication-like inclusions in hMDM. We found that after infection with *C. trachomatis* or eGFP-*C. trachomatis* replicative-like inclusions were present, whereas after infection with *C. pneumoniae* no such inclusions could be found. In addition, we observed that infection with both, wildtype and transgenic, *C. trachomatis* lead to more replicative-like inclusions in hMDM I in comparison to the amount of replicative inclusions in hMDM II (**Figure 38 B-C**).

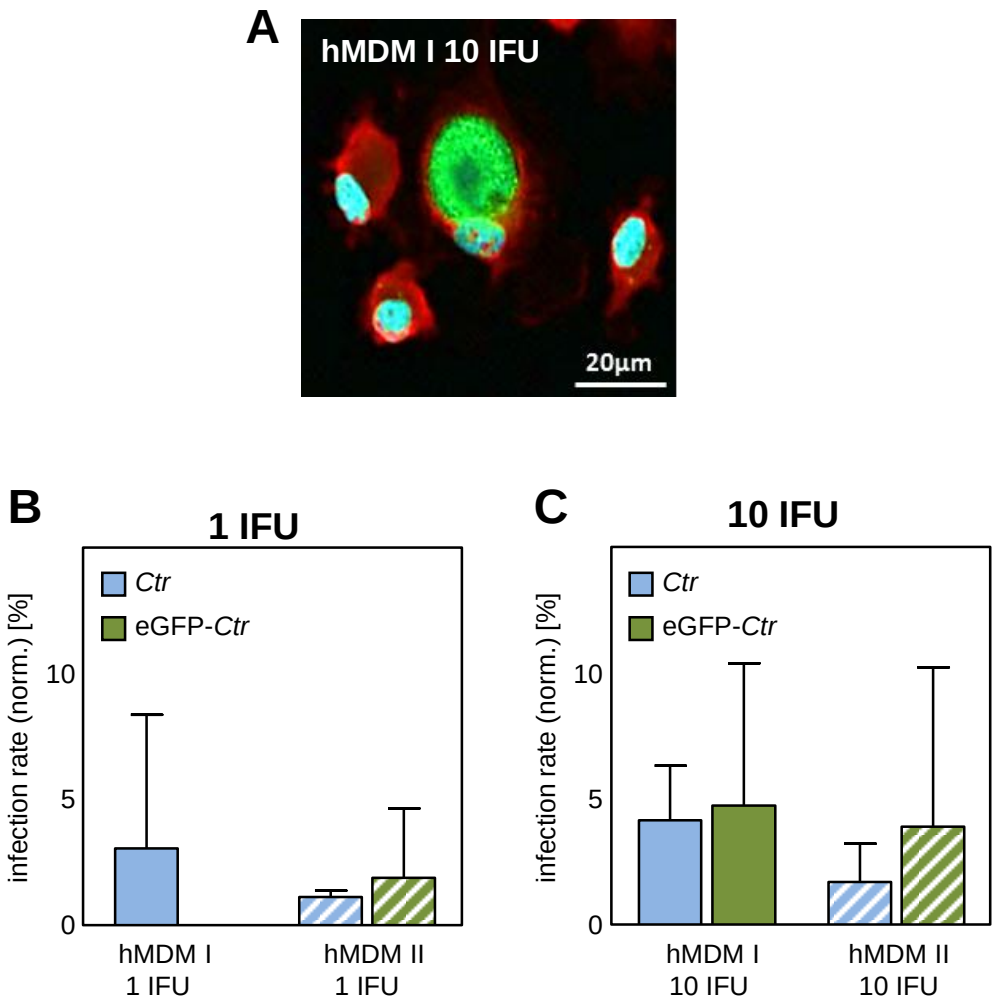

Figure 38: After chlamydiae infection replicative-like inclusions can be found in hMDM I and hMDM II. Human primary macrophages type I (filled bars) or type II (dashed bars) were infected with different doses of either *C. trachomatis* (*Ctr*), eGFP-*C. trachomatis* (eGFP-*Ctr*) or *C. pneumoniae* (*Cpn*). Cells were methanol fixed 48 hpi and immunostained. (**A**) Representative immunofluorescence image of a replicative-like inclusion in hMDM I after infection with 10 IFU of *C. trachomatis.* Occurrence of replicative inclusions was assessed by randomly counting 300 cells after infection with (**B**) 1 IFU or (**C**) 10 IFU. Data, presented as mean ± SD, and immunofluorescence images are representative of three independent experiments (n = 3).

As a consequence of replication, infectious elementary bodies should be present, allowing the chlamydiae to re-infect new cells. To test if the chlamydiae really developed normally, we performed chlamydial recovery experiments. The infected hMDM were lysed and the cell lysates were used for infection of epithelial cells (HEp-2). Interestingly, recovery from hMDM I resulted in larger sized inclusions as compared to recovery from hMDM II (**Figure 39**).

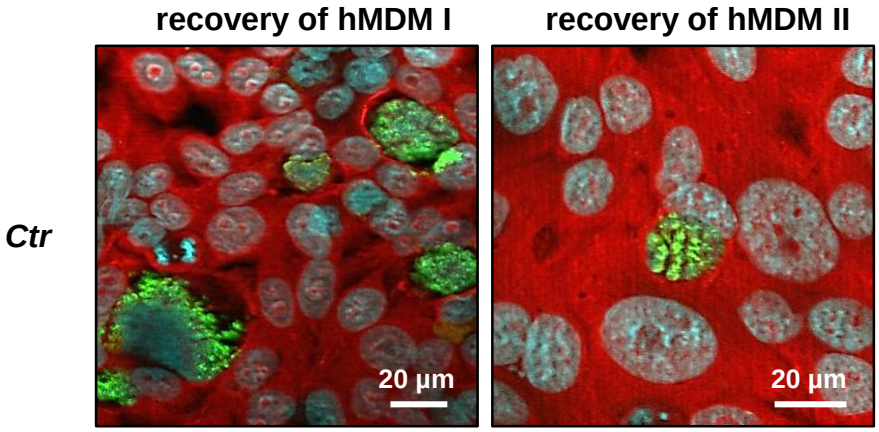

Figure 39: *C. trachomatis* recovery after infection of hMDM I or hMDM II shows the formation of replicative inclusions in Hep-2 cells. Human primary macrophages type I or type II were infected with 10 IFU of *C. trachomatis* for about 48 h. HEp-2 cells were infected with *C. trachomatis* extracted from either infected hMDM I or hMDM II. After 48 h cells were methanol fixed and immunostained with IMAGEN Chlamydia kit (chlamydiae-LPS green; cytoplasm red) and counterstained with DAPI (blue). Immunofluorescence images are representative of three independent experiments (n = 3).

3.2.3 The role of AP-1 in chlamydiae infection of hMDM

In HEp-2 cells, we demonstrated that AP-1 is regulated by chlamydial infection and consequently AP-1 inhibition induced persistence (Krämer et al., 2015). Therefore we now investigated whether AP-1 is also regulated by chlamydiae infection in hMDM, possibly involved in the persistence phenotype we observed. We determined protein expression of c-Jun and c-Fos using Western Blot and densitometry analysis. Focusing on c-Jun first, we found a higher c-Jun protein expression in hMDM I as compared to hMDM II (**Figure 40 A**). In both phenotypes chlamydiae infection did not significantly increase c-Jun protein expression. Over time (48 h) more c-Jun was expressed compared to expression after 24 h. In both phenotypes c-Fos expression was not altered after chlamydiae infection and also did not change over time. Using densitometry we found that, the expression of c-Jun after 24 h, increased upon infection (116.7% ± 31.9%) as compared to uninfected hMDM I (**Figure 40 B**). After 48 h c-Jun expression of uninfected (101.4% ± 27.8%) and infected (101.9% ± 45.7%) hMDM I was comparable. In comparison to the uninfected hMDM I after 24 hours (100% ± 0.0%), c-Jun protein expression in uninfected hMDM II was significantly lower after 24 h (51.7% ± 22.6%) and 48 h (38.1% ± 24.0%). In the infected hMDM II c-Jun protein

expression was reduced was well, but not significantly after 24 h (66.5% ± 31.1%) and 48 h (64.4% ± 38.0%) as compared to uninfected hMDM I cells after 24 h. Although no significant differences of c-Jun protein expression between uninfected and infected hMDM could be detected, the expression between hMDM I and hMDM II strongly differed.

Investigating c-Fos expression, Western Blot analysis showed no difference in protein level between uninfected and infected hMDM. In line, also quantification by densitometry did not show any differences in c-Fos expression in either hMDM I and hMDM II (**Figure 40 C**).

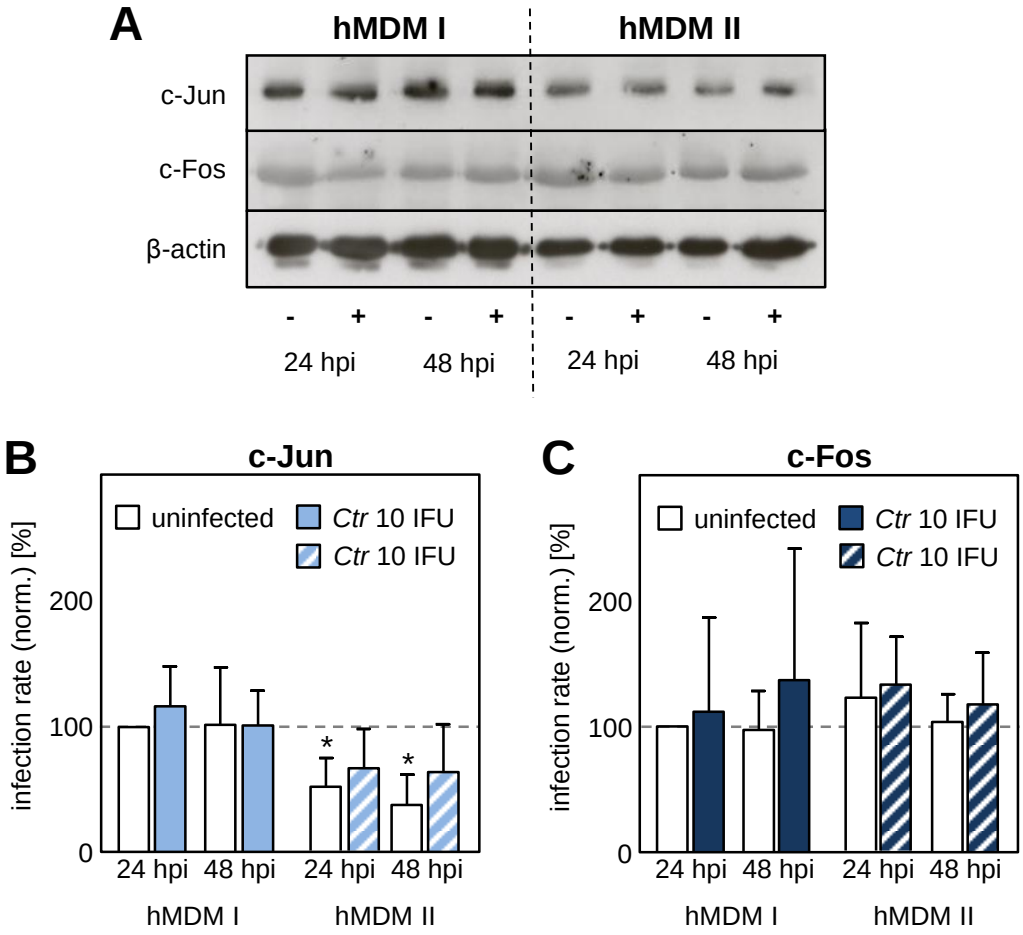

Figure 40: AP-1 proteins c-Jun and c-Fos are not regulated in hMDM I and hMDM II during *C. trachomatis* infection. Human primary macrophages type I (filled bars) or type II (dashed bars) were infected with 10 IFU of *C. trachomatis.* Lysates were prepared 24 hpi and 48 hpi. (**A**) Western Blot analysis of the indicated proteins. Protein expression of (**B**) c-Jun and (**C**) c-Fos was quantified using densitometry. Data, presented as mean ± SD, and immunoblots are representative of three independent experiments (n = 3). *<p 0.05

In addition to Western Blot analysis we used an immunofluorescence staining to detect c-Jun protein. We already showed c-Jun protein expression in hMDM II to be generally lower compared to expression in hMDM I. Furthermore, expression was upregulated after infection, a finding which could also be confirmed by immunofluorescence labeling of c-Jun (compare **Figure 41 A** white arrows with **Figure 41 B** white arrows) (**Figure 41**).

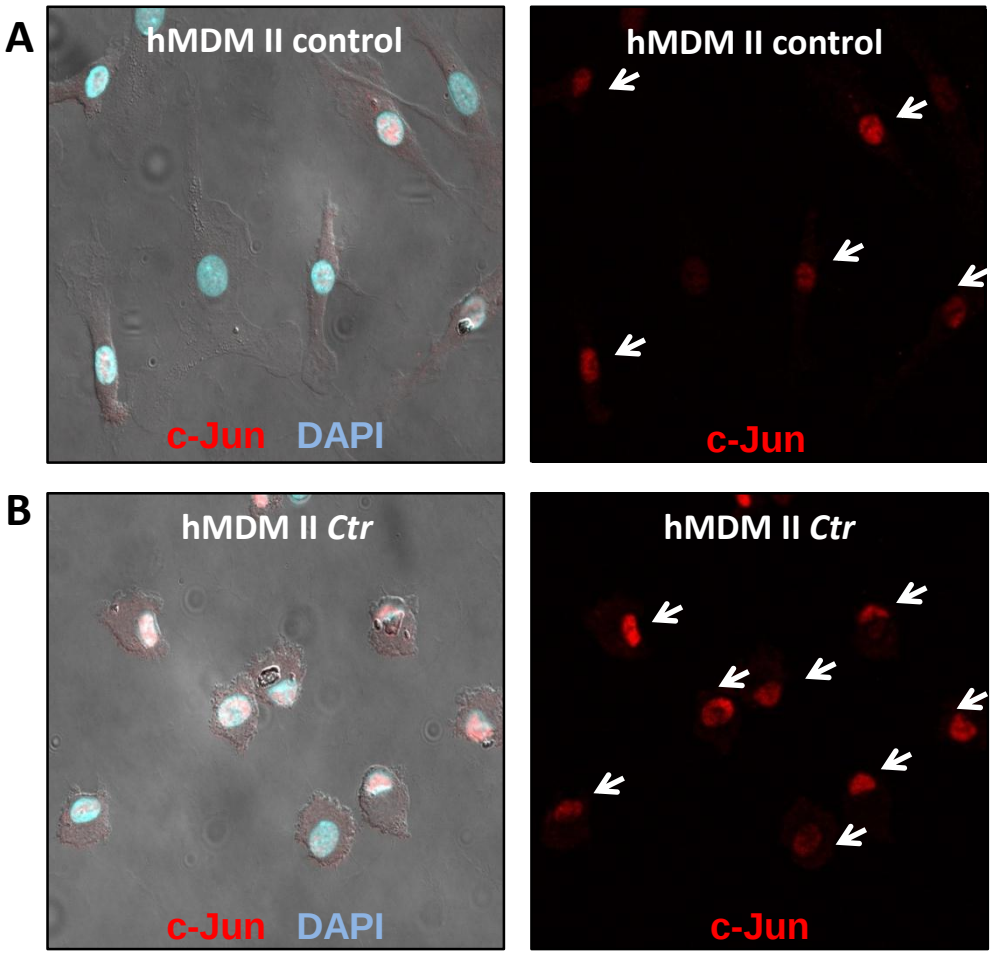

Figure 41: Upon *C. trachomatis* infection c-Jun increases hMDM II. Human primary macrophages type II were infected with 10 IFU of *C. trachomatis* (*Ctr*). After 48 h cells were methanol fixed and immunostained with an antibody against c-Jun (red) and counterstained with DAPI (blue). Expression of c-Jun in (**A**) uninfected (**B**) *C. trachomatis* infected hMDM II. Immunofluorescence images are representative of three independent experiments (n = 3).

3.2.4 Transfer of chlamydiae between HEp-2 cells and primary hMDM

As described above, direct infection of hMDM with chlamydiae usually results in the development of chlamydial persistence. Previous experiments of this research group revealed that the initial route of chlamydial entry appears to be of major importance for the outcome of hMDM infection (Rupp et al., 2009). It was shown that while the direct infection of macrophages led to persistence, the uptake of a chlamydiae-infected apoptotic neutrophil promoted the development of replicative inclusions within the hMDM.

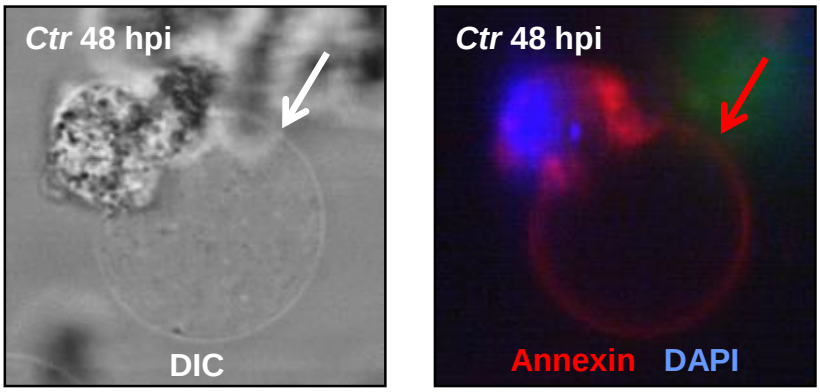

Figure 42: *C. trachomatis* infection leads to formation of Annexin V positive blebs which contain viable chlamydiae. HEp-2 cells were infected with *C. trachomatis* followed by Annexin V (red) and DAPI (blue) staining. Infection was imaged over time.

To gain a better understanding of the process of chlamydiae transfer, we used state of the art microscopy and live cell imaging. First, we investigated the possible formation of apoptotic, chlamydiae-containing blebs. We infected HEp-2 cells with *C. trachomatis* and added fluorescent labeled Annexin V and DAPI to the cells. Annexin V is a common marker for apoptosis as it binds phosphatidylserine and DAPI stains the DNA. Indeed, we found that 24 hpi the infected cells started to develop chlamydiae containing blebs (**Figure 42:** white arrow). Using differential interference contrast (DIC) we were able to visualize blebs, containing fast moving viable chlamydiae. The blebs were surrounded by the Annexin V stain, which is indicative for phosphatidylserine exposure (**Figure 42:** red arrow). In contrast, the uninfected cells did not become apoptotic (data not shown).

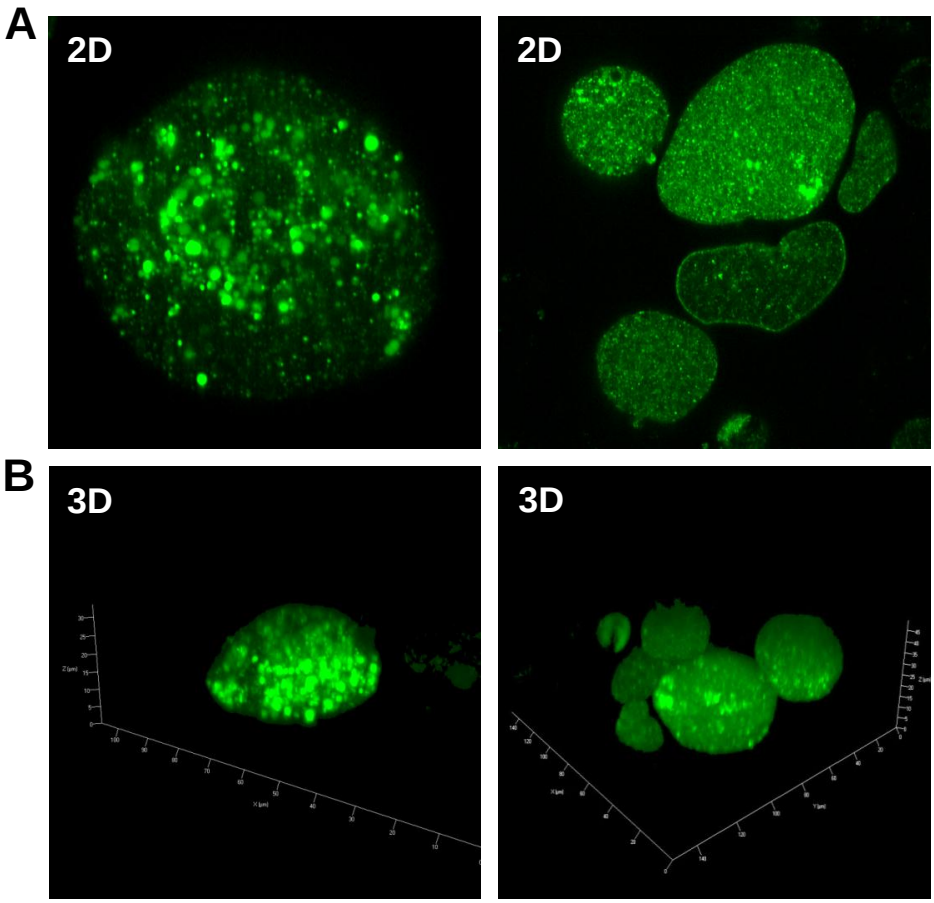

Figure 43: Use of eGFP-*C. trachomatis* enables the visualization of inclusion development over time. HEp-2 cells were infected with 10 IFU of eGFP-*C. trachomatis*. (**A**) Inclusion development was imaged over time. (**B**) Zeiss software ZEN 2012 was used to render live cell imaging data to generate 3D data.

For a better visualization of chlamydiae containing blebs we used eGFP-*C. trachomatis* in combination with live cell imaging. We investigated the chlamydial inclusion development and subsequent bleb release in HEp-2 cells over time. In contrast to wildtype *C. trachomatis* we were now able to clearly visualize the inclusions, containing the moving GFP-expressing chlamydiae (**Figure 43 A**). With the Zeiss software ZEN 2012, we are also able to render the pictures over time to get 3D live imaging data (**Figure 43 B**)

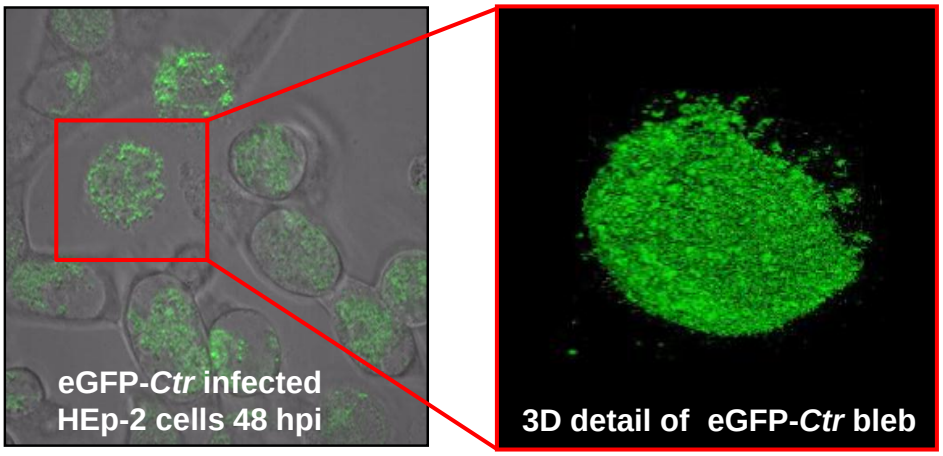

Figure 44: Infection of HEp-2 cells with eGFP-*C. trachomatis* results in the formation of blebs which contain moving chlamydiae. HEp-2 cells were infected with 10 IFU of eGFP-*C. trachomatis*. Bleb formation was imaged over time. Zeiss software ZEN 2012 was used to render bleb to generate 3D image.

As seen for wildtype *C. trachomatis*, we found the formation of the chlamydiae-containing blebs after approximately 24 hpi (data not shown). After 48 h we visualized an eGFP-*C. trachomatis* containing bleb in 2D and rendered it in 3D (**Figure 44**). These bleb structures, containing viable, moving chlamydiae, were observed to float over the other adherent cells.

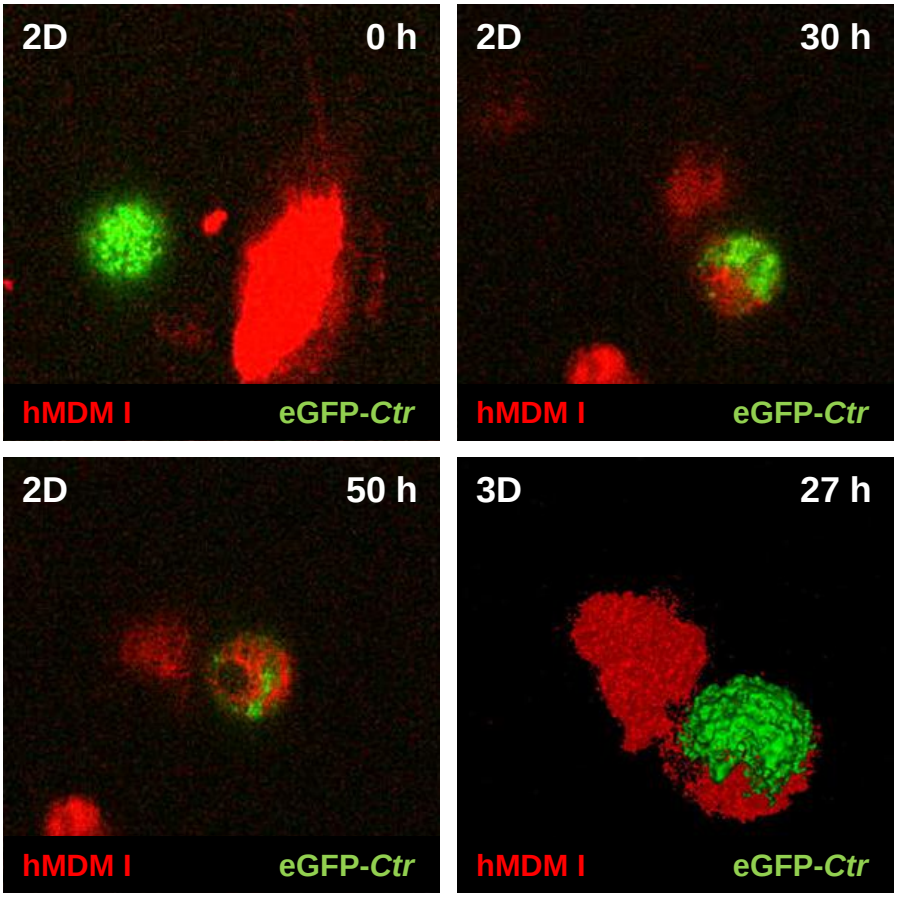

Figure 45: hMDM recognizes and interacts with chlamydial bleb. HEp-2 cells were infected with 10 IFU of eGFP-*C. trachomatis* for 24 h. A mixture of chlamydiae, blebs and cells was added to red stained hMDM I. (**tile 1 – 3**) hMDM I bleb Interaction was imaged over time. (**tile 4**) Zeiss software ZEN 2012 was used to render the hMDM I and the bleb to generate 3D images over time.

Subsequently, infected HEp-2 cells and hMDM were placed in the same well, so that they can interact. We generated hMDM I and used a red plasma stain for their visualization. Transferring a mixture containing HEp-2 cells, blebs and single chlamydiae, at different ratios to the red stained hMDM, we found that the hMDM started to interact with the chlamydiae-containing blebs (**Figure 45**). Over time, we observed a hMDM attaching to a bleb, trying to internalize it and after about 72 h the hMDM started surrounding the bleb (**Figure 45**). The 3D rendering module allowed us to follow this interaction in more detail, demonstrating how the red stained hMDM engulfs more and more of the green bleb (**Figure 45**, tile 4).

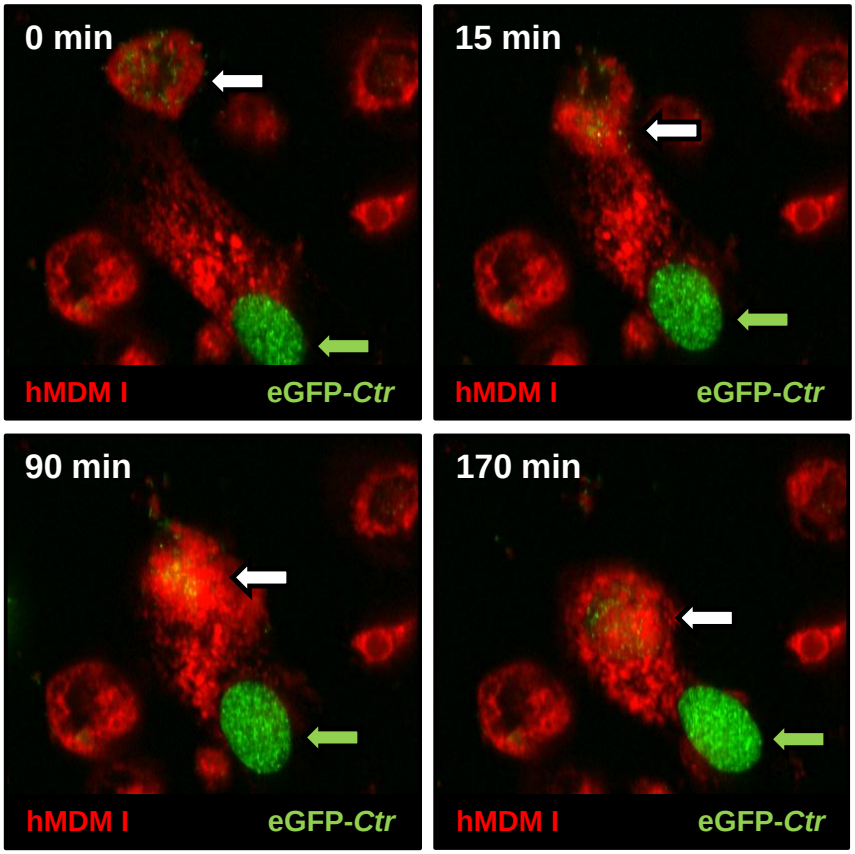

Figure 46: Replicative infected hMDM I internalizes another infected hMDM I. HEp-2 cells were infected with 10 IFU of eGFP-*C. trachomatis* for 24 h. A mixture of chlamydiae, blebs and cells was added to red stained hMDM I. Interactions were imaged over time. (White arrow: apoptotic infected hMDM I; green arrow: replicative infected viable hMDM I)

In addition with live cell imaging we observed how a dead, infected hMDM is internalized by another hMDM (**Figure 46**). Interestingly, the living hMDM itself was replicative infected, as seen by the large inclusion with moving chlamydiae inside. Additionally, we were able to image replicative inclusion development inside an hMDM I (**Figure 47**). We found the formation of multiple inclusions which fused to one big inclusion over time.

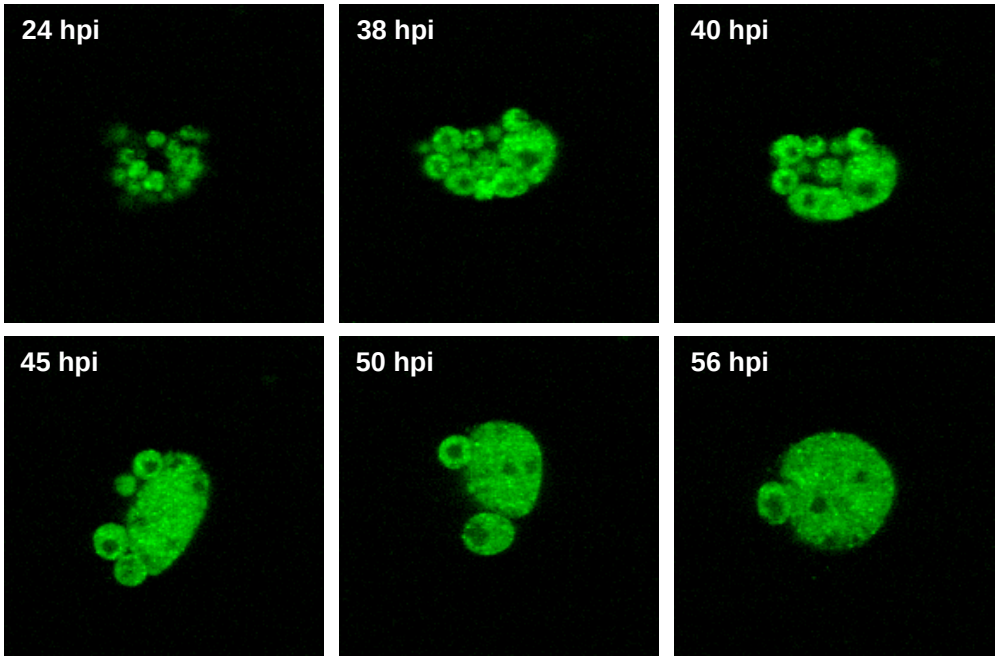

Figure 47: Multiple eGFP-*C. trachomatis* inclusions in a hMDM I fuse to one big inclusion over time. HEp-2 cells were infected with 10 IFU of eGFP-*C. trachomatis* for 24 h. A mixture of chlamydiae, blebs and cells was added to the hMDM I. Inclusion development was imaged over time.

Finally, we wanted to validate the observed replicative inclusions in hMDM using electron microscopy. We again infected hMDM I and hMDM II with *C. trachomatis* and analyzed the infection phenotype after 48 hours with electron microscopy. The presence of elementary bodies, which morphologically differ from reticular bodies, would indicate a replicative phenotype. Preliminary data of infected hMDM II cells did not result in electron micrographs depicting replicative inclusions (data not shown). However, preliminary data of infected hMDM I resulted in some interesting electron micrographs. We observed a hMDM I which was filled with compartment-like structures of different sizes (**Figure 48**). These compartment-like structures resembled chlamydial inclusions and contained a mixture of EB-like (Figure 48, white arrow head) and RB-like (Figure 48, black arrow head) particles. Using live cell imaging, we observed the fusion of multiple inclusions, which is also suggested with this preliminary electron micrograph. However, the typical high number of elementary bodies for a replicative inclusion in its final stage is not yet visible in this electron micrograph.

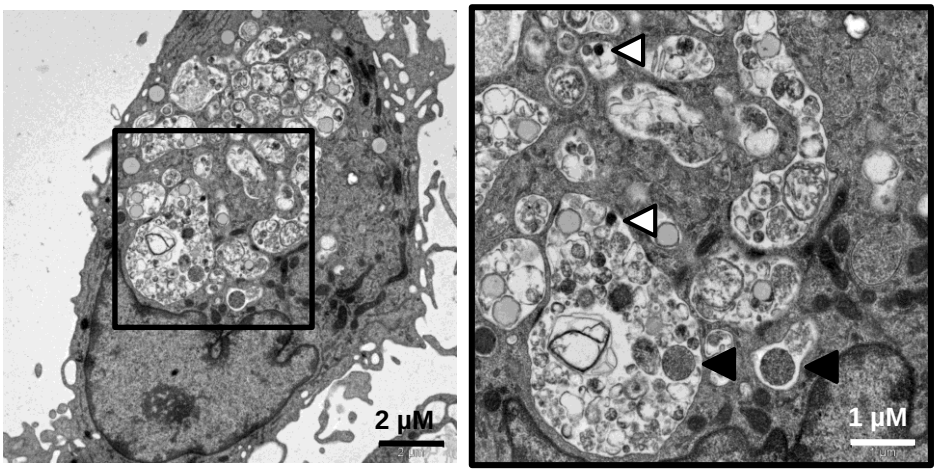

Figure 48: Replicative-like structures in an *C. trachomatis* infected hMDM I. Human primary macrophages type I were infected with 10 IFU of *C. trachomatis* for 48 h and afterwards prepared for electron microscopy.

Taken together, we find replicative-like chlamydiae infection in hMDM, mainly in hMDM I. Even though more hMDM II tend to be infected, the bacterial load and the occurrence of replication were more pronounced in hMDM I. Further experiments are needed to shed light on the question why the hMDM I seem to be a better host for chlamydiae and how single hMDM I differ, as in some replication can occur.

4 Discussion

Due to their obligate intracellular development chlamydiae are efficient modulators of various host cell pathways. A key player in a number of these processes is the transcription factor AP-1. In the first part of this thesis we aimed to elucidate the role of AP-1 for chlamydial development in epithelial cells as we hypothesize that AP-1 plays an important role for the induction of persistence. Indeed, we observed a time and dose dependent regulation of protein expression and phosphorylation of the AP-1 components c-Jun, c-Fos and ATF-2. In contrast to the decrease in c-Fos and ATF-2 protein, c-Jun protein was significantly up-regulated and phosphorylated during *C. pneumoniae* infection. As a consequence of c-Jun siRNA knockdown, the chlamydial load was diminished and accompanied by smaller inclusions and a significant lower chlamydial recovery. To assess if the role of c-Jun in the AP-1 mediated transcription is essential for chlamydial development we used the specific c-Jun/c-Fos AP-1 inhibitor Tanshinone IIA. After Tanshinone IIA treatment the chlamydial load was strongly decreased and the inclusions exhibited a small and aberrant shape. This phenotype was reversible, as the removal of Tanshinone IIA led to a return to normal growth. To identify an underlying mechanism which reveals how Tanshinone IIA alters chlamydiae infection, we assessed mRNA of AP-1 target genes *glut-1* and *c-Jun*, measured ATP level and investigated autophagy induction in presence or absence of Tanshinone IIA.

In the second part of this thesis we focused on the interaction of chlamydiae with human primary cells. We hypothesized that chlamydiae hide inside apoptotic blebs to ensure a silent uptake by macrophages without being visible for the innate immune system.
Initially comparing infection morphology, infection rate and chlamydial load we could demonstrate that both pro- and anti-inflammatory human macrophages are susceptible to infection with different chlamydiae strains. Interestingly, using wildtype *C. trachomatis* and eGFP-*C. trachomatis*, we found more infected hMDM II, but the chlamydial load was higher in hMDM I. In line, more replicative infection in form of large inclusions was observed in hMDM I. Interestingly, we could not determine a role for AP-1 during chlamydiae infection of macrophages. By using high speed live cell imaging and eGFP-*C. trachomatis* we visualized chlamydiae inclusion development inside macrophages. Furthermore we were able to image the formation of apoptotic blebs containing viable chlamydiae, which were recognized and internalized by hMDM, presenting a chlamydiae transfer mechanism to silently sustain infection.

4.1 Part I – the role of AP-1 for chlamydiae development

4.1.1 The role of c-Jun for *C. pneumoniae* development

A role for AP-1 during inflammation was already highlighted for various pathogens, such as microbes or viruses (Ghosh et al., 2002; Seo et al., 2003; Vallejo et al., 2000; Xie et al., 2005; Zachos, 1999). The hepatitis C virus was found to modify AP-1, supporting viral development by promoting cell cycle progression (Koike, 2007). In addition, *Bacillus anthracis* produces the Edema toxin, which was shown to induce AP-1 and to restrict TNF-α production (Comer et al., 2006). Also during *C. pneumoniae* infection AP-1 regulation in smooth vascular muscle cells was observed, leading to the induction of cell proliferation and the stimulation of cell growth (Miller et al., 2000). Recently AP-1 has been demonstrated to be crucial for bacteria growth and for development of the sexual transmittable *C. trachomatis* (Olive et al., 2014). In concordance, we found proteins of the AP-1 family to be regulated upon chlamydiae infection. The regulation of the AP-1 proteins occurred mainly at late time points during development, a finding in line with the recent study focusing on *C. trachomatis* (Krämer et al., 2015; Olive et al., 2014). In this study Olive et al. demonstrated that phosphorylation of c-Jun and c-Fos with subsequent AP-1 dependent transcription is induced at late developmental stage, suggesting that AP-1 is involved in replication or during the re-differentiation process. In our experiments this late phosphorylation was only observed for c-Jun protein. As expression of c-Jun protein was modulated earlier than c-Fos and ATF-2 and protein expression increased, our data suggest that c-Jun plays a more crucial role in chlamydiae development.

The special requirement of c-Jun protein for proper infection development was also described for other pathogens, for instance in viral replication of the H5N1 influenza virus, which was significantly reduced upon specific inhibition of c-Jun expression (Xie et al., 2014). To strengthen this idea in regard to chlamydiae infection, we applied a siRNA knockdown approach of c-Jun to assess the requirement of this AP-1 component for chlamydiae development. Knockdown of c-Jun protein impaired *C. pneumoniae* infection, resulting in 20% smaller inclusions, down-regulation of MOMP, reduction of chlamydial load and a significant decrease in chlamydial recovery. Our findings are indicating suboptimal growth conditions in the absence of the c-Jun protein and are in line with the report of Olive et al, were c-Jun knockdown resulted in significant reduction of IFU production after *C. trachomatis* infection (Olive et al., 2014). In our experiments the knockdown effect on infection was possibly limited, since the siRNA approach resulted in only a partial c-Jun protein reduction. Therefore we suggest that the remaining c-Jun proteins can still dimerize with c-Fos, resulting in AP-1 related transcription.

The prototypic AP-1 heterodimer consists of c-Jun and c-Fos. Since c-Fos protein expression and phosphorylation were significantly down-regulated during infection, we suggest that for chlamydial development c-Jun and not c-Fos protein is required. To investigate this, we tried to establish a c-Fos siRNA knockdown as control. As with c-Jun siRNA knockdown, treatment with c-Fos siRNA reduced the *c-Fos* mRNA levels significantly. However c-Fos protein expression in these cells remained stable. This inverse regulation of c-Fos was already observed during *C. pneumoniae* infection, where c-Fos protein was significantly down-regulated, although mRNA level of *c-Fos* increased. In contrast to *c-Fos*, differences in *c-Jun* mRNA levels always corresponded with changes of c-Jun protein amounts. The stability of c-Fos protein after siRNA treatment was surprising, as c-Fos usually is an unstable and short-lived protein (Basbous et al., 2008; Ferrara et al., 2003). In most tissues gene expression of c-Fos is strongly regulated and increases rapidly upon stimulation of the cell (Basbous et al., 2008; Eferl and Wagner, 2003). The siRNA treatment in our experimental setup seems to stabilize c-Fos protein, possibly by phosphorylation (Ferrara et al., 2003; Okazaki and Sagata, 1995). In all, we are confident that our data concerning c-Fos expression and phosphorylation demonstrate that c-Fos is of minor importance for *C. pneumoniae* development.

4.1.2 Inhibition of c-Jun/AP-1 by Tanshinone IIA impairs *C. pneumoniae* development

To investigate if the presence of c-Jun or the transcriptional activity of c-Jun as part of AP-1 is required for chlamydial development, we used Tanshinone IIA, an isolate of the root of *Salvia miltiorrhiza Bunge* which was shown to specifically inhibit the c-Jun/c-Fos AP-1 complex by preventing DNA binding and the subsequent transcriptional activity (Lee et al., 2008; Park et al., 1999). For *C. trachomatis* the use of Tanshinone IIA was shown to alter infection, resulting in a significant inhibition in the production of infectious progeny (Olive et al., 2014). This finding was in line with our data (Krämer et al., 2015). By performing recovery experiments of *C. pneumoniae* we demonstrated that upon Tanshinone IIA treatment infectious chlamydiae were rarely produced. In the study of Olive et al. Tanshinone IIA treatment impaired the bacterial load of *C. trachomatis* only minimally. However, we observed a strong decrease of *C. pneumoniae* load after Tanshinone IIA treatment. This might be explained by the fact, that they added Tanshinone IIA 20 hpi and not in the beginning as we did (Olive et al., 2014). In addition, our preliminary data suggests a similar effect of Tanshinone IIA treatment on *C. trachomatis* and eGFP-*C. trachomatis* infection as seen for *C. pneumoniae*. For both strains, the chlamydial load decreased and the inclusions size was reduced. Nevertheless, the effect was not as pronounced as for *C. pneumoniae*, for which inclusions showed an aberrant morphology. This might be caused by species

specific differences in chlamydial metabolism, for instance the faster development of *C. trachomatis* (Grieshaber et al., 2002; Nicholson et al., 2003).

The reduced infectivity after Tanshinone IIA treatment was accompanied by a strongly altered inclusion morphology which however was reversible, indicating a persistent *C. pneumoniae* phenotype (Beatty et al., 1993, 1994a; Borel et al., 2014; Harper et al., 2000).

4.1.3 MOMP and cHsp60 as indicator for *C. pneumoniae* persistence

As indicator for persistence, we first determined MOMP and cHsp60 protein expression and subsequently calculated the MOMP:cHsp60 ratio (as described by (Beatty et al., 1994b). We found the MOMP:cHsp60 ratio to be decreased significantly after Tanshinone IIA treatment, which is usually associated with persistence of *C. trachomatis* (Villegas et al., 2008). Several studies concerning *C. trachomatis* persistence found that expression of MOMP was often decreased, while cHsp60 expression remained stable or increases during persistence (Beatty et al., 1993, 1994a; Cevenini et al., 1988; Scidmore-Carlson et al., 1999). For persistent *C. pneumoniae* also contrary data have been published (Hogan et al., 2003; Jones et al., 2001; Mathews et al., 2001; Molestina et al., 2002). In case of *C. pneumoniae* persistence, no significant down-regulation, but a significant up-regulation of MOMP on protein level and transcriptional level following INF-γ induced persistence was observed (Mathews et al., 2001; Molestina et al., 2002). However, in agreement with *C. trachomatis* studies, the level of cHsp60 after INF-γ treatment was found to be maintained or even up-regulated (Beatty et al., 1993; Molestina et al., 2002). In persistence, reduced levels of MOMP could facilitate chlamydiae to avoid the development of protective immunity as MOMP from *C. pneumoniae* can elicit the generation of neutralizing antibodies and T cell mediated immune responses (Bandholtz et al., 2002; Kim et al., 1999; Peterson et al., 1996; Rodríguez et al., 2006). In contrast, cHsp60 accumulation may support chlamydial infection. It is possible that chlamydial Hsp60 induces auto-immunity due to its high identity to human Hsp60, which lays around 48 % in case of *C. trachomatis* (Viale et al., 1994; Yi et al., 1997). In addition to the chlamydiae species, also the inducer of persistence, such as INF-γ or penicillin, is of essential importance for the transcriptional persistence profile measured by expression of MOMP and cHsp60 (Jones et al., 2001; Mathews et al., 2001). As result of these discrepancies, previous publications are in agreement that the MOMP:cHsp60 ratio cannot be used as a universal persistence marker (Hogan et al., 2004; Villegas et al., 2008; Wyrick, 2010). In conclusion, we demonstrated that treatment with Tanshinone IIA, an inducer of persistence, resulted in an unusual *C. pneumoniae* persistence profile, normally found upon *C. trachomatis* infection.

4.1.4 Possible mechanisms of persistence induction by Tanshinone IIA treatment

With electron Microscopy, we demonstrated that Tanshinone IIA treatment switched a replicative infection phenotype into a persistent one (Krämer et al., 2015). So far the best studied *in vitro* model of chlamydial persistence is the persistence induction by treatment with the inflammatory cytokine IFN-γ. IFN-γ increases the enzymatic activity of indole-2,3-dioxygenase (IDO) which is responsible for tryptophan catabolism, thus inducing a faster decrease of the intracellular concentration of tryptophan (Beatty et al., 1993). For chlamydiae this amino acid is essential and as they are not able to synthesize tryptophan alone, they enter a persistence stage upon IFN-γ treatment (Mehta et al., 1998; Pantoja et al., 2001). Given that Tanshinone IIA is a multi-target drug several mechanisms could be of assistance for Tanshinone IIA-induced persistence. Various effects are described for Tanshinone IIA, such as interference with other transcription factors, like NF-κB, and regulation of scavenger receptors, such as CD36 and scavenger receptor-A (Chen et al., 2007; Fan et al., 2009; Jang et al., 2006; Tang et al., 2011). The link between chlamydial development and host autophagy might provide an explanation for the Tanshinone IIA-induced persistence (Al-Younes et al., 2004, 2011; Pachikara et al., 2009; Yasir et al., 2011). Autophagy is a process of self-digestion which involves lysosome-dependent degradation of cytoplasmic components like proteins, neutral lipids and mitochondria, in order to maintain cellular homeostasis, for instance during starvation (Dunn, 1990a, 1990b; Klionsky and Emr, 2000; Maiuri et al., 2010; Mizushima et al., 2008; Reggiori and Klionsky, 2002; Seglen and Bohley, 1992; Stromhaug and Klionsky, 2001). Chlamydiae are highly dependent on nutrients of their host cell which is why limitations in their availability result in persistence (Al-Younes et al., 2001; Coles and Pearce, 1987; Coles et al., 1993; Harper et al., 2000; Raulston, 1997). Furthermore it was shown that in epithelial cells the chlamydial inclusions do not fuse with the lysosome, a function which is involved in autophagy (Al-Younes et al., 1999; Heinzen et al., 1996; Levine et al., 2011; Ooij et al., 1997; Scidmore et al., 2003). Therefore, an interaction with host cell autophagy can be beneficial for chlamydiae and seems likely. The advantage of utilizing the autophagy machinery of the host cell was already described for other pathogens (Crauwels et al., 2015). Indeed, inhibition of autophagy by 3-methyladenine and amino acids was shown to impair the inclusion size, chlamydial morphology or development of infectious progeny of *C. trachomatis* (Al-Younes et al., 2004). Nevertheless, other studies revealed ambiguous interactions between chlamydiae and the host autophagic machinery, as autophagy can also serve as an innate defense mechanism against chlamydiae (Al-Younes et al., 2011; Al-zeer et al., 2013; Yasir et al., 2011). In macrophages autophagy was found to restrict *C. trachomatis* growth (Al-zeer et al., 2013). Tanshinone IIA was shown to inhibit mammalian

target of rapamycin (mTOR) a negative inducer of autophagy thus causing the induction of autophagy (Kondo and Kondo, 2006; Li et al., 2015; Yun et al., 2014). In our experiments we also observed the induction of autophagy upon Tanshinone IIA treatment assessed by detection of LC3 conversion and SQSTM1/p62 (p62) protein expression. Interestingly, the chlamydiae infection alone resulted in an even more pronounced autophagy induction, indicating that they favor autophagy induction. Consequently, Tanshinone IIA induced persistence is not a consequence of autophagy induction. However, further work is required to elucidate the exact role of autophagy in chlamydiae infection.

Another possible explanation for the persistent phenotype induced by Tanshinone IIA is the fact that AP-1 is involved in processes coordinating cell proliferation, which in turn requires a functional host cell metabolism. As Tanshinone IIA treatment leads to suppression of cell proliferation, our data suggest that the interference with AP-1 regulated host cell metabolism affects the chlamydial development (Li et al., 2010; Wang et al., 2005). The intracellular chlamydiae also have a high energy demand during their replicative cycle. As they are hypothesized to be energy parasites, chlamydiae are highly dependent on the host cell for ATP and glucose supply (Moulder, 1970). It is proven that AP-1 regulates genes that are responsible for cellular energy balance, such as glucose transporter 1 (*glut-1*), which was found to exhibit an AP-1 binding site in its promotor (Kozlovsky et al., 1997; Santalucía et al., 2003). Indeed, up-regulation of *glut-1* mRNA expression following *Chlamydia psittaci* infection was already described in later phase of infection, when chlamydial metabolic activity reaches the highest level (Ojcius et al., 1998c; Rupp et al., 2007). In concordance, we also observed a 2-3 fold enhancement of *glut-1* mRNA in late phase of *C. pneumoniae* infection (48 and 72 hpi). However, Tanshinone IIA treatment also increased *glut-1* mRNA expression already after treatment for 24 h and the expression resembled that of infection after 48 and 72 h. This was surprising, as Tanshinone IIA was described to reduce mRNA level of *glut-1* (Li et al., 2015; Rankin et al., 2012; Wang et al., 1995). Also for *c-Jun* mRNA expression an increase after Tanshinone IIA treatment was detected. Tanshinone IIA prevents the AP-1 heterodimer consisting of c-Jun/c-Fos from binding to the DNA (Lee et al., 2008; Park et al., 1999). We would hypothesize that prevention of AP-1 DNA binding leads to accumulation of c-Jun/AP-1 in the cells. As c-Jun protein regulates its own transcription in a positive autoregulation we suggest that the increased presence of c-Jun protein results in up-regulation of *c-Jun* mRNA. We continued to assess other marker for metabolic activity and measured ATP level after infection in presence or absence of Tanshinone IIA. We demonstrated that ATP is up-regulated early (6 and 12 hpi) after *C. pneumoniae* infection, whereas the presence of Tanshinone IIA significantly decreased the ATP levels. The lack of ATP in the phase where differentiation from EB to RB occurs might cause the induction of persistence as the requirements for proper chlamydial development are not provided

anymore (Wolf et al., 2000). In the late stage of development metabolically active RBs are present, in need of ATP for replication and re-differentiation (Omsland et al., 2012). As indicator for metabolic activity of the chlamydial RBs at later time points of infection, NAD(P)H measurement can be used (Solbach et al., 2011). An increase of the fluorescence lifetime of protein-bound NAD(P)H (τ_2-NAD(P)H) in the *C. trachomatis* inclusions using two-photon microscopy and fluorescence live cell imaging (FLIM) was observed during the midphase of infection. This is indicative for the enhanced metabolic activity of RBs. Furthermore it was demonstrated that after induction of persistence with INF-γ treatment the metabolic activity of the RBs was reduced. In cooperation with the group of Prof. Dr. Jan Rupp (Department of Molecular und Clinical Infectious Diseases, UKSH, Lübeck) we used this method to analyze a later developmental stage (48 hpi) of *C. pneumoniae* infection in presence or absence of Tanshinone IIA (Krämer et al., 2015). Thereby it was clearly visible that Tanshinone IIA treatment resulted in a significant decrease of τ_2-NAD(P)H in comparison to untreated infected cells. Thus we hypothesize that Tanshinone IIA treatment results in limitations of glucose and subsequent ATP supply, which is responsible for an incomplete development and leads to persistence (Lee et al., 2001; Ojcius et al., 1998c). This hypothesis is supported by the finding that reduction of host cell ATP synthesis, e.g. by glycolysis inhibition, caused generation of aberrant *C. trachomatis* inclusions and was accompanied by decreased τ_2-NAD(P)H values in the chlamydial inclusions (Solbach et al., 2011).

4.2 Part II – infection and transfer of chlamydiae in human primary macrophages

4.2.1 Transgenic chlamydiae - a new perspective in studying host pathogen interaction

Due to the complex intracellular developmental cycle of chlamydiae, it was a long time not possible to genetically manipulate these bacteria (Binet and Maurelli, 2009; Clarke, 2010; Kari et al., 2011; Tam et al., 1994). Recently a chlamydial plasmid, which was modified to express the green fluorescent protein (GFP), was used as vector shuttle for introduction in a plasmid-free *C. trachomatis* L2 strain with several rounds of penicillin selection (Wang et al., 2011). These genetically modified chlamydiae are now penicillin resistant and express GFP, making them a useful tool in chlamydiae research. However, it should be considered that genetic transformation can induce alterations in infectivity or infection development, as described for the West Nile virus, in which the viral replication was found to be reduced after insertion of a GFP reporter gene (Pierson et al., 2005). In addition, the research group which developed the chlamydial transformation system showed that transformation of

C. trachomatis with another large transforming plasmid extended the development cycle and slightly reduced the chlamydial progeny in comparison to the untransformed strain (Wang et al., 2011). However, in course of our experiments we did not observe significant differences in infection morphology, infection rate or chlamydial load between the wildtype and its transgenic variant. Thus, we concluded that eGFP-*C. trachomatis* is a perfect tool for microscopical studies of chlamydiae host cell interactions.

4.2.2 Chlamydiae infection of human macrophages results in persistent infection phenotype

Until now, most studies regarding chlamydiae infection focused on an epithelial cell infection model, as these cells are the first to be exposed to the bacteria. While chlamydiae infection in epithelial cells is well studied, only little information is available about chlamydiae infection in human primary macrophages. These host immune cells are suggested to play an important role in disease dissemination (Moazed et al., 1998; Zandbergen et al., 2004). Upon infection using *C. trachomatis*, either wildtype or transgenic, but also *C. pneumoniae*, we predominantly observed a persistent phenotype in both pro-inflammatory hMDM I and anti-inflammatory hMDM II. These data are in line with other studies concerning chlamydiae infection of macrophages or monocyte or macrophage derived cell lines. It could be demonstrated that, for example THP-1 and Mono Mac 6, are susceptible for chlamydiae infection, although chlamydial replication is limited (Gaydos et al., 1996; Haranaga et al., 2003; Yamaguchi et al., 2002). Most of the studies performed recovery experiments which revealed that less viable chlamydiae could be obtained from infected macrophages compared to the amount which was used for infection. Furthermore, the observed chlamydial inclusions were small and aberrant and resembled a persistent phenotype, which was not only found *in vitro* but also *in vivo* (Nanagara et al., 1995; Skowasch et al., 2003; Yamaguchi et al., 2002). In addition to this persistence phenotype, we also observed the presence of large, replicative-like inclusions in some macrophages. With first recovery experiments we could confirm that the *C. trachomatis* inclusions from hMDM I and II indeed harbored infectious elementary bodies. This is in concordance with other studies which also found chlamydial recovery after macrophage infection what indicates that chlamydiae are able to replicate inside macrophages (Gaydos et al., 1996; Moazed et al., 1998; Yamaguchi et al., 2002).

4.2.3 Different susceptibility to chlamydiae infection between macrophage phenotypes

Human primary macrophages were found to be susceptible to both *C. trachomatis* and *C. pneumoniae*, however not in a similar extent. Comparing infection of the different chlamydiae species, the infection rates for *C. pneumoniae* were always the lowest. A possible explanation could be due to host cells aberrations, as *C. pneumoniae* usually infects alveolar macrophages which differ from blood monocyte derived macrophages we used in our experiments (Gautier et al., 2012; Hearst et al., 1980). Interestingly, independent of the used species, we found more hMDM II than hMDM I to be infected, indicating a more efficient uptake by anti-inflammatory hMDMs. This finding is in agreement with several studies which also described a higher phagocytic capacity for anti-inflammatory hMDM II, compared to hMDM I. They found a more efficient phagocytosis for hMDM II towards apoptotic cells and various pathogens, e.g. *Leishmania, Mycobacterium bovis* BCG or *Listeria monocytogenes,* probably due to their role in scavenging debris and tissue remodeling (Akagawa, 2002; Bayer et al., 2012; Diget et al., 2013; Neu et al., 2013; Ogden et al., 2005; Verreck et al., 2004; Xu et al., 2006; Zizzo et al., 2012). Regarding the fact that an enhanced uptake of chlamydiae occurred in anti-inflammatory macrophages it was proposed that the increased presence of mannose receptor on this macrophages phenotype may be responsible for the better susceptibility. Mannose receptors were shown to assist in chlamydial uptake as demonstrated for *C. trachomatis*, *C. psittaci* and *C. pneumoniae* in mouse macrophages (Gracey et al., 2013; Kuo et al., 2002). Surprisingly, the chlamydial load, analyzed by detection of 16S rRNA, was more elevated in hMDM I as compared to hMDM II. For most pathogens a better survival in anti-inflammatory type II macrophages is suggested, as fewer pro-inflammatory defense mechanisms are present, such as the anti-microbial peptide LL37, (Bank et al., unpublished data). Intracellular pathogens are able to strategically interfere with the pro-inflammatory defense mechanisms, for example by modulating cytokine production thereby reshaping macrophage phenotypes, as described for *Leishmania, Mycobacterium tuberculosis* and *Francisella tularensis* (Thi et al., 2012). Anti-inflammatory type II mouse macrophages were demonstrated to promote viable *C. muridarum* growth, while pro-inflammatory type I mouse macrophages controlled infection through persistence induction (Gracey et al., 2013). In contrast, using a human macrophage infection model, we demonstrated a higher chlamydial load in the pro-inflammatory hMDM I. Interestingly, also more replicative inclusions were present in this macrophage phenotype. Since large sized replicative-like inclusions possibly contain a higher number of chlamydiae as compared to smaller, aberrant inclusions, we suggest that this explains the increased bacterial load in hMDM I. However, as only small numbers of large sized replicative-like inclusions were found, we cannot exclude that this finding is of minor biological relevance.

4.2.4 Regulation of AP-1 in human macrophages after chlamydiae infection

The finding that chlamydiae development occurred differently in distinct macrophage phenotypes raised the question whether AP-1 may play a decisive role in determining the chlamydiae infection phenotype. As demonstrated for *C. pneumoniae* infection in epithelial cells, we speculated that transcription factor AP-1 may be involved in regulation of replicative or persistent infection of pro- and anti-inflammatory hMDM. As many LPS-inducible genes in macrophages carry AP-1 sites, a role for AP-1 would not be unlikely (Tugal et al., 2013). Inflammatory stimuli such as LPS stimulation cause the induction of a pro-inflammatory immune response in macrophages, amongst others via the c-Jun N-terminal kinase (JNK) signaling pathway, a key regulator of c-Jun/AP-1 (Casals-Casas et al., 2009; Chang and Karin, 2001; Hambleton et al., 1996; Sánchez-Tilló et al., 2007). Following LPS stimulation c-Jun/AP-1 does not only contribute in the induction of pro-inflammatory responses, but counterbalances inflammation by the production of the anti-inflammatory cytokine IL-10 (Das et al., 2014; Pretolani, 1999; Voll et al., 1997). We measured protein level of c-Jun and c-Fos of both hMDM phenotypes with and without *C. trachomatis* infection. The involvement of c-Jun seemed to be more pronounced in the pro-inflammatory response, as we found a significant higher c-Jun expression in pro-inflammatory hMDM I compared to anti-inflammatory hMDM II. In agreement, in murine bone marrow derived macrophages (BMM) which were treated with GM-CSF and M-CSF, respectively, the GM-BMM showed faster and enhanced AP-1 activation in the presence of LPS compared to M-BMM cells (Fleetwood et al., 2007). Surprisingly, we did not observe a pronounced regulation of c-Jun or c-Fos upon *C. trachomatis* infection. A possible explanation may be that chlamydial LPS differs from that of other gram negative bacteria, such as *E.coli* (Cao et al., 2007). In all, we found no evidence for AP-1 involvement in the development of either persistent or replicative chlamydiae infections in human primary macrophages.

4.2.5 Induction of apoptosis for silent chlamydiae transfer

Upon initial infection, epithelial cells are permissive for productive, replicative chlamydiae infection after which they can be transferred to the macrophages. We suggest that the way of cell entry, for instance via apoptotic blebs, may be decisive for the outcome of infection (Byrne and Ojcius, 2004; Zandbergen et al., 2004). The formation of blebs was only observed during chlamydiae infection, whereas the control cells remained viable. These blebs contained viable chlamydiae as identified by their movement in our microscopical investigations. Our preliminary live cell imaging data demonstrated that a proportion of the blebs bared signs of early apoptotic markers such as externalization of phosphatidylserine,

suggestive for chlamydial induction of apoptosis in their host cell. This phenomenon was already described upon infection of neutrophils. It was demonstrated that chlamydiae-infected neutrophils delayed spontaneous apoptosis up to 66 h through stabilization of anti-apoptotic protein Mcl-1 (Sarkar et al., 2015). Then apoptosis occurred and resulted in formation of chlamydiae-containing apoptotic blebs which exposed phosphatidylserine on their surface (Rupp et al., 2009). *In vivo*, neutrophils and monocytes are recruited quickly upon infection and neutrophils are typically the first phagocytes that encounter the site of inflammation (Van Furth et al., 1973; Lehrer et al., 1988; Nathan, 2006; Sunderkötter et al., 2004). Acute *C. trachomatis* infection was found to correlate with infiltration of polymorphonuclear neutrophils (PMNs) (Patton and Kuo, 1989). Also during acute *C. pneumoniae* infection an increased amount of polymorphonuclear neutrophils (PMN) invaded into the lung, as result of IL-8 release from the infected epithelial cells (Molestina et al., 1999). Subsequently, the chlamydiae are rapidly internalized by the PMNs (Zandbergen et al., 2004). Although chlamydiae can survive and multiply inside PMNs/neutrophils their role for chlamydial infection is more likely to function as a vector, similar to a Trojan horse strategy (Rupp et al., 2009). It was demonstrated that the life span neutrophils which normally undergo spontaneous apoptosis within 6 - 10 h was prolonged for up to 90 h upon *C. pneumoniae* infection, demonstrated via annexin V and TUNEL staining (Luo and Loison, 2008; Zandbergen et al., 2004). While induction of apoptosis in initial infection is used by several pathogens to escape immune response, obligate intracellular bacteria, such as chlamydiae and *Rickettsia,* seem to benefit from the inhibition of apoptosis (Galmiche et al., 2000; Hilbi et al., 1997; Müller et al., 2000; Weinrauch and Zychlinsky, 1999). Inhibition of apoptosis enables chlamydiae to complete their development, protects them against cytotoxic T cells and supports the establishment of a long-term infection (Clifton et al., 1998; Dean and Powers, 2001; Fan et al., 1998; Jendro et al., 2004; Perfettini et al., 2003). Another important aspect of delaying apoptosis is the infiltration of macrophages which are supposed to be responsible for systemic dissemination of chlamydiae (Blasi et al., 2004; Maass et al., 2000; Rupp et al., 2009; Shio et al., 2012). The role of macrophages for chlamydial dissemination was already demonstrated for *C. pneumoniae* during *in vivo* experiments with mice (Moazed et al., 1998). Also in human clear evidence exists that macrophages are crucial for systemic dissemination of chlamydiae (Blasi et al., 2004; Rupp et al., 2009; Shio et al., 2012). Moreover, the importance of macrophages as preferred host cell is emphasized by the finding that *C. pneumoniae* infection of THP-1 cells, a human monocytic cell line, and human peripheral blood monocytes actively induced differentiation into macrophages (Yamaguchi et al., 2002). To gain a silent entrance into macrophages, chlamydiae utilize neutrophils and monocytes as vector and misuse apoptosis to achieve their transfer. In line with the result that macrophages internalize apoptotic, chlamydiae-infected neutrophils, we could observe macrophages to interact with blebs,

originating from chlamydiae-infected epithelial cells. These findings strengthen the hypothesis that chlamydial release does not only occur by cell lysis or extrusion, but also by induction of host cell apoptosis and subsequent transfer via apoptotic blebs.

Regarding the release of chlamydiae from their host cell, mainly three ways are discussed, namely host cell lysis, extrusion or induction of host cell apoptosis (Byrne and Ojcius, 2004; Hybiske and Stephens, 2008; Ojcius et al., 1998b; Zandbergen et al., 2004). In contrast to cell lysis and extrusion, the induction of apoptosis and the subsequent uptake by macrophages provides features which are beneficial for a silent uptake. Phagocytosis of apoptotic cells, e.g. neutrophils, is associated with inhibition of pro-inflammatory and release of anti-inflammatory cytokines, like TGF-β and IL-10 (Fadok et al., 1998; Huynh et al., 2002; Silva et al., 2008; Voll et al., 1997). TGF-β in turn leads to suppression of LPS-mediated release of inflammatory cytokines by infected cells (Lucas et al., 2006). Furthermore, the externalization of phosphatydilserine (PS) on the surface of cells is a signal for phagocytosis recognized by T Cell Immunoglobulin Mucin 4 (Tim4), Brain Angiogenesis Inhibitor 1 (Bai1) and Stabilin 1/2 (Devitt and Marshall, 2011). Phagocytosis of PS-exposing apoptotic cells by macrophages leads to secretion of anti-inflammatory cytokines, reduces production of nitric oxide and reactive oxygen species and poor stimulation of T and B cells (Byrne and Ojcius, 2004; Fadok et al., 1998; Goerdt and Orfanos, 1999; Huynh et al., 2002; Ronchetti et al., 1999; Voll et al., 1997).

4.3 Concluding remarks

From the data obtained during this PhD thesis we can conclude that transcription factor AP-1 plays a role in chlamydiae infection of epithelial cells. In our epithelial cell model the chlamydial regulation of especially c-Jun was demonstrated and seems to be essential for a proper chlamydiae development. In addition, we revealed that Tanshinone IIA treatment strongly impaired chlamydiae development leading to the induction of a persistent infection phenotype. The underlying mechanism of Tanshinone IIA-induced persistence still has to be elucidated in future studies. In our infection model using human macrophages as immune host cells, we observed phenotype specific differences in chlamydiae infection. While more anti-inflammatory hMDM got infected, the amount of chlamydiae inside pro-inflammatory hMDM was higher. Together with the finding, that replicative-like infections were predominantly found in pro-inflammatory hMDM, we hypothesize that this macrophage phenotype is more suitable as a host cell for chlamydiae replication. Since the mechanism which determines the development of either a persistent or a replicative infection in macrophages remains elusive, further investigations are required. Regarding the chlamydial transfer, we are confident that the combination of our experimental approaches, using epithelial and human primary cells, with live cell imaging will provide further evidence that apoptotic blebs can be used as strategy for silent chlamydiae infection of macrophages.
In all, these data will contribute to a better understanding of chlamydial host cell modulation and chlamydial immune evasion. Decoding the chlamydial transfer mechanisms is of essential importance for the development of efficient strategies in order to combat the complex chlamydial infections.

5 References

AbdelRahman, Y.M., and Belland, R.J. (2005). The chlamydial developmental cycle. FEMS Microbiol. Rev. *29*, 949–959.

Adams, D.O., and Hamilton, T.A. (1984). The cell biology of macrophage activation. Annu. Rev. Immunol. *2*, 283–318.

Akagawa, K.S. (2002). Functional heterogeneity of colony-stimulating factor-induced human monocyte-derived macrophages. Int. J. Hematol. *76*, 27–34.

Al-Younes, H.M., Rudel, T., and Meyer, T.F. (1999). Characterization and intracellular trafficking pattern of vacuoles containing Chlamydia pneumoniae in human epithelial cells. Cell. Microbiol. *1*, 237–247.

Al-Younes, H.M., Rudel, T., Brinkmann, V., Szczepek, A.J., and Meyer, T.F. (2001). Low iron availability modulates the course of Chlamydia pneumoniae infection. Cell. Microbiol. *3*, 427–437.

Al-Younes, H.M., Brinkmann, V., and Meyer, T.F. (2004). Interaction of Chlamydia trachomatis serovar L2 with the host autophagic pathway. Infect. Immun. *72*, 4751–4762.

Al-Younes, H.M., Al-Zeer, M. a., Khalil, H., Gussmann, J., Karlas, A., Machuy, N., Brinkmann, V., Braun, P.R., and Meyer, T.F. (2011). Autophagy-independent function of MAP-LC3 during intracellular propagation of Chlamydia trachomatis. Autophagy *7*, 814–828.

Al-zeer, M.A., Al-younes, H.M., Lauster, D., Lubad, M.A., and Meyer, T.F. (2013). growth in human macrophages via IFNG-inducible guanylate binding proteins. Autophagy *9*, 50–62.

Amann, R., Springer, N., Schönhuber, W., Ludwig, W., Schmid, E.N., Müller, K.D., and Michel, R. (1997). Obligate intracellular bacterial parasites of acanthamoebae related to Chlamydia spp. Appl. Environ. Microbiol. *63*, 115–121.

Ameyar, M., Wisniewska, M., and Weitzman, J.B. (2003). A role for AP-1 in apoptosis: The case for and against. Biochimie *85*, 747–752.

Angel, P., and Karin, M. (1991). The role of Jun, Fos and the AP-1 complex in cell-proliferation and transformation. Biochim. Biophys. Acta *1072*, 129–157.

Angel, P., Baumann, I., Stein, B., Delius, H., Rahmsdorf, H.J., and Herrlich, P. (1987). 12-O-tetradecanoyl-phorbol-13-acetate induction of the human collagenase gene is mediated by an inducible enhancer element located in the 5'-flanking region. Mol. Cell. Biol. *7*, 2256–2266.

Angel, P., Hattori, K., Smeal, T., and Karin, M. (1988). The jun proto-oncogene is positively autoregulated by its product, Jun/AP-1. Cell *55*, 875–885.

Azenabor, A.A., and Mahony, J.B. (2000). Generation of reactive oxygen species and formation and membrane lipid peroxides in cells infected with Chlamydia trachomatis. Int. J. Infect. Dis. *4*, 46–50.

Bakiri, L., Lallemand, D., Bossy-Wetzel, E., and Yaniv, M. (2000). Cell cycle-dependent variations in c-Jun and JunB phosphorylation: a role in the control of cyclin D1 expression. EMBO J. *19*, 2056–2068.

Bandholtz, L., Kreuger, M.R., Svanholm, C., Wigzell, H., and Rottenberg, M.E. (2002). Adjuvant modulation of the immune responses and the outcome of infection with Chlamydia pneumoniae. Clin. Exp. Immunol. *130*, 393–403.

Basbous, J., Jariel-Encontre, I., Gomard, T., Bossis, G., and Piechaczyk, M. (2008). Ubiquitin-independent- versus ubiquitin-dependent proteasomal degradation of the c-Fos and Fra-1 transcription factors: Is there a unique answer? Biochimie *90*, 296–305.

Bayer, C., Varani, S., Wang, L., Walther, P., Zhou, S., Straschewski, S., Bachem, M., Soderberg-Naucler, C., Mertens, T., and Frascaroli, G. (2012). Human cytomegalovirus infection of M1 and M2 macrophages triggers inflammation and autologous T-cell proliferation. J. Virol.

Beatty, W.L., Byrne, G.I., and Morrison, R.P. (1993). Morphologic and antigenic characterization of interferon gamma-mediated persistent Chlamydia trachomatis infection in vitro. Proc. Natl. Acad. Sci. U. S. A. *90*, 3998–4002.

Beatty, W.L., Morrison, R.P., Byrne, G.I., Beaty, W.L., Morrison, R.P., Byrne, G.I., Beatty, W.L., Morrison, R.P., Byrne, G.I., Beaty, W.L., et al. (1994a). Persistent chlamydiae: from cell culture to a paradigm for chlamydial pathogenesis. Microbiol. Rev. *58*, 686–699.

Beatty, W.L., Morrison, R.P., and Byrne, G.I. (1994b). Immunoelectron-microscopic quantitation of differential levels of chlamydial proteins in a cell culture model of persistent Chlamydia trachomatis infection. Infect. Immun. *62*, 4059–4062.

Beatty, W.L., Belanger, T.A., Desai, A.A., Morrison, R.P., and Byrne, G.I. (1994c). Tryptophan depletion as a mechanism of gamma interferon-mediated chlamydial persistence. Infect. Immun. *62*, 3705–3711.

Beatty, W.L., Morrison, R.P., and Byrne, G.I. (1995). Reactivation of Persistent Chlamydia trachomatis Infection in Cell Culture. *63*, 199–205.

Beeckman, D.S.A., and Vanrompay, D.C.G. (2009). Zoonotic Chlamydophila psittaci infections from a clinical perspective. Clin. Microbiol. Infect. *15*, 11–17.

Belland, R.J., Nelson, D.E., Virok, D., Crane, D.D., Hogan, D., Sturdevant, D., Beatty, W.L., and Caldwell, H.D. (2003). Transcriptome analysis of chlamydial growth during IFN-gamma-mediated persistence and reactivation. Proc. Natl. Acad. Sci. U. S. A. *100*, 15971–15976.

Berry, A., Goodwin, M., Moran, C.L., and Chambers, T.C. (2001). AP-1 activation and altered AP-1 composition in association with increased phosphorylation and

expression of specific Jun and Fos family proteins induced by vinblastine in KB-3 cells. Biochem. Pharmacol. *62*, 581–591.

Binet, R., and Maurelli, A.T. (2009). Transformation and isolation of allelic exchange mutants of Chlamydia psittaci using recombinant DNA introduced by electroporation. Proc. Natl. Acad. Sci. U. S. A. *106*, 292–297.

Blasi, F., Legnani, D., Lombardo, V.M., Negretto, G.G., Magliano, E., Pozzoli, R., Chiodo, F., Fasoli, A., and Allegra, L. (1993). Chlamydia pneumoniae infection in acute exacerbations of COPD. Eur. Respir. J. Off. J. Eur. Soc. Clin. Respir. Physiol. *6*, 19–22.

Blasi, F., Centanni, S., and Allegra, L. (2004). Chlamydia pneumoniae: Crossing the barriers? Eur. Respir. J. *23*, 499–500.

Borel, N., Pospischil, A., Hudson, A.P., Rupp, J., and Schoborg, R. V. (2014). The role of viable but non-infectious developmental forms in chlamydial biology. Front. Cell. Infect. Microbiol. *4*, 97.

Boyle, W.J., Smeal, T., Defize, L.H., Angel, P., Woodgett, J.R., Karin, M., and Hunter, T. (1991). Activation of protein kinase C decreases phosphorylation of c-Jun at sites that negatively regulate its DNA-binding activity. Cell *64*, 573–584.

Brunham, R.C., and Rey-Ladino, J. (2005). Immunology of Chlamydia infection: implications for a Chlamydia trachomatis vaccine. Nat. Rev. Immunol. *5*, 149–161.

Buechler, C., Ritter, M., Orsó, E., Langmann, T., Klucken, J., and Schmitz, G. (2000). Regulation of scavenger receptor CD163 expression in human monocytes and macrophages by pro- and antiinflammatory stimuli. J. Leukoc. Biol. *67*, 97–103.

Bujger, Z., and Ekert, M. Trachoma--an endemic and post-endemic problem. Lijec. Vjesn. *122*, 187–191.

Burton, M.J. (2007). Trachoma: An overview. Br. Med. Bull. *84*, 99–116.

Burton, M.J., and Mabey, D.C.W. (2009). The global burden of trachoma: A review. PLoS Negl. Trop. Dis. *3*.

Bush, R.M., and Everett, K.D.E. (2001). Molecular evolution of the Chlamydiaceae. Int. J. Syst. Evol. Microbiol. *51*, 203–220.

Byrne, G.I., and Ojcius, D.M. (2004). Chlamydia and apoptosis: life and death decisions of an intracellular pathogen. Nat. Rev. Microbiol. *2*, 802–808.

Campbell, L.A., and Kuo, C.C. (2009). Cultivation and laboratory maintenance of Chlamydia pneumoniae. Curr. Protoc. Microbiol.

Campbell, S., Richmond, S.J., and Yates, P.S. (1989). The effect of Chlamydia trachomatis infection on the host cell cytoskeleton and membrane compartments. J. Gen. Microbiol. *135*, 2379–2386.

Cao, F., Castrillo, A., Tontonoz, P., Re, F., and Byrne, G.I. (2007). Chlamydia pneumoniae-induced macrophage foam cell formation is mediated by toll-like receptor 2. Infect. Immun. *75*, 753–759.

Carabeo, R.A., Grieshaber, S.S., Fischer, E., and Hackstadt, T. (2002). Chlamydia trachomatis induces remodeling of the actin cytoskeleton during attachment and entry into HeLa cells. Infect. Immun. *70*, 3793–3803.

Carlin, J.M., and Weller, J.B. (1995). Potentiation of interferon-mediated inhibition of Chlamydia infection by interleukin-1 in human macrophage cultures . Potentiation of Interferon-Mediated Inhibition of Chlamydia Infection by Interleukin-1 in Human Macrophage Cultures. *63*.

Casals-Casas, C., Álvarez, E., Serra, M., de la Torre, C., Farrera, C., Sánchez-Tilló, E., Caelles, C., Lloberas, J., and Celada, A. (2009). CREB and AP-1 activation regulates MKP-1 induction by LPS or M-CSF and their kinetics correlate with macrophage activation versus proliferation. Eur. J. Immunol. *39*, 1902–1913.

Cassol, E., Cassetta, L., Alfano, M., and Poli, G. (2010). Macrophage polarization and HIV-1 infection. J. Leukoc. Biol. *87*, 599–608.

Cevenini, R., Donati, M., and La Placa, M. (1988). Effects of penicillin on the synthesis of membrane proteins of Chlamydia trachomatis LGV2 serotype. FEMS Microbiol. Lett. *56*, 41–45.

Chang, L., and Karin, M. (2001). Mammalian MAP kinase signalling cascades. Nature *410*, 37–40.

Chapuis, F., Rosenzwajg, M., Yagello, M., Ekman, M., Biberfeld, P., and Gluckman, J.C. (1997). Differentiation of human dendritic cells from monocytes in vitro. Eur. J. Immunol. *27*, 431–441.

Chen, T.H., Hsu, Y.T., Chen, C.H., Kao, S.H., and Lee, H.M. (2007). Tanshinone IIA from Salvia miltiorrhiza induces heme oxygenase-1 expression and inhibits lipopolysaccharide-induced nitric oxide expression in RAW 264.7 cells. Mitochondrion *7*, 101–105.

Clarke, I.N. (2010). Chlamydial transformation: facing up to the challenge. In Chlamydial Infections. Twelfth International Symposium on Human Chlamydial Infections,.

Clifton, D.R., Goss, R.A., Sahni, S.K., van Antwerp, D., Baggs, R.B., Marder, V.J., Silverman, D.J., and Sporn, L.A. (1998). NF-kappa B-dependent inhibition of apoptosis is essential for host cellsurvival during Rickettsia rickettsii infection. Proc. Natl. Acad. Sci. U. S. A. *95*, 4646–4651.

Clifton, D.R., Fields, K.A., Grieshaber, S.S., Dooley, C.A., Fischer, E.R., Mead, D.J., Carabeo, R.A., and Hackstadt, T. (2004). A chlamydial type III translocated protein is tyrosine-phosphorylated at the site of entry and associated with recruitment of actin. Proc. Natl. Acad. Sci. U. S. A. *101*, 10166–10171.

Coles, A.M., and Pearce, J.H. (1987). Regulation of Chlamydia psittaci (strain guinea pig inclusion conjunctivitis) growth in McCoy cells by amino acid antagonism. J. Gen. Microbiol. *133*, 701–708.

Coles, A.M., Reynolds, D.J., Harper, A., Devitt, A., and Pearce, J.H. (1993). Low-nutrient induction of abnormal chlamydial development: a novel component of chlamydial pathogenesis? FEMS Microbiol. Lett. *106*, 193–200.

Comer, J.E., Galindo, C.L., Zhang, F., Wenglikowski, A.M., Bush, K.L., Garner, H.R., Peterson, J.W., and Chopra, A.K. (2006). Murine macrophage transcriptional and functional responses to Bacillus anthracis edema toxin. Microb. Pathog. *41*, 96–110.

Crauwels, P., Bohn, R., Thomas, M., Gottwalt, S., Jackel, F., Kramer, S., Bank, E., Tenzer, S., Walther, P., Bastian, M., et al. (2015). Apoptotic-like Leishmania exploit the host's autophagy machinery to reduce T-cell-mediated parasite elimination. Autophagy *11*, 285–297.

Van Dam, H., and Castellazzi, M. (2001). Distinct roles of Jun : Fos and Jun : ATF dimers in oncogenesis. Oncogene *20*, 2453–2464.

Das, A., Ganesh, K., Khanna, S., Sen, C.K., and Roy, S. (2014). Engulfment of apoptotic cells by macrophages: a role of microRNA-21 in the resolution of wound inflammation. J. Immunol. *192*, 1120–1129.

Dautry-Varsat, A., Subtil, A., and Hackstadt, T. (2005). Recent insights into the mechanisms of Chlamydia entry. Cell. Microbiol. *7*, 1714–1722.

Dean, D., and Powers, V.C. (2001). Persistent Chlamydia trachomatis infections resist apoptotic stimuli. Infect. Immun. *69*, 2442–2447.

Devitt, A., and Marshall, L.J. (2011). The innate immune system and the clearance of apoptotic cells. J. Leukoc. Biol. *90*, 447–457.

Diget, E.A., Zuwala, K., Berg, R.K., Laursen, R.R., Søby, S., Østergaard, L., Melchjorsen, J., and Mogensen, T.H. (2013). Characterization of HIV-1 infection and innate sensing in different types of primary human monocyte-derived macrophages. Mediators Inflamm. *2013*.

Distel, R.J., and Spiegelman, B.M. (1990). Protooncogene c-fos as a transcription factor. Adv. Cancer Res. *55*, 37–55.

Doehn, U., Hauge, C., Frank, S.R., Jensen, C.J., Duda, K., Nielsen, J. V., Cohen, M.S., Johansen, J. V., Winther, B.R., Lund, L.R., et al. (2009). RSK Is a Principal Effector of the RAS-ERK Pathway for Eliciting a Coordinate Promotile/Invasive Gene Program and Phenotype in Epithelial Cells. Mol. Cell *35*, 511–522.

Dreses-Werringloer, U., Padubrin, I., Jürgens-Saathoff, B., Hudson, A.P., Zeidler, H., and Köhler, L. (2000). Persistence of Chlamydia trachomatis is induced by ciprofloxacin and ofloxacin in vitro. Antimicrob. Agents Chemother. *44*, 3288–3297.

Droemann, D., Rupp, J., Goldmann, T., Uhlig, U., Branscheid, D., Vollmer, E., Kujath, P., Zabel, P., and Dalhoff, K. (2007). Disparate innate immune responses to

persistent and acute Chlamydia pneumoniae infection in chronic obstructive pulmonary disease. Am. J. Respir. Crit. Care Med. *175*, 791–797.

Dumrese, C., Maurus, C.F., Gygi, D., Schneider, M.K.J., Walch, M., Groscurth, P., and Ziegler, U. (2005). Chlamydia pneumoniae induces aponecrosis in human aortic smooth muscle cells. BMC Microbiol. *5*, 2.

Dunn, W.A. (1990a). Studies on the mechanisms of autophagy: Formation of the autophagic vacuole. J. Cell Biol. *110*, 1923–1933.

Dunn, W.A. (1990b). Studies on the mechanisms of autophagy: Maturation of the autophagic vacuole. J. Cell Biol. *110*, 1935–1945.

Ebers (1875). Papyrus Ebers.

Eferl, R., and Wagner, E.F. (2003). AP-1: a double-edged sword in tumorigenesis. Nat. Rev. Cancer *3*, 859–868.

Ehrt, S., Schnappinger, D., Bekiranov, S., Drenkow, J., Shi, S., Gingeras, T.R., Gaasterland, T., Schoolnik, G., and Nathan, C. (2001). Reprogramming of the macrophage transcriptome in response to interferon-gamma and Mycobacterium tuberculosis: signaling roles of nitric oxide synthase-2 and phagocyte oxidase. J. Exp. Med. *194*, 1123–1140.

Everett, K.D., Bush, R.M., and Andersen, A.A. (1999). Emended description of the order Chlamydiales, proposal of Parachlamydiaceae fam. nov. and Simkaniaceae fam. nov., each containing one monotypic genus, revised taxonomy of the family Chlamydiaceae, including a new genus and five new species, and standards. Int. J. Syst. Bacteriol. *49 Pt 2*, 415–440.

Fadok, V.A., Bratton, D.L., Konowal, A., Freed, P.W., Westcott, J.Y., and Henson, P.M. (1998). Macrophages that have ingested apoptotic cells in vitro inhibit proinflammatory cytokine production through autocrine/paracrine mechanisms involving TGF-??, PGE2, and PAF. J. Clin. Invest. *101*, 890–898.

Fainardi, E., Castellazzi, M., Seraceni, S., Granieri, E., and Contini, C. (2008). Under the microscope: focus on Chlamydia pneumoniae infection and multiple sclerosis. Curr. Neurovasc. Res. *5*, 60–70.

Fan, B.T., Lu, H., Hu, H., Shi, L., Mcclarty, G.A., Nance, D.M., Greenberg, A.H., and Zhong, G. (1998). Inhibition of Apoptosis in Chlamydia-infected Cells : Caspase Activation. *187*.

Fan, G.W., Gao, X.M., Wang, H., Zhu, Y., Zhang, J., Hu, L.M., Su, Y.F., Kang, L.Y., and Zhang, B.L. (2009). The anti-inflammatory activities of Tanshinone IIA, an active component of TCM, are mediated by estrogen receptor activation and inhibition of iNOS. J. Steroid Biochem. Mol. Biol. *113*, 275–280.

Faro, S. (1985). Chlamydia trachomatis infection in women. J. Reprod. Med. *30*, 273–278.

Ferrara, P., Andermarcher, E., Bossis, G., Acquaviva, C., Brockly, F., Jariel-Encontre, I., and Piechaczyk, M. (2003). The structural determinants responsible for c-Fos protein proteasomal degradation differ according to the conditions of expression. Oncogene *22*, 1461–1474.

Fischer, S.F., Schwarz, C., Vier, J., and Häcker, G. (2001). Characterization of antiapoptotic activities of Chlamydia pneumoniae in human cells. Infect. Immun. *69*, 7121–7129.

Fischer, S.F., Vier, J., Kirschnek, S., Klos, A., Hess, S., Ying, S., and Häcker, G. (2004). Chlamydia inhibit host cell apoptosis by degradation of proapoptotic BH3-only proteins. J. Exp. Med. *200*, 905–916.

Fleetwood, A.J., Lawrence, T., Hamilton, J.A., and Cook, A.D. (2007). Granulocyte-macrophage colony-stimulating factor (CSF) and macrophage CSF-dependent macrophage phenotypes display differences in cytokine profiles and transcription factor activities: implications for CSF blockade in inflammation. J. Immunol. *178*, 5245–5252.

Fling, S.P., Sutherland, R.A., Steele, L.N., Hess, B., D'Orazio, S.E., Maisonneuve, J., Lampe, M.F., Probst, P., and Starnbach, M.N. (2001). CD8+ T cells recognize an inclusion membrane-associated protein from the vacuolar pathogen Chlamydia trachomatis. Proc. Natl. Acad. Sci. U. S. A. *98*, 1160–1165.

Franklin, C.C., Sanchez, V., Wagner, F., Woodgett, J.R., and Kraft, A.S. (1992). Phorbol ester-induced amino-terminal phosphorylation of human JUN but not JUNB regulates transcriptional activation. Proc. Natl. Acad. Sci. U. S. A. *89*, 7247–7251.

Fritsche, T.R., Horn, M., Wagner, M., Herwig, R.P., Schleifer, K.H., and Gautom, R.K. (2000). Phylogenetic diversity among geographically dispersed Chlamydiales endosymbionts recovered from clinical and environmental isolates of Acanthamoeba spp. Appl. Environ. Microbiol. *66*, 2613–2619.

Van Furth, R., Diesselhoff-den Dulk, M.C., and Mattie, H. (1973). Quantitative study on the production and kinetics of mononuclear phagocytes during an acute inflammatory reaction. J. Exp. Med. *138*, 1314–1330.

Galmiche, A., Rassow, J., Doye, A., Cagnol, S., Chambard, J.C., Contamin, S., de Thillot, V., Just, I., Ricci, V., Solcia, E., et al. (2000). The N-terminal 34 kDa fragment of Helicobacter pylori vacuolating cytotoxin targets mitochondria and induces cytochrome c release. EMBO J. *19*, 6361–6370.

Gambhir, M., Basáñez, M.G., Turner, F., Kumaresan, J., and Grassly, N.C. (2007). Trachoma: transmission, infection, and control. Lancet Infect. Dis. *7*, 420–427.

Gautier, E.L., Shay, T., Miller, J., Greter, M., Jakubzick, C., Ivanov, S., Helft, J., Chow, A., Elpek, K.G., Gordonov, S., et al. (2012). Gene-expression profiles and transcriptional regulatory pathways that underlie the identity and diversity of mouse tissue macrophages. Nat. Immunol. *13*, 1118–1128.

Gaydos, C.A., Summersgill, J.T., and Sahney, N.N. (1996). Replication of Chlamydia pneumoniae in vitro in human macrophages , endothelial cells , and aortic artery

smooth muscle cells . Replication of Chlamydia pneumoniae In Vitro in Human Macrophages , Endothelial Cells , and Aortic Artery Smooth Muscle Cells.

Gervassi, A.L., Grabstein, K.H., Probst, P., Hess, B., Alderson, M.R., and Fling, S.P. (2004). Human CD8+ T cells recognize the 60-kDa cysteine-rich outer membrane protein from Chlamydia trachomatis. J. Immunol. *173*, 6905–6913.

Ghosh, S., Bhattacharyya, S., Sirkar, M., Sa, G.S., Das, T., Majumdar, D., Roy, S., and Majumdar, S. (2002). Leishmania donovani suppresses activated protein 1 and NF-kappaB activation in host macrophages via ceramide generation: involvement of extracellular signal-regulated kinase. Infect. Immun. *70*, 6828–6838.

Gieffers, J., van Zandbergen, G., Rupp, J., Sayk, F., Krüger, S., Ehlers, S., Solbach, W., and Maass, M. (2004). Phagocytes transmit Chlamydia pneumoniae from the lungs to the vasculature. Eur. Respir. J. *23*, 506–510.

Goerdt, S., and Orfanos, C.E. (1999). Other functions, other genes: alternative activation of antigen-presenting cells. Immunity *10*, 137–142.

Goerdt, S., Politz, O., Schledzewski, K., Birk, R., Gratchev, A., Guillot, P., Hakiy, N., Klemke, C.D., Dippel, E., Kodelja, V., et al. (1999). Alternative versus classical activation of macrophages. Pathobiology *67*, 222–226.

Gordon, S. (2003). Alternative activation of macrophages. Nat. Rev. Immunol. *3*, 23–35.

Gracey, E., Lin, A., Akram, A., Chiu, B., and Inman, R.D. (2013). Intracellular Survival and Persistence of Chlamydia muridarum Is Determined by Macrophage Polarization. PLoS One *8*, 1–10.

Grayston, J.T. (1992). Infections caused by Chlamydia pneumoniae strain TWAR. Clin. Infect. Dis. *15*, 757–761.

Grayston, J.T., Aldous, M.B., Easton, A., Wang, S.P., Kuo, C.C., Campbell, L.A., and Altman, J. (1993). Evidence that Chlamydia pneumoniae causes pneumonia and bronchitis. J. Infect. Dis. *168*, 1231–1235.

Greene, W., Xiao, Y., Huang, Y., McClarty, G., and Zhong, G. (2004). Chlamydia-Infected Cells Continue to Undergo Mitosis and Resist Induction of Apoptosis. Infect. Immun. *72*, 451–460.

Grieshaber, N.A., Fischer, E.R., Mead, D.J., Dooley, C.A., and Hackstadt, T. (2004). Chlamydial histone-DNA interactions are disrupted by a metabolite in the methylerythritol phosphate pathway of isoprenoid biosynthesis. Proc. Natl. Acad. Sci. U. S. A. *101*, 7451–7456.

Grieshaber, S., Swanson, J.A., and Hackstadt, T. (2002). Determination of the physical environment within the Chlamydia trachomatis inclusion using ion-selective ratiometric probes. Cell. Microbiol. *4*, 273–283.

Grieshaber, S.S., Grieshaber, N.A., and Hackstadt, T. (2003). Chlamydia trachomatis uses host cell dynein to traffic to the microtubule-organizing center in a p50 dynamitin-independent process. J. Cell Sci. *116*, 3793–3802.

Hackstadt, T. (1999). Chapter 5 : Cell Biology. In Chlamydia,.

Hackstadt, T., Rockey, D.D., Heinzen, R.A., and Scidmore, M.A. (1996). Chlamydia trachomatis interrupts an exocytic pathway to acquire endogenously synthesized sphingomyelin in transit from the Golgi apparatus to the plasma membrane. EMBO J. *15*, 964–977.

Hackstadt, T., Fischer, E.R., Scidmore, M.A., Rockey, D.D., and Heinzen, R.A. (1997). Origins and functions of the chlamydial inclusion. Trends Microbiol. *5*, 288–293.

Haggerty, C.L., Gottlieb, S.L., Taylor, B.D., Low, N., Xu, F., and Ness, R.B. (2010). Risk of sequelae after Chlamydia trachomatis genital infection in women. J. Infect. Dis. *201 Suppl*, S134–S155.

Hahn, D.L. Role of Chlamydia pneumoniae as an Inducer of Asthma. In Chlamydia Pneumoniae Infection and Disease, pp. 239–262.

Hahn, D.L., Dodge, R.W., and Golubjatnikov, R. (1991). Association of Chlamydia pneumoniae (strain TWAR) infection with wheezing, asthmatic bronchitis, and adult-onset asthma. JAMA *266*, 225–230.

Hai, T., and Curran, T. (1991). Cross-family dimerization of transcription factors Fos/Jun and ATF/CREB alters DNA binding specificity. Proc. Natl. Acad. Sci. U. S. A. *88*, 3720–3724.

Van Hal, S.J., Hillman, R., Stark, D.J., Harkness, J.L., and Marriott, D. (2007). Lymphogranuloma venereum: An emerging anorectal disease in Australia. Med. J. Aust. *187*, 309–310.

Halazonetis, T.D., Georgopoulos, K., Greenberg, M.E., and Leder, P. (1988). c-Jun dimerizes with itself and with c-Fos, forming complexes of different DNA binding affinities. Cell *55*, 917–924.

Hambleton, J., Weinsteint, S.L., Lemt, L., Defrancots, A.L., and Bishop, J.M. (1996). lipopolysaccharide-stimulated macrophages. *93*, 2774–2778.

Haranaga, S., Yamaguchi, H., Ikejima, H., Friedman, H., and Yamamoto, Y. (2003). Chlamydia pneumoniae infection of alveolar macrophages: a model. J. Infect. Dis. *187*, 1107–1115.

Harper, A., Pogson, C.I., Jones, M.L., and Pearce, J.H. (2000). Chlamydial development is adversely affected by minor changes in amino acid supply, blood plasma amino acid levels, and glucose deprivation. Infect. Immun. *68*, 1457–1464.

Hatch, G.M., and McClarty, G. (1998). Cardiolipin remodeling in eukaryotic cells infected with Chlamydia trachomatis is linked to elevated mitochondrial metabolism. Biochem. Biophys. Res. Commun. *243*, 356–360.

Hatch, T.P., Al-Hossainy, E., and Silverman, J.A. (1982). Adenine nucleotide and lysine transport in Chlamydia psittaci. J. Bacteriol. *150*, 662–670.

Hatch, T.P., Miceli, M., and Sublett, J.E. (1986). Synthesis of disulfide-bonded outer membrane proteins during the developmental cycle of Chlamydia psittaci and Chlamydia trachomatis. J. Bacteriol. *165*, 379–385.

Hearst, J.E., Warr, G.A., and Jakab, G.J. (1980). Characterization of murine lung and peritoneal macrophages. J. Reticuloendothel. Soc. *27*, 443–454.

Heinzen, R.A., Scidmore, M.A., Rockey, D.D., and Hackstadt, T. (1996). Differential interaction with endocytic and exocytic pathways distinguish parasitophorous vacuoles of Coxiella burnetii and Chlamydia trachomatis. Infect. Immun. *64*, 796–809.

Von Hertzen, L., Alakärppä, H., Koskinen, R., Liippo, K., Surcel, H.M., Leinonen, M., and Saikku, P. (1997). Chlamydia pneumoniae infection in patients with chronic obstructive pulmonary disease. Epidemiol. Infect. *118*, 155–164.

Hess, J., Angel, P., and Schorpp-Kistner, M. (2004). AP-1 subunits: quarrel and harmony among siblings. J. Cell Sci. *117*, 5965–5973.

Heuer, D., Rejman Lipinski, A., Machuy, N., Karlas, A., Wehrens, A., Siedler, F., Brinkmann, V., and Meyer, T.F. (2009). Chlamydia causes fragmentation of the Golgi compartment to ensure reproduction. Nature *457*, 731–735.

Hilbi, H., Zychlinsky, A., and Sansonetti, P.J. (1997). Macrophage apoptosis in microbial infections. Parasitology *115 Suppl*, S79–S87.

Hodinka, R.L., Davis, C.H., Choong, J., and Wyrick, P.B. (1988). Ultrastructural study of endocytosis of Chlamydia trachomatis by McCoy cells. Infect. Immun. *56*, 1456–1463.

Hogan, R.J., Mathews, S.A., Kutlin, A., Hammerschlag, M.R., and Timms, P. (2003). Differential expression of genes encoding membrane proteins between acute and continuous Chlamydia pneumoniae infections. Microb. Pathog. *34*, 11–16.

Hogan, R.J., Mathews, S. a., Mukhopadhyay, S., Summersgill, J.T., and Timms, P. (2004). Chlamydial Persistence: Beyond the Biphasic Paradigm. Infect. Immun. *72*, 1843–1855.

Holness, C.L., and Simmons, D.L. (1993). Molecular cloning of CD68, a human macrophage marker related to lysosomal glycoproteins. Blood *81*, 1607–1613.

Horn, M., Wagner, M., Müller, K.D., Schmid, E.N., Fritsche, T.R., Schleifer, K.H., and Michel, R. (2000). Neochlamydia hartmannellae gen. nov., sp. nov. (Parachlamydiaceae), an endoparasite of the amoeba Hartmannella vermiformis. Microbiology *146*, 1231–1239.

Huynh, M.L.N., Fadok, V.A., and Henson, P.M. (2002). Phosphatidylserine-dependent ingestion of apoptotic cells promotes TGF-??1 secretion and the resolution of inflammation. J. Clin. Invest. *109*, 41–50.

Hybiske, K., and Stephens, R.S. (2007a). Mechanisms of Chlamydia trachomatis entry into nonphagocytic cells. Infect. Immun. *75*, 3925–3934.

Hybiske, K., and Stephens, R.S. (2007b). Mechanisms of host cell exit by the intracellular bacterium Chlamydia. Proc. Natl. Acad. Sci. U. S. A. *104*, 11430–11435.

Hybiske, K., and Stephens, R.S. (2008). Exit strategies of intracellular pathogens. Nat. Rev. Microbiol. *6*, 99–110.

Igietseme, J.U., Ananaba, G.A., Candal, D.H., Lyn, D., and Black, C.M. (1998). Immune control of Chlamydial growth in the human epithelial cell line RT4 involves multiple mechanisms that include nitric oxide induction, tryptophan catabolism and iron deprivation. Microbiol. Immunol. *42*, 617–625.

Iliffe-Lee, E.R., and McClarty, G. (1999). Glucose metabolism in Chlamydia trachomatis: The “energy parasite” hypothesis revisited. Mol. Microbiol. *33*, 177–187.

Jang, S. Il, Kim, H.J., Kim, Y.-J., Jeong, S.-I., and You, Y.-O. (2006). Tanshinone IIA inhibits LPS-induced NF-kappaB activation in RAW 264.7 cells: possible involvement of the NIK-IKK, ERK1/2, p38 and JNK pathways. Eur. J. Pharmacol. *542*, 1–7.

Jendro, M.C., Fingerle, F., Deutsch, T., Liese, A., Köhler, L., Kuipers, J.G., Raum, E., Martin, M., and Zeidler, H. (2004). Chlamydia trachomatis-infected macrophages induce apoptosis of activated T cells by secretion of tumor necrosis factor-α in vitro. Med. Microbiol. Immunol. *193*, 45–52.

Jewett, T.J., Fischer, E.R., Mead, D.J., and Hackstadt, T. (2006). Chlamydial TARP is a bacterial nucleator of actin. Proc. Natl. Acad. Sci. U. S. A. *103*, 15599–15604.

Jones, M.L., Gaston, J.S., and Pearce, J.H. (2001). Induction of abnormal Chlamydia trachomatis by exposure to interferon-gamma or amino acid deprivation and comparative antigenic analysis. Microb. Pathog. *30*, 299–309.

Kalman, S., Mitchell, W., Marathe, R., Lammel, C., Fan, J., Hyman, R.W., Olinger, L., Grimwood, J., Davis, R.W., and Stephens, R.S. (1999). Comparative genomes of Chlamydia pneumoniae and C. trachomatis. Nat. Genet. *21*, 385–389.

Kari, L., Goheen, M.M., Randall, L.B., Taylor, L.D., Carlson, J.H., Whitmire, W.M., Virok, D., Rajaram, K., Endresz, V., McClarty, G., et al. (2011). Generation of targeted Chlamydia trachomatis null mutants. Proc. Natl. Acad. Sci. U. S. A. *108*, 7189–7193.

Karin, M., Liu, Z.G., and Zandi, E. (1997). AP-1 function and regulation. Curr. Opin. Cell Biol. *9*, 240–246.

Kharkrang (2010). Mechanisms Involved in Type II Macrophage Activation and Effector Functions.

Kim, S.K., Angevine, M., Demick, K., Ortiz, L., Rudersdorf, R., Watkins, D., and DeMars, R. (1999). Induction of HLA class I-restricted CD8+ CTLs specific for the major outer membrane protein of Chlamydia trachomatis in human genital tract infections. J. Immunol. *162*, 6855–6866.

Klionsky, D.J., and Emr, S.D. (2000). Autophagy as a regulated pathway of cellular degradation. Science *290*, 1717–1721.

Koh, W.P., Taylor, M.B., Hughes, K., Chew, S.K., Fong, C.W., and Phoon, M.C. (2002). Seroprevalence of IgG antibodies against Chlamydia pneumoniae in Chinese , Malays and Asian Indians in Singapore. 1001–1007.

Koike, K. (2007). Pathogenesis of HCV-associated HCC: Dual-pass carcinogenesis through activation of oxidative stress and intracellular signaling. Hepatol. Res. *37 Suppl 2*, S115–S120.

Kondo, Y., and Kondo, S. (2006). Autophagy and Cancer Therapy ACKNOWLEDGEMENTS IEN ABBREVIATIONS INTRODUCTION. Autophagy *2*, 85–90.

Kouzarides, T., and Ziff, E. (1988). The role of the leucine zipper in the fos-jun interaction. Nature *336*, 646–651.

Kozlovsky, N., Rudich, a., Potashnik, R., Ebina, Y., Murakami, T., and Bashan, N. (1997). Transcriptional Activation of the Glut1 Gene in Response to Oxidative Stress in L6 Myotubes. J. Biol. Chem. *272*, 33367–33372.

Krämer, S., Crauwels, P., Bohn, R., Radzimski, C., Szaszák, M., Klinger, M., Rupp, J., and van Zandbergen, G. (2015). AP-1 Transcription Factor Serves as a Molecular Switch between Chlamydia pneumoniae Replication and Persistence. Infect. Immun. *83*, 2651–2660.

Krüll, M., Maass, M., Suttorp, N., and Rupp, J. (2005). Chlamydophila pneumoniae. Mechanisms of target cell infection and activation. Thromb. Haemost. *94*, 319–326.

Kuo, C., Puolakkainen, M., Lin, T.-M., Witte, M., and Campbell, L.A. (2002). Mannose-receptor positive and negative mouse macrophages differ in their susceptibility to infection by Chlamydia species. Microb. Pathog. *32*, 43–48.

Kuo, C.C., Jackson, L.A., Campbell, L.A., and Grayston, J.T. (1995). Chlamydia pneumoniae (TWAR). Clin. Microbiol. Rev. *8*, 451–461.

Lad, S.P., Li, J., da Silva Correia, J., Pan, Q., Gadwal, S., Ulevitch, R.J., and Li, E. (2007a). Cleavage of p65/RelA of the NF-kappaB pathway by Chlamydia. Proc. Natl. Acad. Sci. U. S. A. *104*, 2933–2938.

Lad, S.P., Yang, G., Scott, D.A., Wang, G., Nair, P., Mathison, J., Reddy, V.S., and Li, E. (2007b). Chlamydial CT441 Is a PDZ domain-containing tail-specific protease that interferes with the NF-??B pathway of immune response. J. Bacteriol. *189*, 6619–6625.

Lallemand, D., Spyrou, G., Yaniv, M., and Pfarr, C.M. (1997). Variations in Jun and Fos protein expression and AP-1 activity in cycling, resting and stimulated fibroblasts. Oncogene *14*, 819–830.

Landschulz, W.H., Johnson, P.F., and McKnight, S.L. (1988). The leucine zipper: a hypothetical structure common to a new class of DNA binding proteins. Science *240*, 1759–1764.

Lee, C.-Y., Sher, H.-F., Chen, H.-W., Liu, C.-C., Chen, C.-H., Lin, C.-S., Yang, P.-C., Tsay, H.-S., and Chen, J.J.W. (2008). Anticancer effects of tanshinone I in human non-small cell lung cancer. Mol. Cancer Ther. *7*, 3527–3538.

Lee, S.K., Kim, B.S., Yang, W.S., Kim, S.B., Park, S.K., and Park, J.S. (2001). High glucose induces MCP-1 expression partly via tyrosine kinase-AP-1 pathway in peritoneal mesothelial cells. Kidney Int. *60*, 55–64.

Leenen, P.J.M., De Bruijn, M.F.T.R., Voerman, J.S.A., Campbell, P.A., and Van Ewijk, W. (1994). Markers of mouse macrophage development detected by monoclonal antibodies. J. Immunol. Methods *174*, 5–19.

Lehrer, R.I., Ganz, T., Selsted, M.E., Babior, B.M., and Curnutte, J.T. (1988). Neutrophils and host defense. Ann. Intern. Med. *109*, 127–142.

Levine, B., Mizushima, N., and Virgin, H.W. (2011). Autophagy in immunity and inflammation. Nature *469*, 323–335.

Li, G., Shan, C., Liu, L., Zhou, T., Zhou, J., Hu, X., Chen, Y., Cui, H., and Gao, N. (2015). Tanshinone IIA Inhibits HIF-1α and VEGF Expression in Breast Cancer Cells via mTOR/p70S6K/RPS6/4E-BP1 Signaling Pathway. PLoS One *10*, e0117440.

Li, X., Du, J.R., Yu, Y., Bai, B., and Zheng, X.Y. (2010). Tanshinone IIA inhibits smooth muscle proliferation and intimal hyperplasia in the rat carotid balloon-injured model through inhibition of MAPK signaling pathway. J. Ethnopharmacol. *129*, 273–279.

Livak, K.J., and Schmittgen, T.D. (2001). Analysis of relative gene expression data using real-time quantitative PCR and the 2(-Delta Delta C(T)) Method. Methods *25*, 402–408.

Lucas, M., Stuart, L.M., Zhang, A., Hodivala-Dilke, K., Febbraio, M., Silverstein, R., Savill, J., and Lacy-Hulbert, A. (2006). Requirements for apoptotic cell contact in regulation of macrophage responses. J. Immunol. *177*, 4047–4054.

Luo, H.R., and Loison, F. (2008). Constitutive neutrophil apoptosis: Mechanisms and regulation. Am. J. Hematol. *83*, 288–295.

Maass, M., Jahn, J., Gieffers, J., Dalhoff, K., Katus, H.A., and Solbach, W. (2000). Detection of Chlamydia pneumoniae within peripheral blood monocytes of patients with unstable angina or myocardial infarction. J. Infect. Dis. *181 Suppl*, S449–S451.

Mabey, D., and Peeling, R.W. (2002). Lymphogranuloma venereum. Sex. Transm. Infect. *78*, 90–92.

Maiuri, M.C., Criollo, A., and Kroemer, G. (2010). Crosstalk between apoptosis and autophagy within the Beclin 1 interactome. EMBO J. *29*, 515–516.

Mantovani, A., Sica, A., Sozzani, S., Allavena, P., Vecchi, A., and Locati, M. (2004). The chemokine system in diverse forms of macrophage activation and polarization. Trends Immunol. *25*, 677–686.

Martinez, F.O., and Gordon, S. (2014). The M1 and M2 paradigm of macrophage activation: time for reassessment. F1000Prime Rep. *6*, 13.

Martinez, F.O., Gordon, S., Locati, M., and Mantovani, A. (2006). Transcriptional profiling of the human monocyte-to-macrophage differentiation and polarization: new molecules and patterns of gene expression. J. Immunol. *177*, 7303–7311.

Martinez, F.O., Helming, L., and Gordon, S. (2009). Alternative activation of macrophages: an immunologic functional perspective. Annu. Rev. Immunol. *27*, 451–483.

Mathews, S., George, C., Flegg, C., Stenzel, D., and Timms, P. (2001). Differential expression of ompA, ompB, pyk, nlpD and Cpn0585 genes between normal and interferon-gamma treated cultures of Chlamydia pneumoniae. Microb. Pathog. *30*, 337–345.

Matsumoto, A., and Manire, G.P. (1970). Electron microscopic observations on the effects of penicillin on the morphology of Chlamydia psittaci. J. Bacteriol. *101*, 278–285.

McClarty, G. (1999). Chlamydial metabolism as inferred from the complete genome sequence. In Chlamydia, pp. 69–100.

McClarty, G., and Fan, H. (1993). Purine metabolism by intracellular Chlamydia psittaci. J. Bacteriol. *175*, 4662–4669.

McClarty, G., and Qin, B. (1993). Pyrimidine metabolism by intracellular Chlamydia psittaci. J. Bacteriol. *175*, 4652–4661.

Mechta-Grigoriou, F., Gerald, D., and Yaniv, M. (2001). The mammalian Jun proteins: redundancy and specificity. Oncogene *20*, 2378–2389.

Mehlitz, A., and Rudel, T. (2013). Modulation of host signaling and cellular responses by Chlamydia. Cell Commun. Signal. *11*, 90.

Mehta, S.J., Miller, R.D., Ramirez, J.A., and Summersgill, J.T. (1998). Inhibition of Chlamydia pneumoniae replication in HEp-2 cells by interferon-gamma: role of tryptophan catabolism. J. Infect. Dis. *177*, 1326–1331.

Miller, S.A., Selzman, C.H., Shames, B.D., Barton, H. a, Johnson, S.M., and Harken, a H. (2000). Chlamydia pneumoniae activates nuclear factor kappaB and activator protein 1 in human vascular smooth muscle and induces cellular proliferation. J. Surg. Res. *90*, 76–81.

Mills, C.D., Kincaid, K., Alt, J.M., Heilman, M.J., and Hill, A.M. (2000). M-1/M-2 macrophages and the Th1/Th2 paradigm. J. Immunol. *164*, 6166–6173.

Miyairi, I., and Byrne, G.I. (2006). Chlamydia and programmed cell death. Curr. Opin. Microbiol. *9*, 102–108.

Mizushima, N., Levine, B., Cuervo, A.M., and Klionsky, D.J. (2008). Autophagy fights disease through cellular self-digestion. Nature *451*, 1069–1075.

Moazed, T.C., Kuo, C.C., Grayston, J.T., and Campbell, L.A. (1998). Evidence of systemic dissemination of Chlamydia pneumoniae via macrophages in the mouse. J. Infect. Dis. *177*, 1322–1325.

Molestina, R.E., Miller, R.D., Ramirez, J.A., and Summersgill, J.T. (1999). Infection of human endothelial cells with Chlamydia pneumoniae stimulates transendothelial migration of neutrophils and monocytes. Infect. Immun. *67*, 1323–1330.

Molestina, R.E., Klein, J.B., Miller, R.D., Pierce, W.H., Ramirez, J.A., and Summersgill, J.T. (2002). Proteomic Analysis of Differentially Expressed Chlamydia pneumoniae Genes during Persistent Infection of HEp-2 Cells. Infect. Immun. *70*, 2976–2981.

Mosser, D.M. (2003). The many faces of macrophage activation. J. Leukoc. Biol. *73*, 209–212.

Mosser, D.M., and Edwards, J.P. (2008). Exploring the full spectrum of macrophage activation. Nat. Rev. Immunol. *8*, 958–969.

Moulder, J.W. (1970). Glucose Metabolism of L Cells Before and After Infection with Chlamydia psittaci. J. Bacteriol. *104*, 1189–1196.

Moulder, J.W. (1991). Interaction of chlamydiae and host cells in vitro. Microbiol. Rev. *55*, 143–190.

Müller, A., Günther, D., Brinkmann, V., Hurwitz, R., Meyer, T.F., and Rudel, T. (2000). Targeting of the pro-apoptotic VDAC-like porin (PorB) of Neisseria gonorrhoeae to mitochondria of infected cells. EMBO J. *19*, 5332–5343.

Nanagara, R., Li, F., Beutler, A., Hudson, A., and Schumacher, H.R. (1995). Alteration of Chlamydia trachomatis biologic behavior in synovial membranes: Suppression of surface antigen production in reactive arthritis and Reiter's syndrome. Arthritis Rheum. *38*, 1410–1417.

Nathan, C. (2006). Neutrophils and immunity: challenges and opportunities. Nat. Rev. Immunol. *6*, 173–182.

Nathan, C.F. (1987). Neutrophil activation on biological surfaces. Massive secretion of hydrogen peroxide in response to products of macrophages and lymphocytes. J. Clin. Invest. *80*, 1550–1560.

Neeper, I.D., Patton, D.L., and Kuo, C.C. (1990). Cinematographic observations of growth cycles of Chlamydia trachomatis in primary cultures of human amniotic cells. Infect. Immun. *58*, 2042–2047.

Le Negrate, G., Krieg, A., Faustin, B., Loeffler, M., Godzik, A., Krajewski, S., and Reed, J.C. (2008). ChlaDub1 of Chlamydia trachomatis suppresses NF-kappaB activation and inhibits IkappaBalpha ubiquitination and degradation. Cell. Microbiol. *10*, 1879–1892.

Nelson, D.E., Virok, D.P., Wood, H., Roshick, C., Johnson, R.M., Whitmire, W.M., Crane, D.D., Steele-Mortimer, O., Kari, L., McClarty, G., et al. (2005). Chlamydial IFN-gamma immune evasion is linked to host infection tropism. Proc. Natl. Acad. Sci. U. S. A. *102*, 10658–10663.

Neu, C., Sedlag, A., Bayer, C., Förster, S., Crauwels, P., Niess, J.H., van Zandbergen, G., Frascaroli, G., and Riedel, C.U. (2013). CD14-Dependent Monocyte Isolation Enhances Phagocytosis of Listeria monocytogenes by Proinflammatory, GM-CSF-Derived Macrophages. PLoS One *8*.

Nicholson, T.L., Olinger, L., Chong, K., Schoolnik, G., and Stephens, R.S. (2003). Global stage-specific gene regulation during the developmental cycle of Chlamydia trachomatis. J. Bacteriol. *185*, 3179–3189.

Ogden, C.A., Pound, J.D., Batth, B.K., Owens, S., Johannessen, I., Wood, K., and Gregory, C.D. (2005). Enhanced apoptotic cell clearance capacity and B cell survival factor production by IL-10-activated macrophages: implications for Burkitt's lymphoma. J. Immunol. *174*, 3015–3023.

Ojcius, D.M., Hellio, R., and Dautry-Varsat, A. (1997). Distribution of endosomal, lysosomal, and major histocompatibility complex markers in a monocytic cell line infected with Chlamydia psittaci. Infect. Immun. *65*, 2437–2442.

Ojcius, D.M., Bravo de Alba, Y., Kanellopoulos, J.M., Hawkins, R. a, Kelly, K. a, Rank, R.G., and Dautry-Varsat, a (1998a). Internalization of Chlamydia by dendritic cells and stimulation of Chlamydia-specific T cells. J. Immunol. *160*, 1297–1303.

Ojcius, D.M., Souque, P., Perfettini, J.L., and Dautry-Varsat, A. (1998b). Apoptosis of epithelial cells and macrophages due to infection with the obligate intracellular pathogen Chlamydia psittaci. J. Immunol. *161*, 4220–4226.

Ojcius, D.M., Degani, H., Dautry-varsat, A., Ojcius, D.M., Degani, H., Mispelter, J., and Dautry-varsat, A. (1998c). CELL BIOLOGY AND METABOLISM : Enhancement of ATP Levels and Glucose Metabolism during an Infection by Chlamydia : NMR STUDIES OF LIVING Enhancement of ATP Levels and Glucose Metabolism during an Infection by Chlamydia.

Okazaki, K., and Sagata, N. (1995). The Mos/MAP kinase pathway stabilizes c-Fos by phosphorylation and augments its transforming activity in NIH 3T3 cells. EMBO J. *14*, 5048–5059.

Olive, A.J., Haff, M.G., Emanuele, M.J., Sack, L.M., Barker, J.R., Elledge, S.J., and Starnbach, M.N. (2014). Chlamydia trachomatis-induced alterations in the host cell proteome are required for intracellular growth. Cell Host Microbe *15*, 113–124.

Omsland, A., Sager, J., Nair, V., Sturdevant, D.E., and Hackstadt, T. (2012). Developmental stage-specific metabolic and transcriptional activity of Chlamydia trachomatis in an axenic medium. Proc. Natl. Acad. Sci. U. S. A. *109*, 19781–19785.

Ooij, C. Van, Apodaca, G., and Engel, J. (1997). Characterization of the Chlamydia trachomatis vacuole and its interaction with the host endocytic pathway in HeLa cells . Characterization of the Chlamydia trachomatis Vacuole and Its Interaction with the Host Endocytic Pathway in HeLa Cells. *65*.

Ossewaarde, J.M., and Meijer, A. (1999). Molecular evidence for the existence of additional members of the order Chlamydiales. Microbiology *145*, 411–417.

Ouellette, S.P., Belland, R.J., Gieffers, J., and Byrne, G.I. The Biology of Chlamydia pneumoniae in Cardiovascular Disease Pathogenesis. In Chlamydia Pneumoniae Infection and Disease, pp. 135–151.

Pachikara, N., Zhang, H., Pan, Z., Jin, S., and Fan, H. (2009). Productive Chlamydia trachomatis lymphogranuloma venereum 434 infection in cells with augmented or inactivated autophagic activities. FEMS Microbiol. Lett. *292*, 240–249.

Palikhe, A., Lokki, M.-L., Saikku, P., Leinonen, M., Paldanius, M., Seppänen, M., Valtonen, V., Nieminen, M.S., and Sinisalo, J. (2008). Association of Chlamydia pneumoniae infection with HLA-B*35 in patients with coronary artery disease. Clin. Vaccine Immunol. *15*, 55–59.

Pantoja, L.G., Miller, R.D., Ramirez, J.A., Molestina, R.E., and Summersgill, J.T. (2001). Characterization of Chlamydia pneumoniae persistence in HEp-2 cells treated with gamma interferon. Infect. Immun. *69*, 7927–7932.

Park, S., Song, J., Lee, D., and Yang, C. (1999). Suppression of AP-1 Activity by Tanshinone and Cancer Cell Growth Inhibition. *20*, 925–928.

Passegué, E., and Wagner, E.F. (2000). JunB suppresses cell proliferation by transcriptional activation of p16(INK4a) expression. EMBO J. *19*, 2969–2979.

Patton, D.L., and Kuo, C.C. (1989). Histopathology of Chlamydia trachomatis salpingitis after primary and repeated reinfections in the monkey subcutaneous pocket model. J. Reprod. Fertil. *85*, 647–656.

Patton, D.L., Chan, K.Y., Kuo, C.C., Cosgrove, Y.T., and Langley, L. (1988). In vitro growth of Chlamydia trachomatis in conjunctival and corneal epithelium. Investig. Ophthalmol. Vis. Sci. *29*, 1087–1095.

Payne, C.M., Glasser, L., Tischler, M.E., Wyckoff, D., Cromey, D., Fiederlein, R., and Bohnert, O. (1994). Programmed cell death of the normal human neutrophil: An in vitro model of senescence. Microsc. Res. Tech. *28*, 327–344.

Peeling, R.W., and Brunham, R.C. (1996). Chlamydiae as pathogens: new species and new issues. Emerg. Infect. Dis. *2*, 307–319.

Perfettini, J.L., Reed, J.C., Israël, N., Martinou, J.C., Dautry-Varsat, A., and Ojcius, D.M. (2002a). Role of Bcl-2 family members in caspase-independent apoptosis during Chlamydia infection. Infect. Immun. *70*, 55–61.

Perfettini, J.L., Gissot, M., Souque, P., and Ojcius, D.M. (2002b). Modulation of apoptosis during infection with Chlamydia. Methods Enzymol. *358*, 334–344.

Perfettini, J.L., Hospital, V., Stahl, L., Jungas, T., Verbeke, P., and Ojcius, D.M. (2003). Cell death and inflammation during infection with the obligate intracellular pathogen, Chlamydia. Biochimie *85*, 763–769.

Peters, J., Hess, S., Endlich, K., Thalmann, J., Holzberg, D., Kracht, M., Schaefer, M., Bartling, G., and Klos, A. (2005). Silencing or permanent activation: Host-cell responses in models of persistent Chlamydia pneumoniae infection. Cell. Microbiol. *7*, 1099–1108.

Peterson, E.M., Cheng, X., Qu, Z., and De la Maza, L.M. (1996). Characterization of the murine antibody response to peptides representing the variable domains of the major outer membrane protein of Chlamydia pneumoniae. Infect. Immun. *64*, 3354–3359.

Pierson, T.C., Diamond, M.S., Ahmed, A.A., Valentine, L.E., Davis, C.W., Samuel, M.A., Hanna, S.L., Puffer, B.A., and Doms, R.W. (2005). An infectious West Nile Virus that expresses a GFP reporter gene. Virology *334*, 28–40.

Pretolani, M. (1999). Interleukin-10: An anti-inflammatory cytokine with therapeutic potential. Clin. Exp. Allergy *29*, 1164–1171.

Pulverer, B.J., Kyriakis, J.M., Avruch, J., Nikolakaki, E., and Woodgett, J.R. (1991). Phosphorylation of c-jun mediated by MAP kinases. Nature *353*, 670–674.

Rajalingam, K., Al-Younes, H., Müller, A., Meyer, T.F., Szczepek, A.J., and Rudel, T. (2001). Epithelial cells infected with Chlamydophila pneumoniae (Chlamydia pneumoniae) are resistant to apoptosis. Infect. Immun. *69*, 7880–7888.

Rankin, E.B., Wu, C., Khatri, R., Wilson, T.L.S., Andersen, R., Araldi, E., Rankin, A.L., Yuan, J., Kuo, C.J., Schipani, E., et al. (2012). The HIF signaling pathway in osteoblasts directly modulates erythropoiesis through the production of EPO. Cell *149*, 63–74.

Raulston, J.E. (1997). Response of Chlamydia trachomatis serovar E to iron restriction vitro and evidence for iron-regulated chlamydial proteins. Infect. Immun. *65*, 4539–4547.

Reggiori, F., and Klionsky, D.J. (2002). Autophagy in the eukaryotic cell. Eukaryot. Cell *1*, 11–21.

Reynolds, D.J., and Pearce, J.H. (1990). Characterization of the cytochalasin D-resistant (pinocytic) mechanisms of endocytosis utilized by chlamydiae. Infect. Immun. *58*, 3208–3216.

Rockey, D.D., Heinzen, R.A., and Hackstadt, T. (1995). Cloning and characterization of a Chlamydia psittaci gene coding for a protein localized in the inclusion membrane of infected cells. Mol. Microbiol. *15*, 617–626.

Rockey, D.D., Fischer, E.R., and Hackstadt, T. (1996). Temporal analysis of the developing Chlamydia psittaci inclusion by use of fluorescence and electron microscopy. Infect. Immun. *64*, 4269–4278.

Rodríguez, A., Rottenberg, M., Tjärnlund, A., and Fernández, C. (2006). Immunoglobulin A and CD8+ T-cell mucosal immune defenses protect against intranasal infection with Chlamydia pneumoniae. Scand. J. Immunol. *63*, 177–183.

Ronchetti, A., Rovere, P., Iezzi, G., Galati, G., Heltai, S., Protti, M.P., Garancini, M.P., Manfredi, A.A., Rugarli, C., and Bellone, M. (1999). Immunogenicity of apoptotic cells in vivo: role of antigen load, antigen-presenting cells, and cytokines. J. Immunol. *163*, 130–136.

Rupp, J., Gieffers, J., Klinger, M., Zandbergen, G. Van, Wrase, R., Maass, M., Solbach, W., Deiwick, J., and Hellwig-burgel, T. (2007). Chlamydia pneumoniae directly interferes with HIF-1 a stabilization in human host cells. *9*, 2181–2191.

Rupp, J., Pfleiderer, L., Jugert, C., Moeller, S., Klinger, M., Dalhoff, K., Solbach, W., Stenger, S., Laskay, T., and van Zandbergen, G. (2009). Chlamydia pneumoniae hides inside apoptotic neutrophils to silently infect and propagate in macrophages. PLoS One *4*, e6020.

Ryseck, R.P., and Bravo, R. (1991). c-JUN, JUN B, and JUN D differ in their binding affinities to AP-1 and CRE consensus sequences: effect of FOS proteins. Oncogene *6*, 533–542.

Rzomp, K.A., Scholtes, L.D., Briggs, B.J., Whittaker, G.R., and Scidmore, M.A. (2003). Rab GTPases Are Recruited to Chlamydial Inclusions in Both a Species-Dependent and Species-Independent Manner Rab GTPases Are Recruited to Chlamydial Inclusions in Both a Species-Dependent and Species-Independent Manner.

Sánchez-Tilló, E., Comalada, M., Xaus, J., Farrera, C., Valledor, A.F., Caelles, C., Lloberas, J., and Celada, A. (2007). JNK1 is required for the induction of Mkp1 expression in macrophages during proliferation and lipopolysaccharide-dependent activation. J. Biol. Chem. *282*, 12566–12573.

Santalucía, T., Christmann, M., Yacoub, M.H., Brand, N.J., Santalucía, T., Christmann, M., Yacoub, M.H., and Brand, N.J. (2003). H ypertrophic agonists induce the binding of c-Fos to an AP-1 site in cardiac myocytes : implications for the expression of GLUT1. Cardiovasc. Res. *59*, 639–648.

Sarkar, A., Möller, S., Bhattacharyya, A., Behnen, M., Rupp, J., van Zandbergen, G., Solbach, W., and Laskay, T. (2015). Mechanisms of apoptosis inhibition in Chlamydia pneumoniae-infected neutrophils. Int. J. Med. Microbiol. 4–11.

Savage, N.D.L., de Boer, T., Walburg, K. V, Joosten, S.A., van Meijgaarden, K., Geluk, A., and Ottenhoff, T.H.M. (2008). Human anti-inflammatory macrophages

induce Foxp3+ GITR+ CD25+ regulatory T cells, which suppress via membrane-bound TGFbeta-1. J. Immunol. *181*, 2220–2226.

Schachter, J., and Osoba, A.O. (1983). Lymphogranuloma venereum. Br. Med. Bull. *39*, 151–154.

Schachter, J., Stephens, R.S., Timms, P., Kuo, C., Bavoil, P.M., Birkelund, S., Boman, J., Caldwell, H., Campbell, L.A., Chernesky, M., et al. (2006). Erratum: Radical changes to chlamydial taxonomy are not necessary just yet (International Journal of Systematic and Evolutionary Microbiology (2006) vol. 51 (249)). Int. J. Syst. Evol. Microbiol. *56*, 677.

Schöier, J., Ollinger, K., Kvarnström, M., Söderlund, G., and Kihlström, E. (2001). Chlamydia trachomatis-induced apoptosis occurs in uninfected McCoy cells late in the developmental cycle and is regulated by the intracellular redox state. Microb. Pathog. *31*, 173–184.

Schonthaler, H.B., Guinea-Viniegra, J., and Wagner, E.F. (2011). Targeting inflammation by modulating the Jun/AP-1 pathway. Ann. Rheum. Dis. *70 Suppl 1*, i109–i112.

Schreiber, M., Kolbus, A., Piu, F., Szabowski, A., Möhle-Steinlein, U., Tian, J., Karin, M., Angel, P., and Wagner, E.F. (1999). Control of cell cycle progression by c-Jun is p53 dependent. Genes Dev. *13*, 607–619.

Schwarzenbacher, R., Stenner-Liewen, F., Liewen, H., Robinson, H., Yuan, H., Bossy-Wetzel, E., Reed, J.C., and Liddington, R.C. (2004). Structure of the Chlamydia protein CADD reveals a redox enzyme that modulates host cell apoptosis. J. Biol. Chem. *279*, 29320–29324.

Scidmore, M. a., Fischer, E.R., and Hackstadt, T. (2003). Restricted fusion of Chlamydia trachomatis vesicles with endocytic compartments during the initial stages of infection. Infect. Immun. *71*, 973–984.

Scidmore-Carlson, M.A., Shaw, E.I., Dooley, C.A., Fischer, E.R., and Hackstadt, T. (1999). Identification and characterization of a Chlamydia trachomatis early operon encoding four novel inclusion membrane proteins. Mol. Microbiol. *33*, 753–765.

Seglen, P.O., and Bohley, P. (1992). Autophagy and other vacuolar protein degradation mechanisms. Experientia *48*, 158–172.

Seo, J.H., Lim, J.W., Kim, H., and Kim, K.H. (2003). Helicobacter pylori in a Korean isolate activates mitogen-activated protein kinases, AP-1, and NF-κB and induces chemokine expression in gastric epithelial AGS cells. Lab. Investig. *84*, 49–62.

Sessa, R., Schiavoni, G., Borriello, G., Zagaglia, C., Marinelli, F., del Piano, M., and Pozzilli, C. (2007). Real time PCR for detection of Chlamydophila pneumoniae in peripheral blood mononuclear cells of patients with multiple sclerosis. J. Neurol. *254*, 1293–1295.

Shaulian, E., and Karin, M. (2001). AP-1 in cell proliferation and survival. Oncogene *20*, 2390–2400.

Shaulian, E., and Karin, M. (2002). AP-1 as a regulator of cell life and death. Nat. Cell Biol. *4*, E131–E136.

Shaw, E.I., Dooley, C.A., Fischer, E.R., Scidmore, M.A., Fields, K.A., and Hackstadt, T. (2000). Three temporal classes of gene expression during the Chlamydia trachomatis developmental cycle. Mol. Microbiol. *37*, 913–925.

Shen, F., Fan, X., Liu, B., Jia, X., Du, H., You, B., Ye, M., Huang, C., and Shi, X. (2006). Overexpression of cyclin D1-CDK4 in silica-induced transformed cells is due to activation of ERKs, JNKs/AP-1 pathway. Toxicol. Lett. *160*, 185–195.

Shen, Q., Uray, I.P., Li, Y., Krisko, T.I., Strecker, T.E., Kim, H.-T., and Brown, P.H. (2008). The AP-1 transcription factor regulates breast cancer cell growth via cyclins and E2F factors. Oncogene *27*, 366–377.

Shio, M.T., Hassani, K., Isnard, A., Ralph, B., Contreras, I., Gomez, M.A., Abu-Dayyeh, I., and Olivier, M. (2012). Host cell signalling and leishmania mechanisms of evasion. J. Trop. Med.

Silva, M.T., Do Vale, A., and Dos Santos, N.M.N. (2008). Secondary necrosis in multicellular animals: An outcome of apoptosis with pathogenic implications. Apoptosis *13*, 463–482.

Skowasch, D., Yeghiazaryan, K., Schrempf, S., Golubnitschaja, O., Welsch, U., Preusse, C.J., Likungu, J.A., Welz, A., Lüderitz, B., and Bauriedel, G. (2003). Persistence of Chlamydia pneumoniae in degenerative aortic valve stenosis indicated by heat shock protein 60 homologues. J. Heart Valve Dis. *12*, 68–75.

Smeal, T., Angel, P., Meek, J., and Karin, M. (1989). Different requirements for formation of Jun : Jun and Jun : Fos complexes. Genes Dev. *3*, 2091–2100.

Smeal, T., Hibi, M., and Karin, M. (1994). Altering the specificity of signal transduction cascades: positive regulation of c-Jun transcriptional activity by protein kinase A. EMBO J. *13*, 6006–6010.

Smith, W., Feldmann, M., and Londei, M. (1998). Human macrophages induced in vitro by macrophage colony-stimulating factor are deficient in IL-12 production. Eur. J. Immunol. *28*, 2498–2507.

Solbach, W., Rupp, J., Ko, I.R., Szaszák, M., Steven, P., Shima, K., Orzekowsky-Schröder, R., Hüttmann, G., König, I.R., Solbach, W., et al. (2011). Fluorescence lifetime imaging unravels C. trachomatis metabolism and its crosstalk with the host cell. PLoS Pathog. *7*, e1002108.

Solovjov, D.A., Pluskota, E., and Plow, E.F. (2005). Distinct roles for the alpha and beta subunits in the functions of integrin alphaMbeta2. J. Biol. Chem. *280*, 1336–1345.

Squier, M.K., Sehnert, A.J., and Cohen, J.J. (1995). Apoptosis in leukocytes. J. Leukoc. Biol. *57*, 2–10.

Stenner-Liewen, F., Liewen, H., Zapata, J.M., Pawlowski, K., Godzik, A., and Reed, J.C. (2002). CADD, a Chlamydia protein that interacts with death receptors. J. Biol. Chem. *277*, 9633–9636.

Stephens, R.S., Myers, G., Eppinger, M., and Bavoil, P.M. (2009). Divergence without difference: Phylogenetics and taxonomy of Chlamydia resolved. In FEMS Immunology and Medical Microbiology, pp. 115–119.

Stout, R.D., and Suttles, J. (2004). Functional plasticity of macrophages: reversible adaptation to changing microenvironments. J. Leukoc. Biol. *76*, 509–513.

Stromhaug, P.E., and Klionsky, D.J. (2001). Approaching the molecular mechanism of autophagy. Traffic *2*, 524–531.

Summersgill, J.T., Sahney, N.N., Gaydos, C.A., Quinn, T.C., and Ramirez, J.A. (1995). Inhibition of Chlamydia pneumoniae growth in HEp-2 cells pretreated with gamma interferon and tumor necrosis factor alpha. Infect. Immun. *63*, 2801–2803.

Sunderkötter, C., Nikolic, T., Dillon, M.J., Van Rooijen, N., Stehling, M., Drevets, D.A., and Leenen, P.J.M. (2004). Subpopulations of mouse blood monocytes differ in maturation stage and inflammatory response. J. Immunol. *172*, 4410–4417.

Swasdio, K., Rugpao, S., Tansathit, T., Uttavichai, C., Jongusuk, P., Vutayavanich, T., Oranratanachai, A., Pruthitada, N., Peerakom, S., Ittipunkul, W., et al. (1996). The association of Chlamydia trachomatis/gonococcal infection and tubal factor infertility. J. Obstet. Gynaecol. Res. *22*, 331–340.

Tak, T., Tesselaar, K., Pillay, J., Borghans, J. a M., and Koenderman, L. (2013). What's your age again? Determination of human neutrophil half-lives revisited. J. Leukoc. Biol. *94*, 595–601.

Tam, J.E., Davis, C.H., and Wyrick, P.B. (1994). Expression of recombinant DNA introduced into Chlamydia trachomatis by electroporation. Can. J. Microbiol. *40*, 583–591.

Tang, F.-T., Cao, Y., Wang, T.-Q., Wang, L.-J., Guo, J., Zhou, X.-S., Xu, S.-W., Liu, W.-H., Liu, P.-Q., and Huang, H.-Q. (2011). Tanshinone IIA attenuates atherosclerosis in ApoE(-/-) mice through down-regulation of scavenger receptor expression. Eur. J. Pharmacol. *650*, 275–284.

Tang, Y.-W., Sriram, S., Li, H., Yao, S., Meng, S., Mitchell, W.M., and Stratton, C.W. (2009). Qualitative and quantitative detection of Chlamydophila pneumoniae DNA in cerebrospinal fluid from multiple sclerosis patients and controls. PLoS One *4*, e5200.

Thi, E.P., Lambertz, U., and Reiner, N.E. (2012). Sleeping with the enemy: How intracellular pathogens cope with a macrophage lifestyle. PLoS Pathog. *8*.

Thomson, N.R., Holden, M.T.G., Carder, C., Lennard, N., Lockey, S.J., Marsh, P., Skipp, P., O'Connor, C.D., Goodhead, I., Norbertzcak, H., et al. (2008). Chlamydia trachomatis: Genome sequence analysis of lymphogranuloma venereum isolates. Genome Res. *18*, 161–171.

Tipples, G., and McClarty, G. (1993). The obligate intracellular bacterium Chlamydia trachomatis is auxotrophic for three of the four ribonucleoside triphosphates. Mol. Microbiol. *8*, 1105–1114.

Tseng, C.P., and Verma, A.K. (1995). Lack of 12-O-tetradecanoylphorbol-13-acetate responsiveness of ornithine decarboxylase introns which have AP-1 consensus sequences. Mol. Cell. Biochem. *146*, 7–12.

Tuffrey, M., Falder, P., Gale, J., Quinn, R., and Taylor-Robinson, D. (1986). Infertility in mice infected genitally with a human strain of Chlamydia trachomatis. J. Reprod. Fertil. *78*, 251–260.

Tugal, D., Liao, X., and Jain, M.K. (2013). Transcriptional control of macrophage polarization. Arterioscler. Thromb. Vasc. Biol. *33*, 1135–1144.

Tulchinsky, E. (2000). Fos family members: Regulation, structure and role in oncogenic transformation. Histol. Histopathol. *15*, 921–928.

Turner, R., and Tjian, R. (1989). Leucine repeats and an adjacent DNA binding domain mediate the formation of functional cFos-cJun heterodimers. Science *243*, 1689–1694.

Vallejo, J.G., Knuefermann, P., Mann, D.L., and Sivasubramanian, N. (2000). Group B Streptococcus induces TNF-alpha gene expression and activation of the transcription factors NF-kappa B and activator protein-1 in human cord blood monocytes. J. Immunol. *165*, 419–425.

Verreck, F.A.W., de Boer, T., Langenberg, D.M.L., Hoeve, M.A., Kramer, M., Vaisberg, E., Kastelein, R., Kolk, A., de Waal-Malefyt, R., and Ottenhoff, T.H.M. (2004). Human IL-23-producing type 1 macrophages promote but IL-10-producing type 2 macrophages subvert immunity to (myco)bacteria. Proc. Natl. Acad. Sci. U. S. A. *101*, 4560–4565.

Verreck, F.A.W., de Boer, T., Langenberg, D.M.L., van der Zanden, L., and Ottenhoff, T.H.M. (2006). Phenotypic and functional profiling of human proinflammatory type-1 and anti-inflammatory type-2 macrophages in response to microbial antigens and IFN-gamma- and CD40L-mediated costimulation. J. Leukoc. Biol. *79*, 285–293.

Vesely, P.W., Staber, P.B., Hoefler, G., and Kenner, L. (2009). Translational regulation mechanisms of AP-1 proteins. Mutat. Res. - Rev. Mutat. Res. *682*, 7–12.

Viale, A.M., Arakaki, A.K., Soncini, F.C., and Ferreyra, R.G. (1994). Evolutionary relationships among eubacterial groups as inferred from GroEL (chaperonin) sequence comparisons. Int. J. Syst. Bacteriol. *44*, 527–533.

Villegas, E., Camacho, A., Antonio Carrillo, J., Sorlozano, A., Rojas, J., and Gutierrez, J. (2008). Emerging strategies in the diagnosis, prevention and treatment of Chlamydophila pneumoniae infections. Expert Opin. Ther. Pat. *18*, 1175–1189.

Voll, R.E., Herrmann, M., Roth, E.A., Stach, C., Kalden, J.R., and Girkontaite, I. (1997). Immunosuppressive effects of apoptotic cells. Nature *390*, 350–351.

Wagner, E.F. (2001). AP-1--Introductory remarks. Oncogene *20*, 2334–2335.

Wang, Y. (1999). Etiology of trachoma: A great success in isolating and cultivating chlamydia trachomatis. Chin. Med. J. (Engl). *112*, 938–941.

Wang, G.L., Jiang, B.H., Rue, E.A., and Semenza, G.L. (1995). Hypoxia-inducible factor 1 is a basic-helix-loop-helix-PAS heterodimer regulated by cellular O2 tension. Proc. Natl. Acad. Sci. U. S. A. *92*, 5510–5514.

Wang, H., Gao, X., and Zhang, B. (2005). Tanshinone: an inhibitor of proliferation of vascular smooth muscle cells. J. Ethnopharmacol. *99*, 93–98.

Wang, Y., Kahane, S., Cutcliffe, L.T., Skilton, R.J., Lambden, P.R., and Clarke, I.N. (2011). Development of a transformation system for chlamydia trachomatis: Restoration of glycogen biosynthesis by acquisition of a plasmid shuttle vector. PLoS Pathog. *7*, e1002258.

Watson, C., and Alp, N.J. (2008). Role of Chlamydia pneumoniae in atherosclerosis. Clin. Sci. (Lond). *114*, 509–531.

Weinrauch, Y., and Zychlinsky, A. (1999). The induction of apoptosis by bacterial pathogens. Annu. Rev. Microbiol. *53*, 155–187.

WHO (2011). Prevalence and incidence of selected sexually transmitted infections - Chlamydia trachomatis, Neisseria gonorrhoeae, syphilis and Trichomonas vaginalis.

WHO (2015). Trachom - WHO, Fact sheet N°382, Updated May 2015.

Wolf, K., Fischer, E., and Hackstadt, T. (2000). Ultrastructural analysis of developmental events in Chlamydia pneumoniae-infected cells. Infect. Immun. *68*, 2379–2385.

Wolf, K., Fischer, E., Mead, D., Zhong, G., Peeling, R., Whitmire, B., and Caldwell, H.D. (2001). Chlamydia pneumoniae major outer membrane protein is a surface-exposed antigen that elicits antibodies primarily directed against conformation-dependent determinants. Infect. Immun. *69*, 3082–3091.

Wreghitt, T. (1993). Chlamydial infection of the respiratory tract. Commun. Dis. Rep. CDR Rev. *3*, R119–R124.

Wyrick, P.B. (2000). Intracellular survival by Chlamydia. Cell. Microbiol. *2*, 275–282.

Wyrick, P.B. (2010). Chlamydia trachomatis persistence in vitro: an overview. J. Infect. Dis. *201 Suppl*, S88–S95.

Xie, J., Pan, H., Yoo, S., and Gao, S.-J. (2005). Kaposi's sarcoma-associated herpesvirus induction of AP-1 and interleukin 6 during primary infection mediated by multiple mitogen-activated protein kinase pathways. J. Virol. *79*, 15027–15037.

Xie, J., Zhang, S., Hu, Y., Li, D., Cui, J., Xue, J., Zhang, G., Khachigian, L.M., Wong, J., Sun, L., et al. (2014). Regulatory roles of c-jun in H5N1 influenza virus replication and host inflammation. Biochim. Biophys. Acta *1842*, 1–10.

Xu, W., Roos, A., Schlagwein, N., Woltman, A.M., Daha, M.R., and Van Kooten, C. (2006). IL-10-producing macrophages preferentially clear early apoptotic cells. Blood *107*, 4930–4937.

Xu, W., Schlagwein, N., Roos, A., van den Berg, T.K., Daha, M.R., and van Kooten, C. (2007). Human peritoneal macrophages show functional characteristics of M-CSF-driven anti-inflammatory type 2 macrophages. Eur. J. Immunol. *37*, 1594–1599.

Xu, W., Zhao, X., Daha, M.R., and van Kooten, C. (2013). Reversible differentiation of pro- and anti-inflammatory macrophages. Mol. Immunol. *53*, 179–186.

Yamaguchi, H., Haranaga, S., Widen, R., Friedman, H., and Yamamoto, Y. (2002). Chlamydia pneumoniae Infection Induces Differentiation of Monocytes into Macrophages. *70*, 2392–2398.

Yasir, M., Pachikara, N.D., Bao, X., Pan, Z., and Fan, H. (2011). Regulation of chlamydial infection by host autophagy and vacuolar ATPase-bearing organelles. Infect. Immun. *79*, 4019–4028.

Yi, Y., Yang, X., and Brunham, R.C. (1997). Autoimmunity to heat shock protein 60 and antigen-specific production of interleukin-10. Infect. Immun. *65*, 1669–1674.

Ying, S. (2007). Chlamydia Interferes with Host Cell Death : Molecular Analysis of Apoptosis Signaling Pathways Table of Contents. Methods.

Ying, S., Pettengill, M., Latham, E.R., Walch, A., Ojcius, D.M., and Häcker, G. (2008). Premature apoptosis of Chlamydia-infected cells disrupts chlamydial development. J. Infect. Dis. *198*, 1536–1544.

Young, M.R., and Colburn, N.H. (2006). Fra-1 a target for cancer prevention or intervention. Gene *379*, 1–11.

Yun, S.M., Jung, J.H., Jeong, S.J., Sohn, E.J., Kim, B., and Kim, S.H. (2014). Tanshinone IIA induces autophagic cell death via activation of ampk and erk and inhibition of mTOR and p70 S6K in KBM-5 leukemia cells. Phyther. Res. *28*, 458–464.

Zachos, G. (1999). Herpes Simplex Virus Type 1 Infection Stimulates p38/c-Jun N-terminal Mitogen-activated Protein Kinase Pathways and Activates Transcription Factor AP-1. J. Biol. Chem. *274*, 5097–5103.

Zandbergen, G. Van, Gieffers, J., Kothe, H., Rupp, J., Bollinger, A., Aga, E., Klinger, M., Brade, H., Dalhoff, K., Maass, M., et al. (2004). Chlamydia pneumoniae Multiply in Neutrophil Granulocytes and Delay Their Spontaneous Apoptosis 1.

Van Zandbergen, G., Gieffers, J., Kothe, H., Rupp, J., Bollinger, A., Aga, E., Klinger, M., Brade, H., Dalhoff, K., Maass, M., et al. (2004a). Chlamydia pneumoniae multiply in neutrophil granulocytes and delay their spontaneous apoptosis. J. Immunol. *172*, 1768–1776.

Van Zandbergen, G., Klinger, M., Mueller, a., Dannenberg, S., Gebert, a., Solbach, W., and Laskay, T. (2004b). Cutting Edge: Neutrophil Granulocyte Serves as a Vector for Leishmania Entry into Macrophages. J. Immunol. *173*, 6521–6525.

Zenz, R., Eferl, R., Scheinecker, C., Redlich, K., Smolen, J., Schonthaler, H.B., Kenner, L., Tschachler, E., and Wagner, E.F. (2008). Activator protein 1 (Fos/Jun) functions in inflammatory bone and skin disease. Arthritis Res. Ther. *10*, 201.

Zhong, G., Liu, L., Fan, T., Fan, P., and Ji, H. (2000). Degradation of transcription factor RFX5 during the inhibition of both constitutive and interferon gamma-inducible major histocompatibility complex class I expression in chlamydia-infected cells. J. Exp. Med. *191*, 1525–1534.

Zizzo, G., Hilliard, B. a, Monestier, M., and Cohen, P.L. (2012). Efficient clearance of early apoptotic cells by human macrophages requires M2c polarization and MerTK induction. J. Immunol. *189*, 3508–3520.

6 Acronyms and Abbreviations

A. bidest	distilled water
AU	arbitrary unit
APS	Ammoniumpersulfat
ATP	adenosine triphosphate
bp	basepairs
c	chlamydial
CD	cluster of differentiation
cDNA	complementary DNA
cm_2	square centimeter
CO_2	carbon dioxide
CT-value	cycle threshold
DEPC	Diethyl pyrocarbonate
DIC	differential interference contrast
DMEM	Dulbecco´s Modified Eagle Medium
DMSO	Dimethylsulfoxid
DNA	deoxyribonucleic acid
DTT	Dithiothreitol
EDTA	Ethylenediaminetetraacetic acid
EB	elementary body
eGFP	enhanced green fluorescent protein
FCS	fetal calf serum
FITC	Fluorescein isothiocyanate
fwd	forward
g	gravitational force
GAPDH	glyceraldehyde 3-phosphate dehydrogenase
glut-1	glucose transporter 1
GM-CSF	granulocyte-macrophage colony-stimulating factor
h	hour
HEp-2	human epithelial cell line
hMDM	human monocyte derived macrophages
hpi	hours post infection
HRP	horseradish peroxidase
Hsp60	Heat shock protein (60 kDa)
IF	Immunofluorescence
IFU	Inclusion forming unit
IL	Interleukin
INF	Interferon
kDa	kilo dalton
L	liter

LC3	microtubule-associated protein 1A/B-light chain 3
LC3-I	cytosolic form of LC3
LC3-II	lipidated form of LC3
LL37	antimicrobial peptide cathelicidin
LPS	Lipopolysaccharide
LSM	leukocyte separation medium
m	meter
M	Molar
mA	milliampere
M-CSF	macrophage colony-stimulating factor
MDM	monocyte-derived macrophages
MFs	macrophages
MHC	major histocompatibility complex
min	minute
mL	Milliliter
mm	millimeter
mM	millimolar
MOMP	major outer membrane protein
mRNA	Messenger RNA
mTOR	mammalian target of rapamycin
NADPH	oxidase nicotinamide adenine dinucleotide phosphate-oxidase
NEB	New England Biolabs
ng	nanogram
nm	nanometer
nM	nanomolar
PAMPs	pathogen-associated molecular patterns
PBMCs	peripheral blood mononuclear cells
PBS	Phosphate buffered saline
PCR	polymerase chain reaction
PEI	Paul Ehrlich Institute
PFA	paraformaldehyde
PMN	polymorphonuclear neutrophil granulocytes
PRRs	pattern recognition receptors
PS	phosphatidylserine
P/S	penicillin/streptomycin
qRT-PCR	quantitative real-time PCR
RB	reticulate body
rev	reverse
RT	room temperature
RNA	ribonucleic acid
rRNA	ribosomal RNA

SD	standard deviation
SDS-PAGE	sodium dodecyl sulfate polyacrylamide gel electrophoresis
SEM	standard error of the mean
s / sec	second
siRNA	small interfering RNA
TBS	Tris buffered saline
TGF- β	transforming growth factor beta
TNF-α	tumor necrose factor alpha
TUNEL	terminal deoxynucleotidyl transferase (TdT)-mediated dUTP nick end labeling
U	unit
V	Volt
v/v	volume per volume %
WB	Western Blot
WHO	world health organization
w/v	mass per volume %
µg	Microgram
µL	microliter
µM	micromolar
°C	degree celsius
%	percentage
3-MA	3-methyladenine

7 List of figures

8 Declaration of authorship

I hereby declare that I have written the present dissertation with the topic:

“Chlamydiae host cell interaction and immune evasion strategies”

independently, using no other aids then those I have cited. I have clearly mentioned the source of the passages that are taken word for word or paraphrased from other works.

The presented thesis has not been submitted in this or any other form to another Faculty or Examination Institution.

Selbständigkeitserklärung

Hiermit versichere ich, dass ich die vorgelegte Dissertation mit dem Titel

„Chlamydiae host cell interaction and immune evasion strategies“

selbstständig verfasst und keine anderen als die angegebenen Quellen und Hilfsmittel verwendet habe. Die Stellen der Dissertation, die anderen Werken und Veröffentlichungen dem Wortlaut oder dem Sinn nach entnommen wurden, sind durch Quellenangaben gekennzeichnet.

Die Dissertation wurde in der jetzigen oder in ähnlicher Form noch an keiner anderen Hochschule eingereicht und hat noch keinen sonstigen Prüfungszwecken gedient.

Langen, 31. Juli 2015

Susi Krämer

9 Acknowledgements

10 Curriculum Vitae